Universidade de Lisboa

Faculdade de Farmácia

Role of mitofusin-2 in non-alcoholic fatty liver disease and targeting by microRNAs

Pedro Amaral Picado

Dissertation supervised by Dr. Rui E. Castro and co-supervised by Professor Cecília M. P. Rodrigues

Master in Biopharmaceutical Sciences

2020-2021

Universidade de Lisboa

Faculdade de Farmácia

Role of mitofusin-2 in non-alcoholic fatty liver disease and targeting by microRNAs

Pedro Amaral Picado

Dissertation supervised by Dr. Rui E. Castro and co-supervised by Professor Cecília M. P. Rodrigues

Master in Biopharmaceutical Sciences

2020-2021

The studies presented in this thesis were performed at the Research Institute for Medicines (iMed.ULisboa), Faculty of Pharmacy, Universidade de Lisboa, under the supervision of Doutor Rui Eduardo Mota Castro and Professor Cecília Maria Pereira Rodrigues.

This work was supported by Gilead Sciences International Research Scholars Program in Liver Disease and by FCT through research grant PTDC/MED-PAT/31882/2017.

Table of Contents

List of figures and tables

Abstract

Non-alcoholic fatty liver disease (NAFLD) comprises a range of liver lesions, from simple steatosis to non-alcoholic steatohepatitis (NASH), and constitutes a major cause of mortality when progressing to cirrhosis and hepatocellular carcinoma (HCC). Although its risk factors are related with the metabolic syndrome, the biological mechanisms of disease are not entirely known. As such, a better understanding of NAFLD pathogenesis may help in the development of novel targeted therapies for patients suffering from liver disease. In this regard, our research group and others have shown that microRNAs (miRNAs/miRs) have been associated with NAFLD/NASH progression. In parallel, recent evidence also support a crucial role for impaired mitochondrial dynamics in NAFLD development. In particular, mitochondrial fusion protein mitofusin 2 (MFN2) is decreased in the muscle of obese and diabetic patients and its liver-specific silencing in mice leads to numerous metabolic abnormalities. We have additionally shown that MFN2 is reduced in NASH patients and identified miR-222-3p as a direct *Mfn2*-binding miRNA, *in vitro*.

Altogether, the main goal of the work presented in this thesis was to elucidate whether the miR-222-3p:*Mfn2* pathway represents a key, primary event in experimental NAFLD and investigate whether its targeting it could ameliorate disease progression.

First, we aimed to validate an *in vivo* diet-induced NAFLD model based on a modified methionine and choline-deficient (MCD) diet. Our results indicated that this diet leads to modulation of liver genes and proteins associated with NASH. Next, we sought to elucidate whether targeting miR-222-3p counteracted MCD-induced NAFLD progression. Outstandingly, inhibition of miR-222-3p in experimental NASH, through the use of an antagomiR against miR-222-3p, led to significant improvements in NASH-like features, including inflammation, fibrosis, oxidative stress, triglycerides (TGs) accumulation, inflammatory cells activation, and dysregulated lipid metabolism. Finally, we sought to establish if the effect of miR-222-3p in NAFLD was mediated by *Mfn2*, by using liver-specific *Mfn2* knock-out (Mfn2 KO) mice. Surprisingly, inhibition of miR-222-3p in either WT or Mfn2 KO mice yelded similar results.

Overall, our findings highlight the critical role of miR-222-3p in NAFLD/NASH pathogenesis, and suggest that its effects are, mostly, *Mfn2*-independent. Notwithstanding, targeting miR-222-3p could be a promising therapeutic strategy for treating NAFLD.

Keywords: Non-alcoholic fatty liver disease; Non-alcoholic steatohepatitis; miRNA-222-3p; Mitofusin 2; Methionine and choline-deficient diet

Resumo

A doença do fígado gordo não-alcoólico (FGNA) compreende uma gama de lesões hepáticas, desde a esteatose simples à esteatohepatite não-alcoólica (EHNA), podendo progredir para cirrose e carcinoma hepatocelular (CHC). Esta doença está a crescer rapidamente em todo o mundo, com quase todos os países a exibirem um aumento da prevalência do FGNA. A prevalência mundial de FGNA é estimada em ~25%, enquanto na Europa cerca de 24% da população vive com FGNA. Por sua vez, de entre todos os casos de FGNA, aproximadamente 20% são classificados como EHNA. Estima-se que, apenas nos Estados Unidos, o FGNA tenha sido responsável por 1,27 milhões de mortes em 2015, com projecções que apontam que este número aumente para 1,83 milhões até 2030, o que significa um total de mais de 24 milhões de mortes durante 2015-2030. Esta tendência de agravamento do FGNA/EHNA é vastamente influenciada por vários fatores de risco, tais como a obesidade, diabetes, resistência à insulina (RI), e síndrome metabólica. A obesidade está a tornar-se mais comum e já é 6 vezes mais prevalente desde 1975. Em 2016, quase 2 mil milhões de adultos tinham excesso de peso, dos quais 671 milhões foram considerados obesos. Além disso, foi demonstrado que a síndrome metabólica constitui um reforço significativo para o FGNA, e os doentes que sofrem de síndrome metabólica são 12 vezes mais susceptíveis de terem mortes relacionadas com o fígado. Por conseguinte, uma melhor compreensão da patogénese da doença pode ajudar no desenvolvimento de novas terapias orientadas para os doentes que sofrem de doenças hepáticas.

No geral, a RI promove a disfunção do tecido adiposo (TA), resultando num aumento de lipólise e, consequentemente, libertação de ácidos gordos livres (AGLs) para o fígado. Um dos principais eventos na patogénese do FGNA é a lipotoxicidade. AGLs acumulam-se no fígado quando a sua disponibilidade é elevada, até um ponto em que excedem a capacidade do fígado para a sua metabolização, armazenamento e exportação, tornando-se assim espécies lipotóxicas. Por sua vez, a acumulação de triglicéridos (TGs) e AGLs no fígado promove a lipotoxicidade, desencadeando uma cascata de disfunção mitocondrial e gerando espécies reactivas de oxigénio (ROS) e stress do retículo endoplasmático (RE). Todos estes factores contribuem para a inflamação hepática que surge na sequência da libertação de citocinas pró-inflamatórias, tais como a interleucina 8 (IL-8), a interleucina 1 beta (IL-1β), e o fator de necrose tumoral-alfa (TNF-α). A disfunção mitocondrial foi estabelecida como uma peça fundamental na patogénese do FGNA. Conduz à sobreprodução de ROS e citocinas, contribuindo para a inflamação e fibrose hepática. Em particular, a proteína de fusão mitocondrial mitofusina 2 (MFN2) é uma proteína da membrana externa mitocondrial (MEM) composta por 757 resíduos, encontrando-se também nos locais de contacto do RE-

mitocondria, controlando desta forma ligação entre ambos organelos. Para além do seu papel na fusão mitocondrial, a MFN2 é também um modulador crucial do metabolismo mitocondrial no músculo esquelético e no fígado. Na verdade, a MFN2 está reduzida no músculo de doentes obesos e diabéticos e o seu silenciamento específico no fígado em ratinhos origina numerosas anomalias metabólicas. Mais recentemente, o nosso grupo colaborou num estudo mais amplo onde mostrámos que a expressão da MFN2 está diminuída no fígado de doentes com EHNA e em diferentes modelos animais de EHNA induzida pela dieta. Além disso, ratinhos com silenciamento (*knock-out*;KO) da *Mfn2* especificamente no fígado (hepatócitos) apresentaram-se com inflamação hepática exacerbada, acumulação de TGs, fibrose e progressão para cancro do fígado. Notavelmente, a reexpressão da *Mfn2* melhorou o fenótipo da EHNA.

Os microRNAs (miRNAs/miRs) são pequenos RNAs não codificantes de cadeia simples, com aproximadamente 22 nucleótidos de comprimento, que se ligam à região 3' não traduzida (UTR) dos mRNAs alvo, reprimindo a sua tradução. Os miRNAs têm sido associados à progressão do FGNA/EHNA, e a sua desregulação altera o metabolismo lipídico, o stress oxidativo, a fibrogénese, a proliferação celular e a apoptose. A este respeito, diferentes estudos estabeleceram uma associação entre um padrão de miRNAs em circulação alterado e a progressão do FGNA. Em particular, mostrámos já que doentes com FGNA apresentam níveis de expressão do miR-222-3p elevados, níveis esses que continuam a aumentar, progressivamente, com a gravidade da doença. Neste contexto, o nosso grupo identificou, *in vitro*, que o miR-222-3p se liga diretamente à *Mfn2* e que a desregulação da MFN2 na EHNA deveu-se, pelo menos em parte, à modulação directa pelo miR-222-3p.

Tudo em conta, o principal objetivo do trabalho apresentado nesta tese foi elucidar se a via miR-222-3p:*Mfn2* representa um evento chave e primário no FGNA experimental e investigar se a modulação desta via pode melhorar a progressão da doença.

Em primeiro lugar, o nosso objetivo era validar um modelo *in vivo* de FGNA, induzido por uma dieta deficiente em metionina e colina (MCD). Aqui, os nossos resultados indicaram que esta dieta induz características hepáticas de EHNA no fígado num curto período de tempo, incluindo inflamação, fibrose, stress oxidativo, acumulação de TGs, activação de células inflamatórias, e metabolismo lipídico desregulado. Em seguida, procurámos elucidar se a inibição do miR-222-3p contrariava a progressão do FGNA induzido pela dieta MCD. Notavelmente, a inibição do miR-222-3p, usando um antagomiR contra o miR-222-3p, levou a melhorias significativas nas características que definem a EHNA no nosso modelo experimental. Finalmente, procurámos estabelecer se o efeito do miR-222-3p no FGNA era mediado pela *Mfn2*. Para o efeito, usamos ratinhos com a *Mfn2* silenciada especificamente no fígado e que foram alimentados com a dieta MCD ou uma dieta controlo. Contudo, a

inibição do miR-222-3p nestes animais, ou seja, na ausência da *Mfn2* hepática, teve efeitos semelhantes aos da inibição em ratinhos *wild type* (WT).

Globalmente, apesar do seu efeito ser independente da *Mfn2* hepática, os nossos resultados salientam o papel crítico do miR-222-3p na patogénese do FGNA/EHNA ao contribuir para a inflamação, fibrose, e desenvolvimento de stress oxidativo com acumulação de TG, activação de células inflamatórias, e metabolismo lipídico desregulado. Assim sendo, o miR-222-3p pode representar um alvo terapêutico promissor para o tratamento do FGNA.

Palavras-chave: Fígado gordo não-alcoólico; Esteatohepatite não-alcoólica; miRNA-222-3p; Mitofusina 2; dieta deficiente em metionina e colina

Acknowledgments

Primeiro, gostava de começar por agradecer ao professor Rui, orientador desta tese, por me ter recebido no seu grupo de investigação tão bem e sempre ter confiado no meu trabalho. Mais importante ainda, por sempre ter estado disponível para me ajudar e aconselhar sempre que precisei e ter tornado todo este trabalho possível.

À professora Cecília, coorientadora desta tese, agradeço o acompanhamento e por sempre ter mostrado interesse e me ter motivado para que esta tese tivesse êxito.

Ao André, pessoa fulcral para o desenvolvimento desta tese, um enorme obrigado por estares sempre disponível para me ajudar e por todos os ensinamentos ao longo deste ano que possibilitaram que eu me fosse tornando cada vez mais autónomo dentro do laboratório. Desculpa se te chateei muito de vez em quando, mas sem dúvida que sem a tua ajuda isto não teria corrido tão bem.

À Daniela e aos restantes membros do laboratório, um obrigado por todos os momentos bem passados, por me terem acompanhado nesta caminhada e estarem sempre prontos para ajudar e esclarecer qualquer dúvida.

A ti Carolina, o maior agradecimento de todos, por me amparares nos dias menos bons e me motivares e acreditares em mim quando eu o deixo de fazer. Obrigado por me teres acompanhado, não teria feito sentido de outra forma.

Aos meus pais e a toda a minha família, agradeço por sempre me incentivarem e puxarem por mim ao longo da minha vida académica para dar sempre o meu máximo em tudo o que faça, que agora culmina nesta tese de mestrado.

Por fim, agradecer a todos os meus amigos, que apesar de ter falhado algumas vezes com eles, de uma forma ou de outra também contribuíram para o sucesso deste trabalho, seja com tardes/noites de folga bem passados ou de trabalho intenso no DEEC.

Abbreviations

α-SMA – Alpha-smooth muscle actin

AASLD – American Association for the Study of Liver Diseases

ACOX1 – Acyl-Coenzyme A oxidase 1

AGO2 – Argonaute 2

AGPAT – 1-acylglycerol-3-phosphate O-acyltransferases

AKT – Protein kinase B

ALD – Alcoholic liver disease

ALT – Alanine aminotransferase

AMPK – 5'-adenosine monophosphate-activated protein kinase

ANOVA – One-way analysis of variance

APRI – AST:platelet ratio index

AST – aspartate aminotransferase

AT – Adipose tissue

ATP – Adenosine triphosphate

BMI – Body mass index

CAP – Controlled attenuation parameter

CCL2 – C-C motif chemokine ligand 2

CCl4 – Carbon tetrachloride

CCR2 – C-C chemokine receptor 2

CD36 – Fatty acid translocase

CDAA – Choline-deficient L-amino-defined

CDKN1B – Cyclin-dependent kinase inhibitor 1B

Clec4f – C-type lectin domain family member f

CREB – cAMP response element-binding protein

DAMP – Danger-associated molecular pattern

DCF – 2', 7'-dichlorofluorescein

DGAT – Diacylglycerol-acyltransferases

DGCR8 – DiGeorge syndrome critical region gene 8

DNL – *De novo* lipogenesis

DRP1 – Dynamin-related protein 1

dsRNA – Double-stranded RNA

DTT – Dithiothreitol

EASD – European Association for the Study of Diabetes

EASL – European Association for the Study of the Liver

EASO – European Association for the Study of Obesity

ECM – Extracellular matrix

EMA – European Medicines Agency

ER – Endoplasmic reticulum

ERRα – Estrogen-related receptor-alpha

ETC – Electron transport chain

F4/80 – Adhesion G protein-coupled receptor

FDA – U.S. Food and Drug Administration

FF – Fast food

FFA – Free fatty acid

FIB-4 – Fibrosis-4

FIS1 – Mitochondrial fission 1 protein

FLI – Fatty liver index

FXR – Farnesoid X receptor

GBD – Global burden of disease

GGT – γ-glutamyl transferase

GLP-1 – Glucagon-like peptide-1

H_2DCFDA – 2', 7'-dichlorodihydrofluorescein diacetate

H_2O_2 – Hydrogen peroxide

HAT1 – Histone acetyltransferase 1

HBV – Hepatitis B virus

HBC – Hepatitis C virus

HCC – Hepatocellular carcinoma

HDL – High-density lipoprotein

HF – High-fat

HFD – High-fat diet

HO-1 – Heme oxygenase-1

HPRT – Hypoxanthine-guanine phosphoribosyltransferase

HSC – Hepatic stellate cell

HUVEC – Human umbilical vein endothelial cells

IFN-γ – Interferon-gamma

IL-1β – Interleukin 1 beta

IL-4 – Interleukin 4

IL-6 – Interleukin 6

IL-8 – Interleukin 8

IL-10 – Interleukin 10

IL-13 – Interleukin 13

IL-18 – Interleukin 18

IMM – Inner mitochondrial membrane

IR – Insulin resistance

JNK- C-jun N-terminal kinase

KC – Kupffer cell

KD – Knock-down

KO – Knock-out

LCFA – Long-chain free fatty acid

LDL – Low-density lipoprotein

LPS – Lipopolysaccharide

LSEC – Liver sinusoidal endothelial cell

MAFLD – Metabolic (dysfunction) associated fatty liver disease

MCD – Methionine and choline-deficient

MFF – Mitochondrial fission factor

MFN1 – Mitofusin-1

MFN2 – Mitofusin-2

Mfn2 KO – Mitofusin 2 knock-out

MiRNAs/miR – MicroRNA

MPTP – Mitochondrial permeability transition pore

MRS – Magnetic resonance spectroscopy

MtDNA – Mitochondrial DNA

NAFL – Non-alcoholic fatty liver

NAFLD – Non-alcoholic fatty liver disease

NAS – NAFLD activity score

NASH – Non-alcoholic steatohepatitis

NEFA – Non-esterified fatty acid

NF-kβ – Nuclear factor-kappa beta

NFS – NAFLD fibrosis score

NLRP3 – Nod-like receptor protein 3

NPC – Non-parenchymal cell

NRF-1 – Nuclear respiratory factor-1

NRF-2 – Nuclear respiratory factor-2

$O_2^{\bullet}$ - Superoxide radical

OCA – Obeticholic acid

OMM – Outer mitochondrial membrane

OPA1 – Optic atrophy 1

PAMP – Pathogen-associated molecular pattern

PBS – Phosphate buffer saline

PE – Phosphatidylethanolamine

PERK – Protein kinase RNA-like ER kinase

PI3K – Phosphoinositide 3-kinase

PGC-1α – Peroxisome proliferator-activated receptor gamma coactivator-1alpha

PGC-1β – Peroxisome proliferator-activated receptor gamma coactivator-1beta

PNPLA3 – Patatin-like phospholipase 3

PPARγ – Peroxisome proliferator-activated receptor gamma

PPARα – Peroxisome proliferator-activated receptor alpha

PPARδ – Peroxisome proliferator-activated receptor delta

PPP2R2A – Protein phosphatase 2 regulatory subunit B alpha

pre-miRNA – Precursor miRNA

pri-miRNA – Primary miRNA

PS – Phosphatidylserine

PTEN – Phosphatase and tensin homolog

PUFA – Polyunsaturated fatty acid

PUMA – P53 up-regulated modulator of apoptosis

qPCR – Real-Time PCR

RAN-GTP – Ras-related nuclear protein-guanosine triphosphate

RISC – RNA-induced silencing complex

ROS – Reactive oxygen species

RT – Room temperature

RT-PCR – Reverse transcription-polymerase chain reaction

SAF – steatosis, activity, and fibrosis

SDS-PAGE – Sodium dodecyl sulfate-polyacrylamide gel electrophoresis

S.E.M – Standard error of the mean

SGLT-2 – Sodium-glucose co-transporter-2

SIRT1 – Silent information regulator-1

snoRNA – Small nucleolar RNA

snRNA – Small nuclear RNA

SREBP1c – Sterol regulatory binding protein-1c

T2DM – Type 2 diabetes mellitus

TFAM – Mitochondrial transcription factor A

TG – Triglyceride

TGF-β – Transforming growth factor-beta

THRβ – Thyroid hormone receptor beta

TIMP3 – Tissue inhibitor metalloproteinases 3

TLR – Toll-like receptor

TLR4 – Toll-like receptor 4

TNF-α – Tumor necrosis factor-alpha

TRAIL – Tumor necrosis factor-related apoptosis-inducing ligand

TRBP – Trans-activation response RNA-binding protein

UCP-2 – Uncoupling protein-2

UPR – Unfolded protein response

UTR – Untranslated region

VLDL – Very-low-density lipoprotein

WHO – World health organization

WT – Wild-type

Chapter 1 | Introduction

1.1. Burden of liver diseases

Chronic liver diseases constitute a major public health problem, with a high economic burden, and include alcoholic liver disease (ALD), non-alcoholic fatty liver disease (NAFLD), and viral hepatitis, both hepatitis B virus (HBV) and hepatitis C virus (HCV) (Paik et al., 2020). Worldwide, around 2 billion people are obese, 400 million have diabetes and over 75 million experience alcohol use disorders, conditions which represent the major risk factors associated with chronic liver diseases. Liver diseases affect around 1.5 billion people with approximately 2 million deaths per year. In this context, cirrhosis represents the 11th leading cause of death with 1.16 million deaths per year and hepatocellular carcinoma (HCC) the 16th cause of death and the 3rd most common cause of cancer-related death, leading to 788 thousand deaths each year. These numbers have been consistently rising over the years, in the year 2000, 3% of all deaths were related to chronic liver diseases, while in 2015 they already represented 3.5% of all deaths (Asrani et al., 2019; Marcellin & Kutala, 2018).

The liver is the second most common organ transplanted in the world (22%), with the first being kidney transplantation (66.5%). Still, less than 10% of the patients who need a liver transplant are given one. This discrepancy is largely due to kidney transplantations being more accessible and easier to perform from living donors compared to liver transplantation. For instance, while many kidney donations in the European Union in 2015 came from living donors (21%), most liver transplants were performed from deceased patients and only 3% originated from living donors (Asrani et al., 2019). Chronic liver diseases have a huge economic impact on daily life. In the United States, patients with chronic liver diseases are more frequently unemployed than people without the disease (55% vs 30% respectively). In addition, annually, liver disease patients have higher health care expenditures ($19,390 vs $5,567). It is estimated that NAFLD alone is responsible for medical expenditures of $103 billion in the United States and €35 billion, just in Germany, France, Italy, and United Kingdom together (Asrani et al., 2019; Cotter et al., 2020).

As mentioned earlier, alcohol consumption, obesity, diabetes, and viral hepatitis represent major risk factors associated with liver diseases. Europe has the largest burden of liver disease in the world by presenting the highest per capita alcohol consumption and increased prevalence of obesity. Higher alcohol consumption is directly correlated to a higher incidence of cirrhosis. In particular, around 50% of all cirrhosis-related deaths are linked to alcohol consumption (Asrani et al., 2019). In 2017, a report from the Global Burden of Disease (GBD) indicated that the prevalence of cirrhosis was around 833 per 100,000 persons with an incidence of 26.0 per 100,000 inhabitants every year (James et al., 2018; Moon et al., 2020). According to the World Health of Organization (WHO), in 2015, Europe had an associated

prevalence of 1600 and 1500 cases per 100,000 inhabitants of HBV and HCV respectively, and 61.8 new cases of HCV per 100,000 inhabitants every year (WHO, 2017). In 2015, in Europe, at least 151,523 people died of complications from liver disease (Pimpin et al., 2018). In Portugal, from 2015 to 2017, around 1,000 people died from cirrhosis and chronic liver disease each year, overall accounting for 0.9% of all deaths. These numbers have been steadily decreasing in the last years due to improvement of some risk factors. For example, alcohol consumption has been decreasing and, in 2015, Portugal approved the access to direct-acting antivirals for hepatitis C. Since the approval, over 18,000 patients have been authorized for therapy, for which an even bigger impact on liver disease reduced related mortality is expected in the future (Silva et al., 2021).

1.2. Non-alcoholic fatty liver disease

1.2.1. Staging and diagnosis

NAFLD is mainly characterized by an excessive fat deposition in the liver, resulting in macrovesicular steatosis, in the absence of excessive consumption of alcohol (<20 g/day for women and <30 g/day for men). NAFLD patients may fail to present with any symptoms for years, while in others the disease starts to manifest as non-alcoholic fatty liver (NAFL), characterized by simple steatosis. NAFL has a considerable risk of progressing to non-alcoholic steatohepatitis (NASH), characterized by advanced steatosis, inflammation, hepatocyte ballooning, and different stages of fibrosis. Then, NASH can be potentially aggravated to cirrhosis and/or HCC with associated complications and, ultimately, liver failure. The exact factors that accelerate disease progression are not yet fully understood, with hepatic fibrosis being the most differentiated predictor of the disease severity (Estes et al., 2018; Friedman et al., 2018; Younossi et al., 2019). Fibrosis is staged from F1-F4, with F1 being characterized by fibrosis in the perisinusoidal/pericellular zone; F2 by F1 plus periportal fibrosis; F3 by F2 plus bridging fibrosis; and F4 by cirrhosis (Koch & Yeh, 2018). Fibrosis progression occurs at a slow rate of about 0.09 stage/year, suggesting that it takes about 30 years to progress from minimal fibrosis (F1) to cirrhosis (F4) (Asrani et al., 2019). As a liver disease, NAFLD is vastly influenced by several risk factors, such as obesity, diabetes/insulin resistance (IR), and metabolic syndrome (Estes et al., 2018). NAFLD is strongly associated with metabolic syndrome, which is characterized by obesity, diabetes, hypertension, and hypertriglyceridemia (Sanyal, 2011). In fact, over 80% of patients that present with the metabolic syndrome have NAFLD. Recently, international experts have even started to discuss renaming NAFLD to metabolic (dysfunction) associated fatty liver disease (MAFLD), as a more suitable nomenclature for the disease (Fouad et al., 2020).

In 1999, the first system to grade and stage NASH was proposed. The grade comprehends scores from 0-3 for steatosis, ballooning degeneration, and inflammation (Brunt et al., 1999). Later, in 2005, the NASH Clinical Research Network Pathology Committee validated a new scoring system, called the NAFLD Activity Score (NAS). The NAS is obtained from the sum of scores for steatosis (0-3), lobular inflammation (0-3), and ballooning (0-2). However, due to the lack of information related to fibrosis staging, these scoring systems are not particularlly useful to diagnose NASH but rather to indicate the severity of NAFLD and to monitor changes over time. In 2012, a new system was proposed, evaluating steatosis, activity, and fibrosis (SAF), and that shows a good correlation between its evaluation diagnosis and liver biopsy diagnosis (Bedossa et al., 2012; Koch & Yeh, 2018).

NALFD diagnosis is extremely important to know whether a patient presents advanced disease (NASH) or simple steatosis, and what is the risk of developing more severe complications, such as cirrhosis and HCC. At the moment, the only way to accurately diagnose NASH and fibrosis stage is by means of a liver biopsy. However, the biopsy is an extremely invasive method to perform in all potential NAFLD patients for routine screening. As such, alternative non-invasive strategies for diagnosis and staging of NAFLD/NASH are of extreme importance (Castera et al., 2013; Koch & Yeh, 2018; Smiderle et al., 2021). There are two possible approaches in non-invasive methods, namely using imaging techniques or serum biomarkers. The grade of steatosis in the liver can be determined through ultrasonography, a simple and widely used technique, although its sensitivity drops when <30% of the liver is infiltrated by fat and in patients with BMI> 40 kg/m^2. Other imaging techniques are the controlled attenuation parameter (CAP), an exam based on control transient elastography (like FibroScan® and VCTE™), and magnetic resonance spectroscopy (MRS) (Castera et al., 2013). MRS is a significantly sensitive method that demonstrates high accuracy, with results correlating to liver biopsy for steatosis. However, MRS is very time-consuming, expensive and is not widely available (Koch & Yeh, 2018). Regarding serum biomarkers, several tests diagnose steatosis, such as the SteatoTest™, FibroTest™-ActiTest, the fatty liver index (FLI), among others. All these scores are based on algorithms that take into account several variables including BMI, cholesterol, triglycerides (TG), waist circumference, γ-glutamyl transferase (GGT), age, gender, etc (Castera et al., 2013). For example, FLI is an equation useful to assess hepatic steatosis that only involves measurements of BMI, waist circumference, TG, and GGT (J.-Y. Kim et al., 2020). However, they are not very popular given the limited information they provide compared to other techniques. Liver fibrosis can be staged by hepatic transient elastography (FibroScan®), which measures liver stiffness by calculating the velocity a wave propagates through the liver and it is a useful technique to exclude severe fibrosis and cirrhosis in NASH (Castera et al., 2013). For an estimative of liver fibrosis from serum, the aspartate aminotransferase:alanine aminotransferase (AST:ALT) ratio and the

AST:platelet ratio index (APRI) can be used, as there is a strong association between AST:ALT>1 and AST:platelet>1 and advanced fibrosis on liver biopsy. Other scoring systems such as, FIB-4 index, BARD score, NAFLD fibrosis score (NFS), APRI, FibroMeter^{TM}, and HepaScore help in selecting patients at risk for more severe complications (HCC and cirrhosis), who need to face liver biopsy (Koch & Yeh, 2018). In particular, NFS has been approved by both the European Association for Study of the Liver (EASL) and the American Association for the Study of Liver Disease (AASLD) guidelines to predict whether a patient presents advanced fibrosis (F3-F4) or not. Combined, all these scores and indexes might help separate the patients at low risk of developing advanced fibrosis from the patients who need to undergo liver biopsy for further confirmation of NAFLD (Castera et al., 2013; J.-Y. Kim et al., 2020; Koch & Yeh, 2018; Smiderle et al., 2021).

1.2.2. Epidemiology

There is currently no national public health policy focusing on NAFLD. This disease is rapidly growing all over the world, with almost every country exhibiting an increase in NAFLD prevalence (Ge et al., 2020). The worldwide prevalence of NAFLD is estimated to be ~25%, whereas in Europe about 24% of the population lives with NAFLD (Younossi et al., 2019). A recent meta-analysis study in the United States estimated that in 2015, 83.1 million people had NAFLD, corresponding to a 25.8% prevalence in the general population. By 2030, NAFLD prevalence is projected to increase to 28.4% (Estes et al., 2018). Globally, NASH is prevalent in about 4% of the population (Younossi et al., 2019). And if we account for NASH cases between patients with NAFLD, approximately 20% of NAFLD cases could also be classified as NASH, with expectations to increase to 27% by 2030. In 2015, in the United States, there were 16.52 million cases of NASH, being estimated that by 2030 the prevalence of NASH will increase by 63% to 27 million cases. Also, 20% of those who have NASH feature at least stage 3 of fibrosis (3.31 million people), with estimations of reaching almost 29% in 2030 (8 million). NAFLD was estimated to be responsible for 1.27 million deaths in 2015, with projections to increase to 1.83 million by 2030, meaning a total of over 24 million deaths during 2015-2030 only in the United States. Consequently, NASH-related cirrhosis and HCC will also increase by 168% and 137% (Estes et al., 2018; Younossi et al., 2019). Accordingly, the incidence and mortality of liver cancer originated by NAFLD/NASH is rising globally. From 2012 to 2017, NAFLD-related liver cancer incidence and deaths grew by 26.43% and 22.49% respectively. Asia regions are among the most affected, suffering around 47,880 losses to NAFLD-related liver cancer. Altogether, 16 out of the 21 GBD regions were shown to be moving in a negative direction in terms of incidence and mortality of NAFLD-related cirrhosis. In 2017, NAFLD was responsible for 9% of global cirrhosis deaths, a 15% increase since 2012 (Paik et al., 2020).

Noteworthy, in patients with NAFLD or NASH, the most common cause of death is from cardiovascular disease, accounting for around 7.5% of total deaths, and less likely due to liver disease. Moreover, the risk in patients with NASH is 2 to 3 times higher compared to NAFLD patients (Younossi et al., 2019).

The worsening trend of NAFLD/NASH is tightly associated with the increasing epidemic of diabetes and obesity. NAFLD and NASH prevalence is even higher in cohorts of patients with diabetes or/and class III obesity who undergo weight reduction surgery (Asrani et al., 2019). If we only consider patients with type 2 diabetes mellitus (T2DM), the global prevalence reaches 61% for NAFLD and 10% for NASH. In addition, patients with NAFLD in the presence of T2DM are two times more likely to suffer liver-related death (Younossi et al., 2019). Obesity is becoming more common and has increased 6-fold since 1975. In 2016, almost 2 billion adults were overweight, of which 671 million were considered obese (BMI≥30 Kg/m^2) (Asrani et al., 2019). Among obese patients who undergo weight reduction surgery, NAFLD prevalence exceeds 95%. However, in some regions, the increased prevalence of NAFLD does not always associate to higher caloric consumption, suggesting the importance of other factors beyond obesity. In fact, around 8% and 20 % of patients with NAFLD are “lean” in the United States and in Europe, respectively. These “lean” patients appear to be more metabolically normal than obese subjects (Asrani et al., 2019; Younossi et al., 2019). Additionally, metabolic syndrome was shown to constitute a significant booster for NAFLD, and patients who suffer from metabolic syndrome are 12 times more susceptible to liver-related death. Age, sex, and ethnicity might also play an influence on the disease outcome. Older patients tend to be more susceptible to NAFLD, with NAFLD prevalence increasing with age, being higher in males, who are responsible for approximately 60% of all cases, and in individuals with hispanic ethnicity, where 45% of the population have NAFLD (Ge et al., 2020; Younossi et al., 2019).

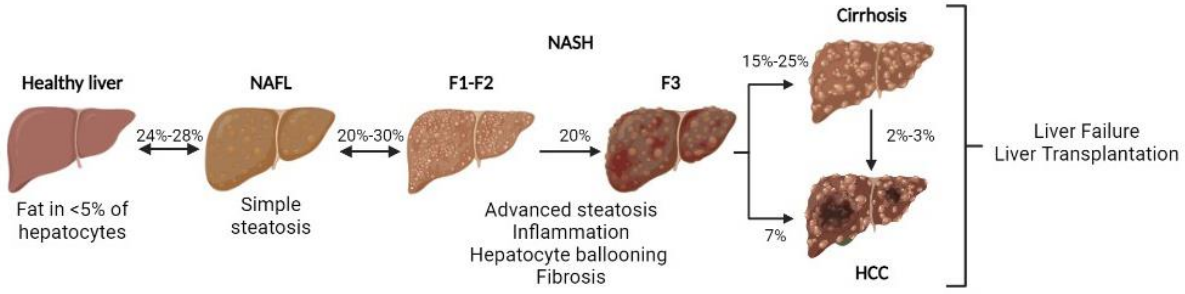

Figure 1.1. | NAFLD spectrum. NAFLD encompasses a spectrum of several disease stages, ranging from simple steatosis to NASH, each associating with specific disease hallmarks, such as hepatic lipid accumulation, inflammation, ballooning, and fibrosis. Further, NASH can progress to cirrhosis and/or HCC, both contributing to increased mortality. It is estimated that approximately 25% of the world population presents some form of NAFLD. Of all the patients who have NAFLD, about 20% have NASH, with 20% of those presenting stage 3 fibrosis. Over time, around 22% of individuals in this stage go on to develop cirrhosis, whereas HCC is prevalent in 7% of the

cases. Lastly, approximately 2% of cirrhotic patients will develop HCC within 3 years. F1, fibrosis stage 1; F2, fibrosis stage 2; F3, fibrosis stage 3; HCC, hepatocellular carcinoma; NAFL, non-alcoholic fatty liver; NASH, non-alcoholic steatohepatitis. Adapted from (Ferguson & Finck, 2021).

1.2.3. Pathogenesis

NAFLD was first described in 1980 (Lindenmeyer & McCullough, 2018). The first theory of NAFLD pathogenesis, known as the "two-hit hypothesis", was proposed in 1998 (Day & James, 1998). According to this theory, a first "hit" characterized by hepatic TG accumulation resulting from a high-fat diet, sedentarism and eventually, obesity and IR, leads to hepatic steatosis, thus triggering the disease. After this first "hit", the liver becomes more vulnerable to other factors and a second "hit" is needed to induce NASH. The second "hit" is characterized by inflammatory cytokines, mitochondrial dysfunction or oxidative stress and, consequently, significant lipid peroxidation, necroinflammation, and fibrogenesis. However, this perspective started to seem too simplistic to explain NAFLD pathogenesis and a new one emerged, named the "multiple-hit model" (Buzzetti et al., 2016; Day & James, 1998; Fang et al., 2018; Tilg & Moschen, 2010). Tilg and his colleagues proposed this new model suggesting that multiple factors from different tissues may act in parallel in NAFLD/NASH pathogenesis and progression (Tilg & Moschen, 2010). Dietary habits, epigenetic and genetic factors influence the development of obesity and IR, which in turn results in changes in gut microbiota and triggers major alterations in several organs and in the relations between them (Buzzetti et al., 2016; Fang et al., 2018; Tilg & Moschen, 2010). In general, IR promotes adipose tissue (AT) dysfunction, resulting in AT lipolysis and consequently increasing the release of free fatty acids (FFAs) to the liver. In turn, accumulation of TG and FFAs in the liver promote lipotoxicity, triggering a cascade of mitochondrial dysfunction with oxidative stress, generating reactive oxygen species (ROS) and endoplasmic reticulum (ER) stress. All these factors contribute to hepatic inflammation leading to the release of pro-inflammatory cytokines, such as interleukin 8 (IL-8), interleukin 1 beta (IL-1β), and tumor necrosis factor-alpha (TNF-α) (Buzzetti et al., 2016).

Diet ingredients have a critical impact on NAFLD progression. For example, diets with high levels of calories and added sugars from processed foods and fast-food increase hepatic *de novo* lipogenesis (DNL) and consequently the risk of obesity and NAFLD (Buzzetti et al., 2016; Fang et al., 2018; Prasun et al., 2021). In addition, genetic factors might also predispose for NAFLD triggering and progression (Tilg & Moschen, 2010). For example, patatin-like phospholipase 3 (*PNPLA3*) gene polymorphisms influence the development of NAFLD. *PNPLA3* encodes for adiponutrin, a lipid droplet protein involved in lipid metabolism. *PNPLA3* single nucleotide polymorphism I148M is associated with increased steatosis (Buzzetti et al.,

2016). Furthermore, *PNPLA3* I148M allele carriers have more than 2-fold hepatic fat content than non-carriers, increasing the risk of NAFLD (Fang et al., 2018).

1.2.3.1. Lipotoxicity in steatosis and fibrosis

One of the main events in NAFLD pathogenesis is lipotoxicity. FFA accumulate in the liver when its availability is high, up to a point where it exceeds the liver capacity for its use, storage, and exportation, thus becoming lipotoxic species (Rada et al., 2020). FFAs and non-esterified fatty acids (NEFA) in the liver originate from three major sources: 60% from AT lipolysis; 26% are produced in the liver from excessive carbohydrates through DNL; and the remaining 14% from excessive dietary intake (Nassir et al., 2015; Parthasarathy et al., 2020; Prasun et al., 2021). In adipocytes, metabolic dysregulation, such as IR, contributes to excess lipolysis of triglycerides (TGs), resulting in the release of FFAs into circulation. FFA uptake by the liver is facilitated by membrane proteins, such as fatty acid translocase (CD36), whose expression levels are known to be increased in obesity (Rada et al., 2020). In addition, carbohydrates, such as glucose and fructose, undergo DNL via upregulation of sterol regulatory binding protein-1c (SREBP1c), producing more FFAs and, consequently, hepatic steatosis (Cobbina & Akhlaghi, 2017; Prasun et al., 2021). FFAs in the liver are metabolized by either β-oxidation or esterification to TG. TG functions as a FFA storage mechanism and seems to work as an adaptive and protective mechanism against toxic amounts of FFA. However, when this mechanism is overwhelmed, metabolic dysregulation, hepatocyte cell death, inflammation, and fibrosis ensues. TGs are exported as very-low-density lipoproteins (VLDL) or stored as lipid droplets (Friedman et al., 2018; Parthasarathy et al., 2020; Prasun et al., 2021). Secretion of TGs as VLDL increases proportionally with the amount of hepatic TG. However, when hepatic TG content exceeds 10%, VLDL secretion reaches a plateau, resulting in its accumulation in the liver (Nassir et al., 2015). Lipid droplets can suffer lipolysis, releasing FFA back into hepatocytes and contributing to NAFLD/NASH progression.

Besides the amount, the type of FFAs that accumulate in the liver also differentially account for NAFLD pathogenesis. Saturated FFAs are more toxic compared to unsaturated FFAs, probably because unsaturated FFAs are stored into TGs more efficiently (Rada et al., 2020). In the NAFLD liver, there are significantly higher levels of saturated fatty acids compared to unsaturated fatty acids. Apart from saturated fatty acids, diacylglycerol, ceramides, and cholesterol are also lipotoxic for hepatocytes (Friedman et al., 2018). In NASH patients, palmitate, a saturated fatty acid (C16:0), is found elevated in plasma accumulating in the esterified form in the liver. Lipotoxicity, specifically the presence of saturated FFAs, is associated with increased intrinsic and extrinsic pathways of hepatocyte apoptosis, ER stress, and release of calcium (Prasun et al., 2021). For example, palmitate activates intrinsic and

extrinsic apoptotic pathways in the hepatocytes, such as c-jun N-terminal kinase (JNK) and p53 up-regulated modulator of apoptosis (PUMA), sensitizing cells to tumor necrosis factor-related apoptosis-inducing ligand (TRAIL) induced cell death. All these pathways result in the release of cytochrome *c* and, consequently, activation of caspases, triggering cell death. In turn, cell death activates inflammatory signaling, and immune cells release apoptotic mediators resulting in a positive feedback loop. On the other hand, unsaturated fatty acids attenuate palmitate toxicity *in vitro*, reducing steatosis, IR, inflammation, and promoting TG formation, indicating that TG formation might have a cytoprotective effect (Parthasarathy et al., 2020; Rada et al., 2020).

1.2.3.2. Inflammation

Beyond releasing FFA into circulation, the AT also secretes adipokines. Early in NAFLD, there is an increased secretion of pro-inflammatory adipokines, such as leptin, and a decreased secretion of adiponectin, an anti-inflammatory adipokine, leading to AT inflammation and IR (Prasun et al., 2021). In the liver, lipotoxicity causes the release of several intracellular molecules that activate non-parenchymal cells (NPCs), such as kupffer cells (KCs), hepatic stellate cells (HSCs), and liver sinusoidal endothelial cells (LSECs), which exhibit different responses to these signals (Rada et al., 2020). For example, steatosis can lead to nuclear factor kappa beta (NF-kβ) activation, thus inducing the production of pro-inflammatory cytokines, such as TNF-α, interleukin 6 (IL-6), and IL-1β. In turn, these mediators induce the recruitment and activation of KCs (Cobbina & Akhlaghi, 2017).

Liver macrophages include KCs and bone marrow monocyte-derived macrophages. Macrophages can show two different phenotypes depending on the surrounding environment. They can be classically activated (M1) or alternatively activated (M2). M1 macrophages exhibit pro-inflammatory properties in response to interferon-γ (IFNγ) and TNF-α, producing significant amounts of pro-inflammatory cytokines that contribute to liver inflammation. Contrastingly, M2 macrophages exhibit anti-inflammatory properties in response to interleukin 4 (IL-4), interleukin 10 (IL-10), interleukin 13 (IL-13), and transforming growth factor-beta (TGF-β). M2 KCs further induce M1 macrophage apoptosis, attenuating NAFLD in mice, indicating that M2 macrophages play a protective role in NAFLD development (Cha et al., 2018; Huang et al., 2020).

KCs are present in the sinusoidal space where they remove bacteria from the intestine. In NAFLD, the accumulation of cholesterol and lipid droplets in hepatocytes associates with the aggregation of KCs and fibrosis. KCs play a role in early NASH by producing TNF-α, IL-1β, C-C motif chemokine ligand 2 (CCL2), and other pro-inflammatory cytokines. In turn, by interacting with its C-C chemokine receptor 2 (CCR2), expressed by monocytes, CCL2

facilitates the recruitment of bone marrow monocyte-derived macrophages (Kazankov et al., 2019; Parthasarathy et al., 2020; Rada et al., 2020). Together, both types of immune cells contribute to NASH progression by boosting liver inflammation. This pro-inflammatory phenotype change has been observed in primary KCs treated with palmitate. On the other hand, when treated with oleate, macrophages changed to an anti-inflammatory phenotype. Further, depletion of KCs and monocyte-derived macrophages recruitment in a murine model of NASH resulted in decreased steatosis, inflammation, fibrosis and hepatic IR, delaying NASH progression (Huang et al., 2020; Parthasarathy et al., 2020; Rada et al., 2020).

Besides macrophages, HSCs are also activated upon exposure to FFAs, producing pro-inflammatory cytokines and pro-fibrogenic cytokines, such as TGF-β, alpha-smooth muscle actin (α-SMA), and collagen. LSECs role in NAFLD pathogenesis is still not entirely elucidated. While some studies suggest that they may act to attenuate fibrosis development, they also appear to become dysfunctional upon lipotoxicity and injury, therefore contributing to disease (Rada et al., 2020). Nod-like receptor protein 3 (NLRP3) is mainly expressed in injured hepatocytes, KCs, HSCs, and LSECs. NLRP3 inflammasome is activated by pathogen-associated molecular patterns (PAMPs), like lipopolysaccharide (LPS) product of gut harmful bacteria that reach the liver through the portal circulation, and danger-associated molecular patterns (DAMPs), such as saturated FFAs. NLRP3 inflammasome activation leads to the secretion of pro-inflammatory cytokines such as IL-1β, IL-6, and interleukin 18 (IL-18) and induces apoptosis through caspase-1 activation (Friedman et al., 2018; Parthasarathy et al., 2020). In NASH patients, NLRP3 inflammasome activity is increased while in healthy hepatocytes is low. In agreement, NLRP3 inhibition leads to improvements in NASH pathogenesis. DAMPs and PAMPs can also activate toll-like receptors (TLRs) that initiate a cascade of events releasing pro-inflammatory cytokines and inducing immune cell activation. For example, due to gut dysbiosis and increased permeability for bacteria, there is an increase in LPS release that activates toll-like receptor 4 (TLR4) in KCs, promoting secretion of pro-inflammatory cytokines, such as IL-6, IL-8, and TGF-β, that activate HSCs to secrete collagen contributing to hepatic fibrosis. Thus, TLR4 is known to be highly expressed in patients with NASH (Parthasarathy et al., 2020; Prasun et al., 2021). Last but not least, neutrophils also play a role in NASH by releasing ROS, and B cells, Th1 and Th17 release more pro-inflammatory cytokines, while Th2 release less anti-inflammatory cytokines (Parthasarathy et al., 2020). Also, they are extremely involved in the production and deposition of extracellular matrix components (ECM) (Huang et al., 2020).

1.2.3.3. Oxidative stress through mitochondrial dysfunction

NAFLD is highly associated with mitochondrial dysfunction and deregulated fatty acid oxidation, resulting in overproduction of ROS and oxidative stress (Cobbina & Akhlaghi, 2017). Mitochondria represent the cell's primary site of energy production in the form of adenosine triphosphate (ATP). In addition, mitochondria play a critical role in energy metabolism by metabolizing fatty acids and glucose via β-oxidation and citric acid cycle respectively (Prasun et al., 2021).

Mitochondria can also be the major source of ROS production in cells mainly due to impaired fatty acid oxidation and deficient electron flow through the electron transport chain (ETC). ATP is produced due to the movement of electrons down the ETC. In healthy conditions, a very small fraction of electrons, about 2 %, escape from the ETC and can react with molecular oxygen producing superoxide radicals triggering a cascade of reactions that lead to the production of ROS. However, ETC dysfunction provokes an over leakage of electrons and, consequently, excessive ROS production, such as superoxide radical ($O_2^{\bullet}$) and hydrogen peroxide (H_2O_2) (Mantena et al., 2008; Prasun et al., 2021; Rada et al., 2020). This is called oxidative stress, one of the key players in NASH pathogenesis. Indeed, NAFLD patients show increased oxidative stress and lipid peroxidation and decreased activity of antioxidant enzymes (Rada et al., 2020).

Mitochondrial dysfunction results in impaired β-oxidation, impaired ETC, and depletion of mitochondrial DNA (mtDNA). Inhibition of enzymes involved in mitochondrial β-oxidation and depletion of mtDNA induces hepatic steatosis. In NASH patients, mitochondria are bigger, more swollen, and fewer in number. Also, they present lower activity of complexes I, III, IV, and V of the ETC and, consequently, lower ATP production (Wei et al., 2008). Excessive ROS induces cell injury, typically apoptosis. It results in outer mitochondrial membrane (OMM) permeabilization, facilitating the release of proapoptotic factors such as cytochrome *c*, which in turn activates a cascade of reactions leading to caspase-3 activation. ROS also provokes mitochondrial permeability transition pores (MPTPs) in the inner mitochondrial membrane (IMM), causing the loss of mitochondrial membrane potential, decreased ATP synthesis, and mitochondrial swelling (Prasun et al., 2021).

Mitochondrial dysfunction has been established as a key player in NAFLD pathogenesis. It leads to overproduction of ROS and cytokines, contributing to hepatic fibrosis and inflammation (Wei et al., 2008). In the end, NAFLD pathogenesis seems to be a vicious cycle between, lipotoxicity, inflammation, oxidative stress, and cell death (Cobbina & Akhlaghi, 2017).

1.2.3.3.1 Mitochondrial dynamics

Maintenance and coordination of mitochondrial biogenesis, fission, and fusion are critical for healthy mitochondrial homeostasis (Figure 1.2.). In turn, dysfunction of either one of these processes may contribute to disease triggering and progression, including metabolic diseases like obesity and T2DM (López-Lluch et al., 2008; Popov, 2020). Mitochondrial biogenesis consists of replication of pre-existing mitochondria and is influenced by exogenous factors such as environmental stress, exercise, diet, and endogenous factors such as oxidative stress and cell division and renewal. Mitochondrial biogenesis increases the oxidative phosphorylation capacity, the repair of mitochondrial dysfunctions, and decreases pathologic oxidative stress (Jornayvaz & Shulman, 2010; Popov, 2020). Peroxisome proliferator-activated receptor gamma (PPARγ) coactivator-1alpha (PGC-1α), a co-transcriptional regulation factor, is the major regulator of mitochondrial biogenesis. Early on, PGC-1α activation is triggered by different signaling molecules such as AMPK, silent information regulator-1 (SIRT1), and cAMP response element-binding protein (CREB) (Jornayvaz & Shulman, 2010; López-Lluch et al., 2008; Scarpulla et al., 2012). AMPK facilitates transcription by relaxing the chromatin-DNA structure through histone acetyltransferase 1 (HAT1) activation. SIRT1/PGC-1α activation is known to be enhanced during mitochondria proliferation, oxidative phosphorylation, and energy production (Popov, 2020). PGC-1α stimulates several nuclear transcription factors, such as nuclear respiratory factor-1 (NRF-1), nuclear respiratory factor-2 (NRF-2), and estrogen-related receptor-alpha (ERRα). Next, these proteins, induce the expression of the mitochondrial transcription factor A (TFAM), which binds to mtDNA promoting the transcription and replication of mtDNA and mitochondria itself (Picca et al., 2017).

Mitochondria are extremely dynamic organelles, balancing between different architecture and function states, namely fusion and fission. These shape changes represent constant adaptations to the surrounding environment and altered physiological needs (R. Li et al., 2020). Thus, mitochondrial fission and fusion are pivotal in maintaining functional mitochondria in a metabolic stress environment (Youle & van der Bliek, 2012). A balance between these two mechanisms also impacts mitochondrial growth and distribution. Interestingly, in hepatocytes of NAFLD patients, giant and swollen mitochondria with crystallin insertions and loss of mitochondrial cristae have been observed (Longo et al., 2021; van der Bliek et al., 2013).

Mitochondrial fission is characterized by the split of a single mitochondrion into two, or more, smaller mitochondria. Normally, fission occurs when oxidative stress damages mitochondria, surging the need to be segregated from the healthy ones. Dynamin-related protein 1 (DRP1), mitochondrial fission 1 protein (FIS1), and mitochondrial fission factor (MFF) are the main proteins involved in this mechanism. FIS1 and MFF recruit and activate DRP1 from the cytosol to OMM. Here, DRP1 forms a spiral homomultimeric structure around OMM that constricts and

divides the mitochondria. This pathway is induced by SIRT1 and AMPK, which phosphorylates FIS1 and MFF. In the end, damaged mitochondria are degraded by mitophagy (Archer, 2013; Longo et al., 2021; López-Lluch et al., 2008; Youle & van der Bliek, 2012).

Mitochondrial fusion is associated with high oxidative phosphorylation capacity and mitochondrial elongation. This mechanism is ensued by three major proteins, mitofusin-1 (MFN1), mitofusin-2 (MFN2), and optic atrophy 1 (OPA1). MFN1 and MFN2 are responsible for the merging of OMMs, with MFN1 having a higher affinity for mitochondrial bridging and MFN2 playing a crucial role in both mitochondria-mitochondria and ER-mitochondria tethering. Next, OPA1 mediates IMMs fusion and cristae shaping remodeling (Archer, 2013; R. Li et al., 2020; Longo et al., 2021). Mitochondrial fusion works as a compensatory mechanism to restore damaged mitochondria functionality and maintain cellular homeostasis by mixing partially damaged mitochondria with healthy mitochondria. However, when severely damaged, depolarized mitochondria need to be eliminated by mitophagy. Thus, fusion/fission processes originate new mitochondria and contribute to the elimination of damaged ones (R. Li et al., 2020; Youle & van der Bliek, 2012). Overall, an increased fusion/fission rate is associated with low levels of stress, since dysfunctional mitochondria are mixed with healthy ones, helping to reduce stress. On the other hand, decreased fusion/fission rate occurs with high levels of stress (van der Bliek et al., 2013). As such, any dysregulation in fusion/fission results in defective mitochondrial function and homeostasis leading to disease development and/or progression (R. Li et al., 2020; López-Lluch et al., 2008). In particular, MFN2 imbalances associate with metabolic abnormalities, including NAFLD.

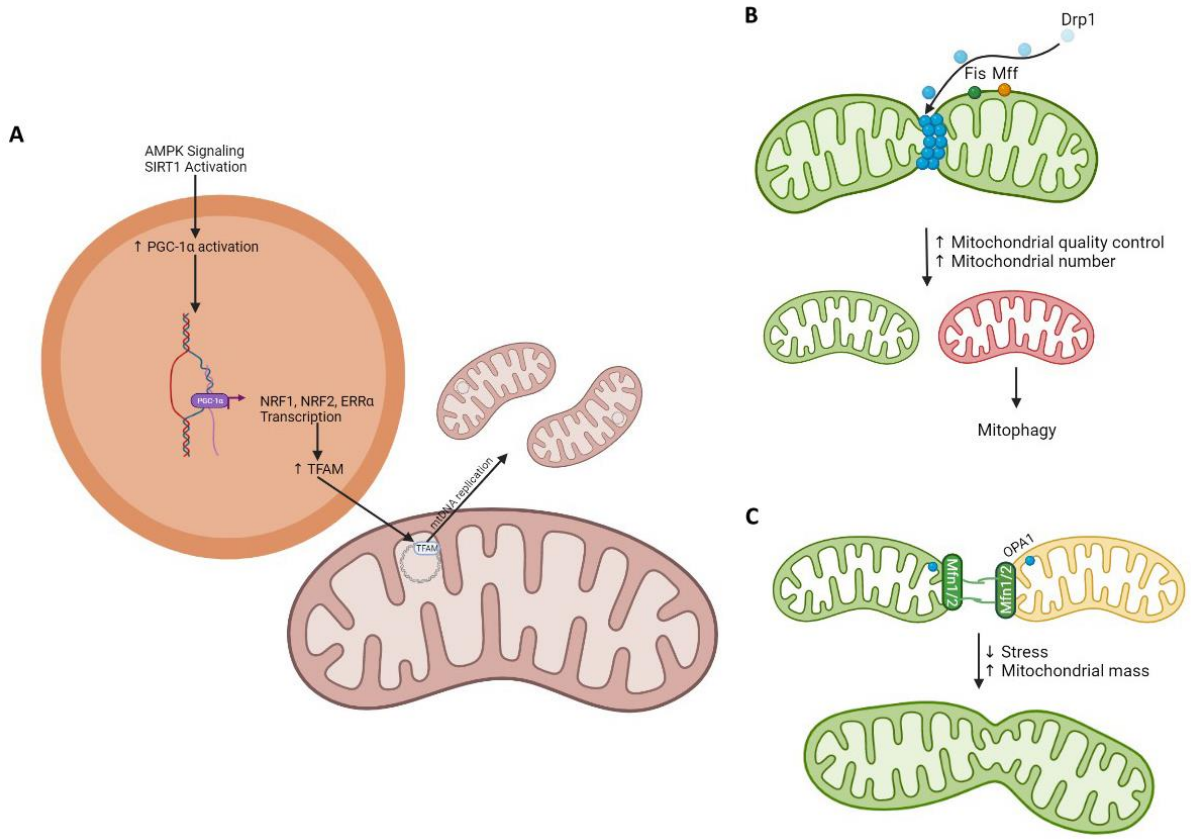

Figure 1.2. | Mitochondrial biogenesis and dynamics. A. Mitochondrial biogenesis. This mechanism is triggered by AMPK/SIRT1 signaling, which induces PGC-1α activation in the nucleus, promoting the expression of NRF1, NRF2, and ERRα transcription. In turn, these proteins increase the expression of TFAM, which is transported to the mitochondria and binds to mtDNA, promoting its transcription and replication of the mitochondria. **B.** Mitochondrial fission. This process is initiated by FIS1 and MFF proteins, which recruit DRP1 to form a structure around the OMM that divides the mitochondria into two different organelles. Eventually, damaged mitochondria generated from mitochondrial fission are degraded by mitophagy, ensuring high quality control. **C.** Mitochondrial fusion. Fusion is mediated by MFN1, MFN2 and OPA1. While MFN1 and MFN2 are responsible for the merging of OMMs, OPA1 coordinates the fusion of the IMMs. This process attenuates stress by allowing functional mitochondria to compensate for a partially dysfunctional one. AMPK, 5'-adenosine monophosphate-activated protein kinase; DRP1, dynamin-related protein 1; ERRα, estrogen-related receptor-alpha; FIS, mitochondrial fission 1 protein; MFF, mitochondrial fission factor; MFN1/2, mitofusin 1/2; mtDNA, mitochondrial DNA; NRF1, nuclear respiratory factor-1; NRF-2, nuclear respiratory factor-2; OPA1, optic atrophy 1; PGC-1α, peroxisome proliferator-activated receptor-gamma coactivator-1alpha; SIRT1, silent information regulator-1; TFAM, mitochondrial transcription factor A. Adapted from (Archer, 2013; Picca et al., 2017; Youle & van der Bliek, 2012).

1.2.3.3.2 Metabolic roles of MFN2

In humans, MFN2 is an OMM protein composed of 757 residues that is also located in the ER mitochondrial contact sites controlling its tethering with the mitochondria. MFN2 seems to play a fundamental role in normal body function, as *Mfn2* knock-out (KO) mice die early in gestation due to a placental defect (Segalés et al., 2013; Zorzano et al., 2010). Apart from its role in mitochondrial fusion, MFN2 is also a crucial modulator of mitochondrial metabolism in

skeletal muscle and liver. Early studies in 2005 discovered that MFN2 plays a regulatory role in muscle metabolism. It was observed that MFN2 is involved in mitochondrial energization independently of its role in mitochondrial fusion, mainly by regulating the expression of the oxidative phosphorylation system (D. Bach et al., 2005; Mingrone et al., 2005; Pich et al., 2005). For instance, *Mfn2* deficiency in muscle cells causes mitochondrial dysfunction, inhibiting pyruvate, glucose, and palmitate oxidation and reducing mitochondrial membrane potential (Pich et al., 2005; Zorzano, 2009). In addition, subunits of oxidative phosphorylation complexes I, II, III, and V are suppressed. In opposition, *Mfn2* overexpression induces glucose oxidation, mitochondrial membrane potential, and expression of complexes I, IV, and V subunits. Curiously, a truncated form of MFN2, incapable of inducing mitochondrial fusion, exerted a similar effect, suggesting that the role of MFN2 in mitochondrial metabolism is independent of its role as a mitochondrial fusion protein. *Mfn2* expression has been found to be significantly decreased in obesity in both obese patients and Zucker rats (Mingrone et al., 2005; Pich et al., 2005). In agreement, the activity of subunits of complexes I, II, III, and V was decreased in obese rats. Moreover, *in vivo* and *in vitro* studies have suggested that MFN2 has repressing effects in cell proliferation by provoking G0/G1 cell-cycle arrest (Pich et al., 2005).

Along with mitochondrial metabolism, MFN2 has been identified as a key player in the maintenance of the mitochondrial network architecture (Daniel Bach et al., 2003; Mingrone et al., 2005). *Mfn2* inhibition in muscle cells leads to morphological and functional disorganization of the mitochondrial network, originating independent clusters (Pich et all). This leads to decreased glucose oxidation, mitochondrial membrane potential, mitochondrial leak of protons, and cell respiration in both muscle and non-muscle cells (Daniel Bach et al., 2003; Yong Zhang et al., 2011). Therefore, MFN2 plays a crucial role in mitochondrial metabolism through the preservation of the mitochondrial network architecture. *Mfn2* mRNA expression is reduced in the skeletal muscle of obese patients, both male and female, and in T2DM patients, both lean and obese (Daniel Bach et al., 2003; Sebastian et al., 2012; Segalés et al., 2013). In fact, *Mfn2* expression is inversely proportional to BMI and is positively correlated with insulin sensitivity. *Mfn2* muscle expression significantly increases after weight reduction by biliopancreatic diversion or bariatric surgery (Daniel Bach et al., 2003; Zorzano, 2009). In addition, upon weight loss in obese patients, this increase in *Mfn2* expression is stronger compared to other mitochondrial genes (Mingrone et al., 2005).

In certain conditions, *Mfn2* expression is differently regulated (Figure 1.3.). For example, *Mfn2* expression is upregulated in the skeletal muscle during exercise. This finding suggests a correlation between MFN2 and exercise-induced PGC co-activators, as PGC-1α and PGC-1β positively regulate *Mfn2* expression in the muscle. PGC-1α indirectly activates *Mfn2* by activating ERRα that binds to the *Mfn2* promoter. Notably, PGC-1α overexpression induces a higher increase in *Mfn2* mRNA expression and protein levels compared to other genes

normally induced under the same conditions (Zorzano, 2009; Zorzano et al., 2010). PGC-1β deficiency leads to downregulation of *Mfn2* in muscle, liver, and heart, while its overexpression upregulates *Mfn2* mRNA expression mainly through ERRα activation as well. Moreover, it was observed that *Mfn2* knock-down (KD) limits PGC-1α effectiveness on mitochondrial membrane potential. Thus, PGC-1α effects on mitochondrial energization are dependent on MFN2's normal functioning. However, in obese nondiabetic subjects, exercise increases nuclear genes *PGC-1α* and *ERRα* but not *Mfn2*, and subjects with T2DM show little capacity to induce both *Mfn2* and *PGC-1α* expression. Therefore, dysfunctional PGC-1α/*Mfn2* and PGC-1β/*Mfn2* interactions are associated with the development of metabolic diseases (Hernandez-Alvarez et al., 2010; Zorzano, 2009).

MFN2 also plays a direct role in mitigating ER stress. As a result, the ER expands and there is excessive activation of the unfolded protein response (UPR). Protein kinase RNA-like ER kinase (PERK), one arm of the UPR, directly interacts with *Mfn2* upon ER stress, being suppressed by *Mfn2*. Loss of this interaction due to *Mfn2* deficiency affects ROS production, mitochondrial morphology and respiration, and Ca^{2+} signaling (Muñoz et al., 2013). Neurons are particularly sensitive to *Mfn2* dysfunction. Indeed, more than one hundred *Mfn2* gene mutations are the primary cause of Charcot-Marie-Tooth neurotype 2A, an autosomal dominant neuropathy. Characterized by chronic axonal neuropathy, *Mfn2* loss-of-function compromises energy production along the axon, promoting axon degeneration (Daniel Bach et al., 2003; Pich et al., 2005).

By playing a pivotal role in metabolic homeostasis, *Mfn2* associates with obesity and T2DM (Gan, 2013). Liver-specific *Mfn2* KO mice display several metabolic abnormalities, such as glucose intolerance and increased hepatic gluconeogenesis. In addition, *Mfn2* deficiency promotes ER stress, increases the production of H_2O_2, and activates JNK, impairing insulin signaling in the liver and muscle (Sebastian et al., 2012). Hepatic steatosis was demonstrated to be alleviated through omega-3 polyunsaturated fatty acids (PUFAs)-induced upregulation of *Mfn2*. In particular, liver cells incubated with omega-3 PUFAs show increased mitochondrial fusion and ATP production, and decreased oxidative stress, via upregulation of *Mfn2* expression. In turn, cells incubated with long-chain free fatty acids (LCFAs) lead to *Mfn2* inhibition, suggesting that *Mfn2* could play a role in NAFLD progression (Yong Zhang et al., 2011). In this regard, *Mfn2* expression has been found significantly downregulated in a HFD-induced animal model of NASH, with its overexpression restoring insulin sensitivity (Gan, 2013). More recently, our group collaborated in a larger study where we showed that *Mfn2* expression is decreased in the liver of NASH patients and in different diet-induced NASH mouse models. Liver-specific *Mfn2* KO mice displayed exacerbated liver inflammation, TG accumulation, fibrosis, and progression to liver cancer. Noteworthy, *Mfn2* re-expression improved the NASH phenotype. We further showed that MFN2 is instrumental for lipid transport

and phospholipid synthesis in mitochondria by binding to phosphatidylserine (PS), mobilizing to the mitochondrial membrane and promoting phosphatidylethanolamine (PE) synthesis. In agreement, liver-specific *Mfn2* KO mice display disrupted ER-mitochondrial PS transport and PE synthesis, which contributes to ER stress and NASH development (Hernández-Alvarez et al., 2019).

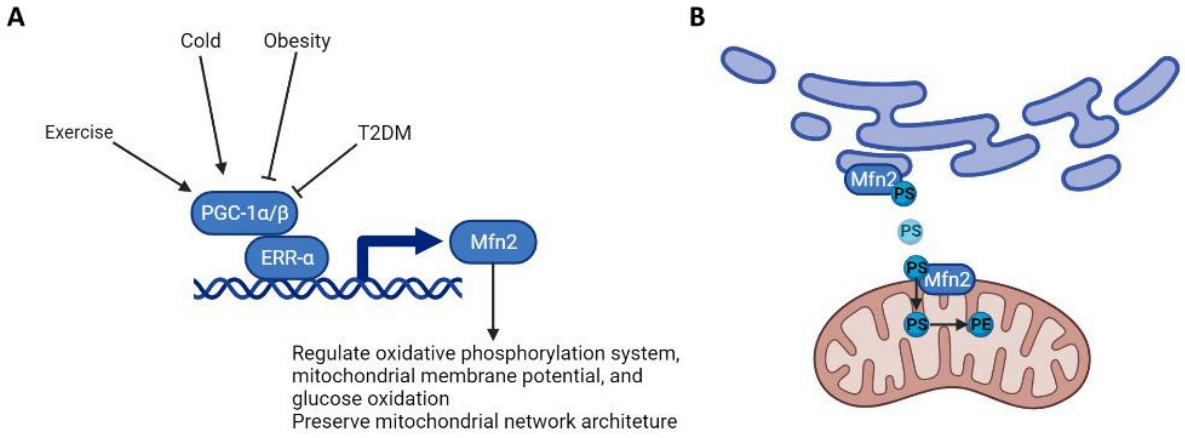

Figure 1.3. | *Mfn2* regulation and metabolic roles. A. *Mfn2* transcriptional regulation. ERRα, which is co-activated by PGC1α/β, binds to the *Mfn2* promoter inducing its transcription. **B.** MFN2 function in lipid transport. MFN2 controls ER-mitochondria tethering. Here, MFN2 helps in transporting PS to the mitochondria, where it is converted into PE. ERR-α, estrogen-related receptor-alpha; Mfn2, mitofusin 2; PGC-1α/β, peroxisome proliferator-activated receptor-gamma coactivator-1alpha/beta; PE, phosphatidylethanolamine; PS, phosphatidylserine. Adapted from (Chandhok et al., 2018; Hernández-Alvarez et al., 2019; Zorzano, 2009).

1.2.4. Inter-organ crosstalk

Organ crosstalk is the communication between different organs through signaling mediators. This inter-organ communication is essential to maintain homeostasis. In fact, dysfunction in any organ may cause dysfunction of others. Circulating molecules, such as cytokines and chemokines, play a key role in organ crosstalk, and a dysregulated release of these factors can induce dysfunction in other organs. Disrupted inter-organ communication represents a key NAFLD feature (Armutcu, 2019). Some of the organs that are involved in inter-organ crosstalk in the NAFLD context include the liver, AT, skeletal muscle, gut, among others (Figure 1.4.). For example, altered gut microbiota and permeability influence circulating levels of LPS, FFAs, bile acids, and pro-inflammatory cytokines, stimulating profibrotic and pro-inflammatory pathways in the liver and contributing to fibrosis and IR (Armutcu, 2019; X. Zhang et al., 2018).

Inter-organ crosstalk between the liver, AT and skeletal muscle plays an important role in NAFLD development (Altajar & Baffy, 2020). In particular, the AT represents a source of FFAs that are released into circulation and delivered into the liver and skeletal muscle (X. Zhang et

al., 2018). In addition, the AT is an endocrine organ that produces and secretes adipokines that metabolically affect other organs, such as the liver and skeletal muscle. Adiponectin and leptin are the two major adipokines. Adiponectin presents many beneficial activities, such as activating 5'-adenosine monophosphate-activated protein kinase (AMPK), which possesses an anti-inflammatory role by inhibiting the NF-kβ pathway and secreting anti-inflammatory cytokines, negatively regulating apoptosis, and promoting hepatic insulin sensitivity. Leptin is the other major adipokine secreted by the AT, responsible for regulating appetite and energy metabolism. High leptin levels induce inflammation and fibrogenesis in the liver (Altajar & Baffy, 2020; X. Zhang et al., 2018). As adipocytes accumulate more fatty acids, they secrete less adiponectin and higher levels of leptin and pro-inflammatory cytokines. In NAFLD patients, leptin levels are exacerbated, increasing proportionally with the severity of the disease (Altajar & Baffy, 2020; Armutcu, 2019; X. Zhang et al., 2018).

Skeletal muscle dysfunction, such as myosteatosis or sarcopenia, is directly linked to increased risk of NAFLD (Chakravarthy et al., 2020). Myosteatosis results from the incapability of the AT to store excessive FFAs, leading to ectopic fat accumulation in skeletal muscle. Sarcopenia is characterized by low skeletal muscle mass. Loss of skeletal muscle mass promotes metabolic impairments, being associated with the prevalence of NAFLD (Altajar & Baffy, 2020; Cai et al., 2020; G. Kim et al., 2018). Consequently, dysfunctional skeletal muscle composition provokes a dysregulated secretion of myokines, such as myostatin, irisin, and myonectin. Myostatin promotes liver inflammation and fibrosis through HSCs activation, while increasing adiposity. Oppositely, inhibition of myostatin in mice increases muscle mass and browning of the AT, ameliorating NAFLD. Irisin induces browning of the AT, increasing energy expenditure, insulin sensitivity, and inducing β-oxidation in the liver. Myonectin induces the uptake of FFAs by the AT and the liver, and inhibits autophagy in the liver (Altajar & Baffy, 2020; Chakravarthy et al., 2020). During NAFLD, the skeletal muscle secretes elevated levels of myostatin, while myonectin and irisin production is reduced. Thus, aggravation of skeletal muscle dysfunction directly correlates with NAFLD progression. Altogether, liver-AT-muscle axis disruption increases with the aggravation of NAFLD (Chakravarthy et al., 2020).

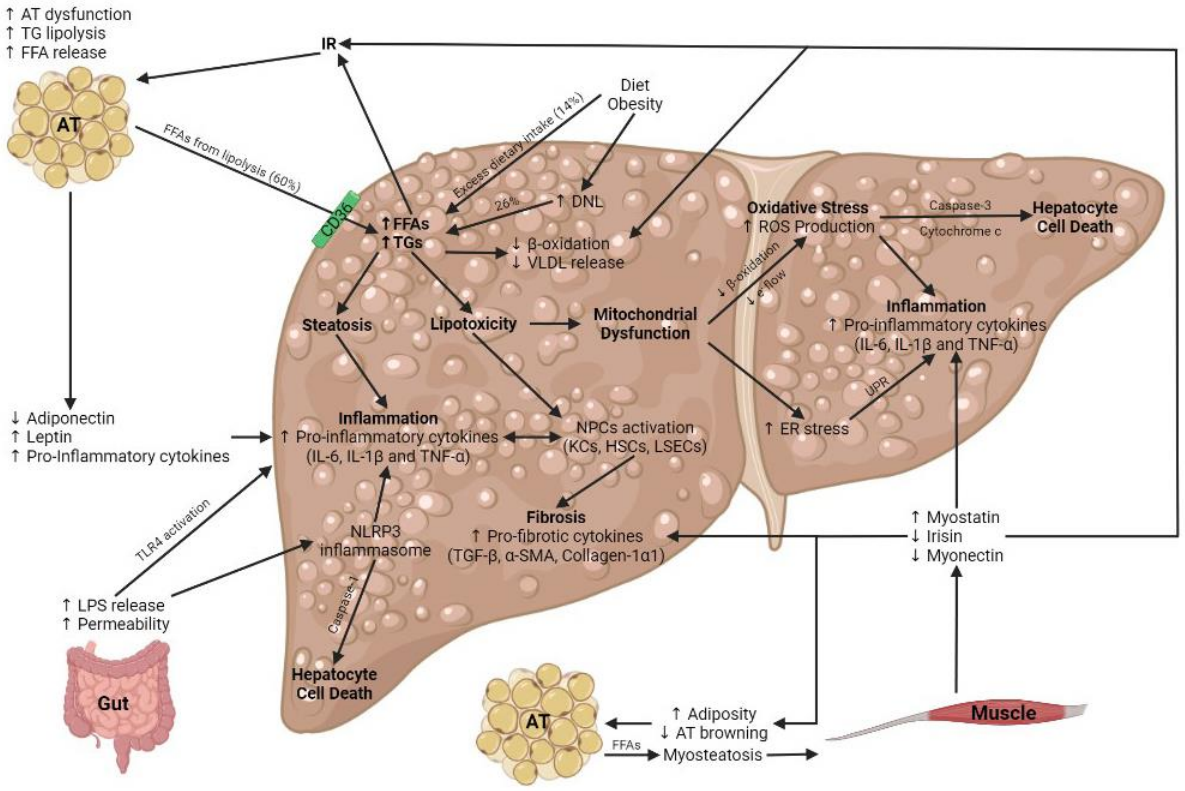

Figure 1.4. | Dysfunctional inter-organ crosstalk in NAFLD pathogenesis. NAFLD pathogenesis involves loss of or dysfunctional inter-organ communication between the liver and other organs, such as the AT, skeletal muscle, and the gut. IR in adipocytes induces TG lipolysis, increasing the flux of FFAs to the liver. The excessive accumulation of FFAs in the liver results in lipotoxicity, steatosis, inflammation, decreased β-oxidation, and VLDL release. In turn, lipotoxicity impairs mitochondrial viability and induces NPCs activation, including KCs that promote more inflammation, and HSCs that release pro-fibrogenic cytokines, including TGF-β, α-SMA, and collagen-1α1. Mitochondrial dysfunction due to impaired β-oxidation and electron flow leads to increased ROS production and ER stress, resulting in the release of pro-inflammatory cytokines, such as IL-6, IL-1β, and TNF-α, and hepatocyte cell death through caspase-3 activation. In addition to FFAs released from the AT, dysregulated secretion of adipokines, myokines, and LPS by the AT, skeletal muscle, and gut, respectively, contribute to the worsening of inflammation and fibrosis. In the NAFLD pathological state, the AT releases less adiponectin and higher levels of leptin and pro-inflammatory cytokines, whereas the skeletal muscle secretes more myostatin and lower levels of irisin and myonectin. Dysfunctional gut, due to increased permeability, promotes elevated circulating levels of LPS, which are recognized by TLR4 in liver cells, contributing to inflammation. AT, adipose tissue; CD36, fatty acid translocase; DNL, *de novo* lipogenesis; e^-, electron; ER, endoplasmic reticulum; FFA, free fatty acid; HSC, hepatic stellate cell; IL-1β, interleukin 1 beta; IL-6, interleukin 6; IR, insulin resistance; KC, kupffer cell; LPS, lipopolysaccharide; LSEC, liver sinusoidal endothelial cell; NLRP3, nod-like receptor protein 3; NPC, non-parenchymal cell; ROS, reactive oxygen species; TG, triglyceride; TGF-β, transforming growth factor-beta; TNF-α, tumor necrosis factor-alpha; UPR, unfolded protein response; VLDL, very-low-density lipoprotein; α-SMA, alpha-smooth muscle actin. Adapted from (Altajar & Baffy, 2020; Buzzetti et al., 2016; X. Zhang et al., 2018)

1.2.5. Animal models of NAFLD

Animal models should mimic the full spectrum of NAFLD pathogenesis in humans so that they allow the study of NAFLD/NASH pathogenesis and the development of new therapeutic

strategies. Over 3500 different animal models of NAFLD have been reported in the literature, depicting variations in age, sex, genetic background, and dietary composition (Table 1.1). The best-suited model should mimic both the histopathology and pathophysiology of human NAFLD/NASH. Still, no model yet appears to recapitulate all features of human NAFLD (Im et al., 2021; Takahashi, 2012).

There are three types of mice models of NAFLD, namely diet-induced, genetically modified, and chemically-induced. Also, several models are the result of the combination of more than one type to induce a more severe hepatic histopathology, closer to human NAFLD/NASH. Chemically-induced models show fewer metabolic features of NAFLD, being usually used as complementary models. *Ob/ob* and *db/db* are examples of genetic mice models that possess spontaneous mutations in the leptin gene and leptin receptor gene, respectively. Despite exhibiting liver steatosis and several characteristics of the metabolic syndrome, these models fail to develop NASH in the absence of a secondary stimulus, such as a methionine and choline-deficient (MCD) diet or a high-fat diet (HFD) (Takahashi, 2012).

The MCD diet is composed of high amounts of sucrose (40%) and fat (10%), in the absence of methionine and choline. These two nutrients are important for glutathione synthesis, hepatic TG secretion in the form of VLDL, and mitochondrial β-oxidation. Ultimately, its absence results in FFAs accumulation in the liver (Denk et al., 2019; Jahn et al., 2019). The major advantages of the MCD diet model are the similarity between its hepatic histopathology with human NASH, and the presence of macrovesicular steatosis, perisinusoidal fibrosis, inflammation, hepatocyte ballooning, apoptosis, and mitochondrial abnormalities with just a few weeks of feeding (2-10 weeks) (Jahn et al., 2019). In this model, steatohepatitis starts at day 10, pericellular fibrosis generally occurs around 9 weeks, and after 10 weeks extensive macrovesicular steatosis can be observed (Takahashi, 2012). Also, serum alanine aminotransferase (ALT) levels are increased in mice fed a MCD diet and KCs are activated. In addition, the presence of cirrhosis in under 20 weeks and HCC under 30 weeks are also observed in choline-deficient diets (Im et al., 2021). However, the metabolic profile of these animals is the opposite of human NASH, and mice suffer significant weight loss (>20%), display low plasma TGs, cholesterol and leptin levels, and increased insulin sensitivity (Takahashi, 2012). To overcome these disadvantages, MCD-diet can be fed to genetically modified mice, such as the *ob/ob* and *db/db*, or additional diet modifications can be introduced. For example, mice fed a choline-deficient L-amino-defined (CDAA) diet, after a long time, start to develop obesity, IR, and elevated TG and cholesterol levels (Denk et al., 2019).

Among the wide variety of animal models of NAFLD, the high-fat (HF), high-fructose diet models are probably the ones that most resemble the human phenotype of NAFLD. These diets vary in the relative contents of fat, fructose, sucrose and cholesterol, and induce NAFLD, IR and increase adiposity (Im et al., 2021). The HFD consists of 71% energy from fat, 11%

from carbohydrates, and 18% from proteins. Mice fed a HFD present the complete span of NAFLD metabolic features with hepatic lipid accumulation, obesity, IR, oxidative stress, panlobular steatosis, inflammation, and fibrosis. The major stepback is that steatosis, inflammation, and fibrosis in the HFD model present a high variability, whereas the MCD diet model promotes a sharper liver injury. In addition, to induce inflammation and fibrosis with a HFD, mice must be fed for a long period of at least 1 year. To overcome time-limiting restrictions, HFDs supplemented with increased levels of cholesterol and/or fructose led to more significant liver inflammation and fibrosis, in a shorter timeframe (Jahn et al., 2019; Takahashi, 2012). Altogether, due to the wide alternatives, it is very important to choose the best-suited model according to the objective of the study.

Table 1.1. | NAFLD animal models. Pathological characteristics of common NASH models. CDAA, choline-deficient L-amino-defined; F2, fibrosis stage 2; F3, fibrosis stage 3; F4, fibrosis stage 4; HF, High-fat; HFD, High-fat diet; IR, insulin resistance; MCD, methionine and choline-deficient. Adapted from (Denk et al., 2019; Im et al., 2021).

Model	Type of Model	Steatosis	Inflammation	Hepatocyte Ballooning	Fibrosis	IR	Obesity
Ob/ob	Genetic	+	+	+	-	+	+
Db/db	Genetic	+	+	+	-	+	+
MCD	Diet	+	+	+	+ (F2-F3)	-	-
HFD	Diet	+	+	+	-	+	+
MCD+HFD	Diet	+	+	+	+ (F4)	+	-
CDAA	Diet	+	+	+	+ (F4)	±	-
HF, high-fructose	Diet	+	+	+	+ (F2)	+	+
HF, high-fructose, and high-cholesterol	Diet	+	+	+	+ (F2-F3)	+	+
Ob/ob, HF, high-fructose, and high-cholesterol	Diet	+	+	+	+ (F3)	+	+

1.4. Biogenesis of microRNAs

MicroRNAs (miRNAs) are small non-coding single-stranded RNAs, with approximately 22 nucleotides in length, that bind to the 3' untranslated region (UTR) of target mRNAs, repressing

its translation (Murchison & Hannon, 2004). The first described miRNA was lin-4, discovered in *Caenorhabditis elegans* in 1993. In humans, it is estimated that around 2000 miRNA genes exist, regulating approximately 30% of all protein-coding genes (Murchison & Hannon, 2004; Vishnoi & Rani, 2017). Due to each miRNA presenting a moderate affinity with its target, a single miRNA may inhibit the expression of several different mRNAs. MiRNAs play an important role in physiological homeostasis and disease onset, being involved in cell proliferation, apoptosis, differentiation, among others (Tétreault & De Guire, 2013).

In humans, miRNA biogenesis begins with transcription of the miRNA as a long primary miRNA (pri-miRNA) composed of thousands of nucleotides and stem-loop structures. Pri-miRNA transcription takes place in the nucleus by RNA polymerase II. Then, the RNAse III enzyme Drosha interacts with DiGeorge syndrome critical region gene 8 (DGCR8) and associated proteins, forming a complex called microprocessor (Michlewski & Cáceres, 2019; Tétreault & De Guire, 2013). The microprocessor will cleave the pri-miRNA releasing a stem-loop structure of approximately 70 nucleotides called precursor miRNA (pre-miRNA). Next, the pre-miRNA is transported from the nucleus to the cytoplasm through Exportin-5 in a Ras-related nuclear protein-guanosine triphosphate (RAN-GTP)-dependent manner. Once in the cytoplasm, RNAse III enzyme Dicer cleaves the hairpin precursors into a double-stranded RNA (dsRNA), composed of the mature miRNA and its complementary strand of 21-23 nucleotides. This dsRNA is then incorporated into an effector complex called RNA-induced silencing complex (RISC), by binding to the trans-activation response RNA-binding protein (TRBP) that recruits Argonaute 2 (AGO2), a major component of the RISC complex. Finally, RISC has the role of selecting and recruiting the miRNA strand that has the lowest thermodynamic stability at its 5' end, releasing the complementary strand (Murchison & Hannon, 2004; Tétreault & De Guire, 2013; Vishnoi & Rani, 2017). Finally, RISC will induce mRNA cleavage, translation suppression, degradation, or deadenylation of the mRNA complementary to the mature miRNA (Figure 1.5.) (Ha & Kim, 2014). Still, there are other not so common alternative pathways to miRNA biogenesis, such as mirtrons, miRNAs originated from pre-miRNA from specific introns, and small nucleolar RNA (snoRNA) precursors (Michlewski & Cáceres, 2019).

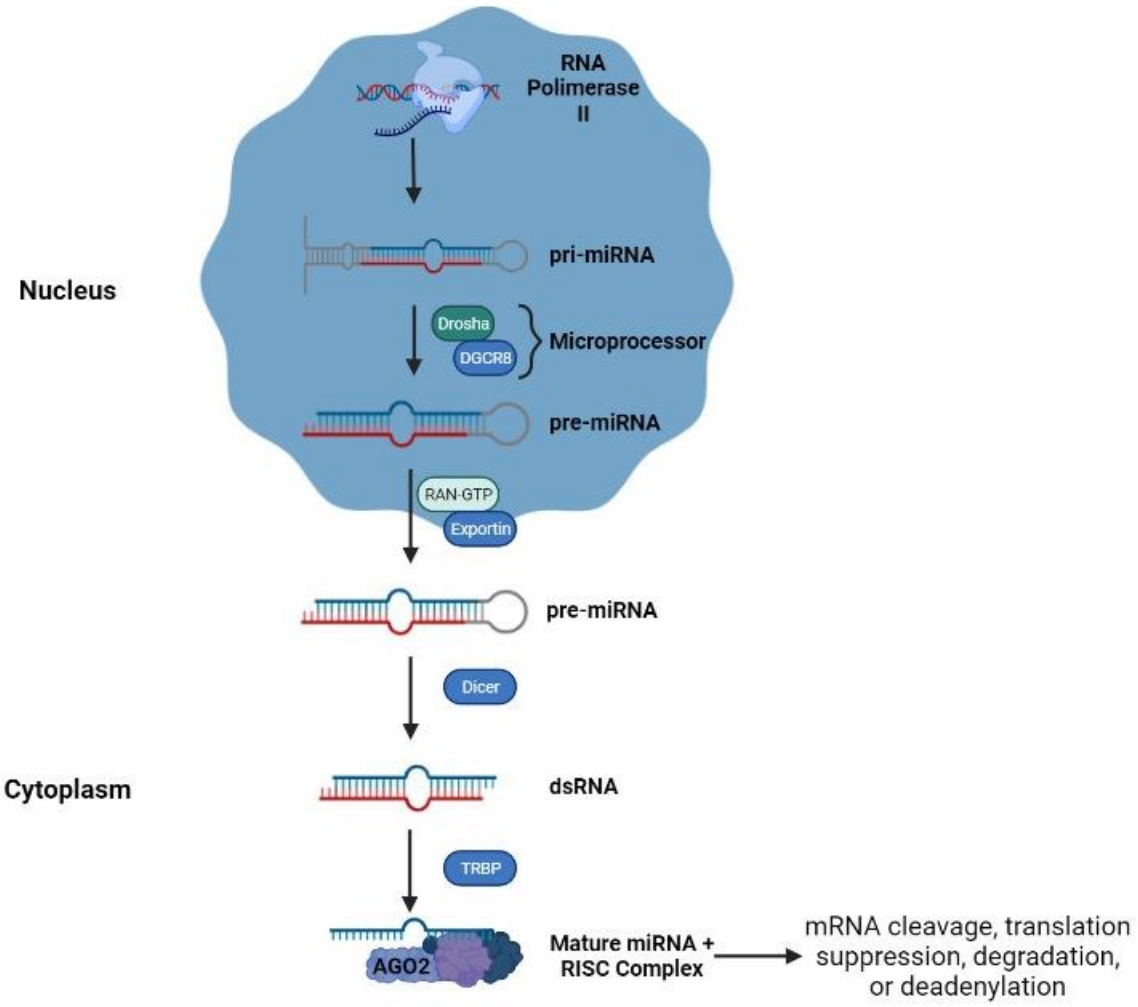

Figure 1.5. | MiRNA biogenesis. MiRNA biogenesis begins with transcription of the pri-miRNA by RNA polymerase II. This is followed by the cleavage of the pri-miRNA into a pre-miRNA by the microprocessor complex. Next, the pre-miRNA is transported to the cytoplasm in a RAN-GTP dependent-manner by a protein called exportin. In the cytoplasm, the pre-miRNA is cleaved again by the RNase III enzyme Dicer into a dsRNA. Finally, the dsRNA binds to TRBP that recruits AGO2, a major component of the RISC complex, which is responsible for the selection of the active miRNA and inducing the cleavage, translation suppression, degradation, or deadenylation of the complementary mRNA. AGO2, argonaute 2; DGCR8, DiGeorge syndrome critical region gene 8; dsRNA, double-stranded RNA; Pre-miRNA, precursor miRNA; Pri-miRNA, primary miRNA: RAN-GTP, ras-related nuclear protein-guanosine triphosphate; RISC, RNA-induced silencing complex; TRBP, trans-activation response RNA-binding protein. Adapted from (Tétreault & De Guire, 2013; Vishnoi & Rani, 2017).

1.4.1. Role of miRNAs in NAFLD pathogenesis

MiRNAs are known to play diverse roles during NAFLD progression, and its dysregulation offsets lipid metabolism, oxidative stress, fibrogenesis, cell proliferation, and apoptosis (Figure 1.6.) (He et al., 2016; Szabo & Csak, 2016). MiRNA profile changes have also been associated with transition from NAFLD to HCC (Tessitore et al., 2016). Finally, miRNAs have potential as non-invasive biomarkers in the diagnosis, staging and prognosis of NAFLD (Szabo & Csak,

2016). In this regard, different studies have established an association between an altered circulating miRNAs pattern and NAFLD progression. One study observed that, during disease progression, three major miRNAs were found dysregulated, namely miR-301a-3p, miR-34a-5p, and miR-375. Specifically, while miR-301a-3p showed a positive correlation with steatosis-to-NASH progression and cirrhosis, miR-375 presented a negative (Guo et al., 2016). More recently, another study found alterations in nine miRNAs in serum of severe NAFLD patients, which included miR-122, miR-34a, miR-21, miR-192, miR-27b, and miR-30c. In addition, miR-27b and miR-30c appeared significantly altered in both NASH and advanced fibrosis (López-Riera et al., 2018). In terms of staging, augmented circulating levels of miR-122 and miR-34a showed moderate accuracy in distinguishing NAFLD from healthy patients, and NASH from NAFL respectively (C.-H. Liu et al., 2018). Another study identified a panel composed of miR-122-5p, miR-1290, miR-27b-3p and miR-192-5p, that showed a higher diagnostic accuracy for NAFLD with more sensitivity and specificity than ALT and FIB-4 (Tan et al., 2014).

miR-122 represents 70% of the total miRNAs pool in the liver, being involved in several pathways related to FFA, TGs, and cholesterol metabolism, in part, via downregulation of both AMPK and peroxisome proliferator-activated receptor alpha (PPARα) (Dongiovanni et al., 2018; Gatfield et al., 2009; He et al., 2016). Remarkably, miR-122 and miR-192 levels have been found significantly increased in NASH patients when compared to controls, increasing by 7.2-fold and 4.4-fold respectively. In addition, miR-122 levels increased by 3.1-fold from simple steatosis to NASH. However, in the liver, miR-122 expression was significantly downregulated by 10-fold in NASH patients, compared to simple steatosis, suggesting that the liver releases high levels of miR-122 into circulation during NASH progression (Pirola et al., 2015; Szabo & Csak, 2016). Of note, other studies reported a positive correlation between serum miR-122 levels and hepatic steatosis, with miR-122 deficient mice developing steatosis and progressing towards NASH, fibrosis, and HCC. However, serum miR-122 levels may possess low specificity, as they can also be found increased in additional liver pathologies, such as ALD and chronic hepatitis C (He et al., 2016; Pirola et al., 2015). In addition, although miR-122 is significantly increased in the serum of NASH patients, its levels in patients with advanced fibrosis have not yet been elucidated, for which miR-122 may not be an ideal biomarker for NASH and, particularly, fibrosis (López-Riera et al., 2018).

MiRNA expression profiles also change in the liver during NAFLD progression. In NAFLD, several miRNAs have already been associated with development of steatosis (miR-155, miR-34a, others), fibrosis (miR-200, miR-221/222, miR34a, others), cirrhosis (miR-34a, miR-21, others) and HCC (miR-21, miR-200, others) (Tessitore et al., 2016). Most information available has been obtained from diet-induced NAFLD animal models. It should be noted though, that different NAFLD-inducing diets induce different liver miRNAs profiles (M. Zhu et al., 2018). Our group has recently shown that in a fast food (FF) diet model, miR-21 levels were increased in

the liver and muscle, and consequently, PPARα expression was downregulated (Rodrigues et al., 2017). It appears that miR-21 expression is enhanced by unsaturated fatty acids in a NF-kβ-dependent manner, playing a role in inhibiting PPARα (Loyer et al., 2016; Vinciguerra et al., 2009). Also, we found that miR-21/PPARα interaction was amplified in liver, muscle, and serum of NAFLD patients. Further, miR-21-deficient mice showed improvements in steatosis, inflammation, and fibrosis. Strikingly, miR-21 KO in mice supplemented with obeticholic acid (OCA) a farnesoid X receptor (FXR) agonist, known to induce fatty acid β-oxidation through PPARα activation, resulted in minimal steatosis, inflammation, oxidative stress, and cholesterol accumulation mainly through targeting PPARα (Rodrigues et al., 2017). More recently, our group further showed that miR-34a was increased in the muscle of NAFLD patients and mice fed three different NAFLD-inducing diets. In addition, activation of the miR-34a/SIRT1:AMPK pathway was amplified, leading to mitochondrial dysfunction. Further, we found that muscle miR-34a indirectly modulates Mfn2 through the SIRT1:AMPK pathway (Simão et al., 2019).

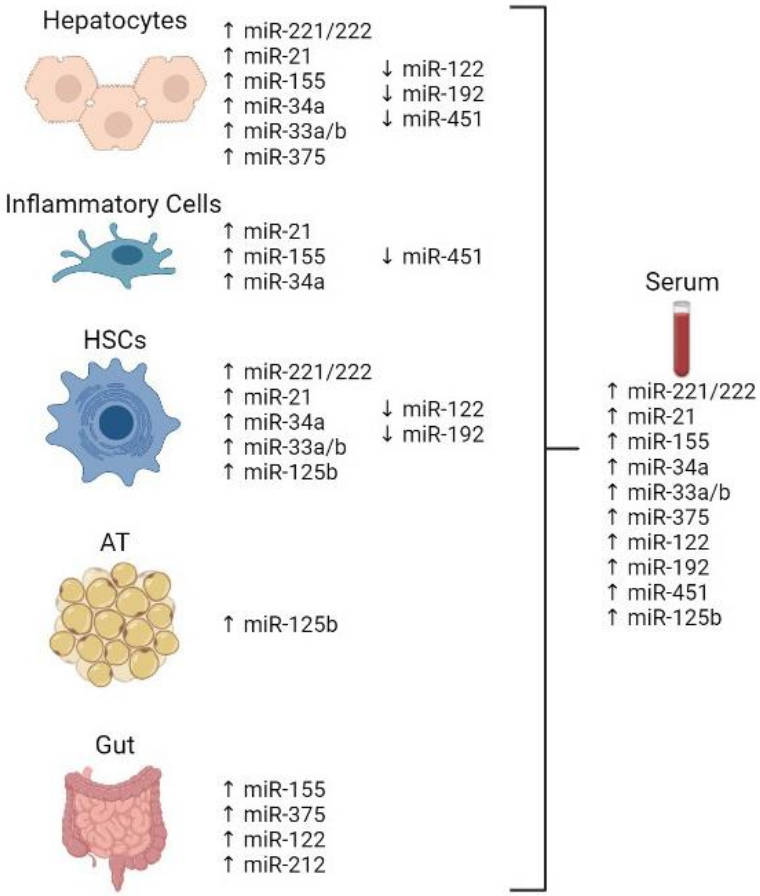

Figure 1.6. | MiRNA signatures in NAFLD. Illustration of miRNAs reported to be differently expressed in different liver cell types (hepatocytes, inflammatory cells, and HSCs) and extra-hepatic tissues (AT and gut), during NAFLD progression. MiRNAs can be secreted into circulation, serving as putative diagnostic and predictive biomarkers. AT, adipose tissue; HSC, hepatic stellate cell. Adapted from (Dongiovanni et al., 2018)

1.4.2. MiRNAs directly targeting *Mfn2*

miRNAs have been increasingly described to regulate mitochondrial function, including mitochondrial fission and fusion. Noteworthy, some miRNAs have already been described to directly target *Mfn2*, dysregulating its function (P. Li et al., 2012). MiR-106b was the first described miRNA to directly target Mfn2. Researchers found that, in insulin-resistant cultured C2C12 myotubes, miR-106b was upregulated and its ablation increased Mfn2 expression levels, resulting in improved IR. Thus, miR-106b may regulate skeletal muscle mitochondrial function and insulin sensitivity through *Mfn2* targeting (Ying Zhang et al., 2013). MiR-214 represents another miRNA directly targeting *Mfn2*. In a Huntington's disease cell model, increased expression of miR-214 inhibits *Mfn2* expression, altering mitochondrial morphology and dysregulating the cell cycle (Bucha et al., 2015). In HCC tissues, miR-761 was found upregulated and identified as a *Mfn2* direct targeting miRNA. Furthermore, inhibition of miR-761 enhanced the expression of *Mfn2* that repressed tumor growth and metastasis both *in vitro* and *in vivo* (Zhou et al., 2016).

More recently, our group showed that *Mfn2* is a direct target of miR-222-3p. Furthermore, *Mfn2* downregulation in NASH was, at least in part, due to direct modulation by miR-222-3p. In agreement, miR-222-3p inhibition in mice NASH models resulted in increased MFN2 protein levels, ameliorating steatosis, inflammation, and mitochondrial dysfunction. Thus, miR-222-3p contributes to NAFLD pathogenesis, in part, by inhibiting *Mfn2* expression (unpublished results).

1.4.2.1. MiR-222-3p

MiR-222-3p was first described in human umbilical vein endothelial cells (HUVECs) (Z. Wang et al., 2020). Human miR-222 and miR-221 form a cluster and are transcribed in the same pri-miRNA that is encoded from a gene located in chromosome Xp11.3. These two miRNAs have similar seed sequences differing in only four nucleotides (Hao et al., 2012; Jeong et al., 2017). In the liver, the miR-221/222 cluster plays an important role in regulating lipid metabolism, inflammation, and fibrosis, with its expression being found increased in the liver of NASH patients and mouse models of NAFLD. Moreover, miR-221/222 were shown to be the most upregulated miRNAs in HCC. Further, hepatic miR-221/222 deletion in MCD-fed and carbon tetrachloride (CCl4)-treated mice NASH models ameliorated liver fibrosis, lipid accumulation, and inflammation. In agreement, miR-221/222 re-expression resulted in worsening of hepatic steatosis and fibrosis. Therefore, antagomiRs against miR-221/222 effectively reduce steatosis and fibrosis in NASH mice models (Jiang et al., 2018). MiR-222-3p has also been reported to be significantly upregulated in several cancers, such as HCC,

breast, pancreatic, kidney, prostate, and thyroid cancer, and in metastatic tumors, compared to non-metastatic tumors, being responsible for tumor progression, cell proliferation, survival, and metastasis (Z. Liu et al., 2018; Y.-F. Yang et al., 2014). For instance, suppression of miR-222-3p impacts numerous pro-oncogenic pathways, tumor growth and, consequently, HCC aggressiveness (de Conti et al., 2017; Y.-F. Yang et al., 2014). Finally, miR-222-3p has been found significantly elevated in both *in vivo* and *in vitro* NAFLD models, in the liver of *ob/ob* mice, and mice fed a HF and sucrose diet. Similar observations were found in NASH patients, as well as in the AT of diabetic, and obese patients and mice models (Cheung et al., 2008; J.-J. Wang et al., 2019).

Several direct targets of miR-222-3p have already been described, such as p27, phosphatase and tensin homolog (PTEN), tissue inhibitor metalloproteinases 3 (TIMP3) among others. P27, a cell cycle inhibitor and tumor suppressor encoded in the cyclin-dependent kinase inhibitor 1B (*CDKN1B*) gene, is one of the most characterized target genes of miR-222-3p. Low levels of p27 are linked to increased tumor aggressiveness and poor patient survival. In agreement, increased expression of miR-222-3p inhibits p27 gene expression, inducing tumor growth (le Sage et al., 2007). In parallel, p27 is downregulated in HCC, associating with advanced tumor stage, lower survival, and higher proliferation (Fornari et al., 2008). *In vitro*, overexpression of miR-222-3p in HepG2 cells negatively regulates p27 expression promoting cell proliferation (Y.-F. Yang et al., 2014). Moreover, miR-222-3p directly targets tumor suppressors PTEN and TIMP3, inducing resistance to TRAIL-induced cell death and, consequently, cellular migration through protein kinase B (AKT) dephosphorylation (de Conti et al., 2017; Garofalo et al., 2009). PTEN is one of the most dysregulated tumor suppressors in human cancers and regulates the phosphoinositide 3-kinase (PI3K)/AKT pathway, whereas TIMP3 induces the activation of caspase-8 and caspase-9. Thus, targeting miR-221/222 ameliorates NASH, at least in part, through targeting TIMP3 and PTEN (Jiang et al., 2018). Furthermore, PUMA is a promoter of cell apoptosis that is also directly targeted by miR-222-3p. Inhibition of miR-222-3p reduces cell proliferation and induces apoptosis through PUMA/caspase-3 pathway activation (Z. Liu et al., 2018). In L02 cells, miR-222-3p overexpression leads to increased triglyceride accumulation, through inhibition of acyl-Coenzyme A oxidase 1 (ACOX1), a key enzyme in fatty acid β-oxidation (J.-J. Wang et al., 2019). In a murine model of biliary atresia, miR-222-3p directly suppresses protein phosphatase 2 regulatory subunit B alpha (PPP2R2A) expression, increasing AKT activation and HSCs activation. Thus, upregulation of PPP2R2A through miR-222-3p suppression may improve liver fibrosis (Dong et al., 2015; Shen et al., 2014).

1.5. Therapeutic approaches for NAFLD

Currently, there are no pharmacological therapies approved by the U.S. Food and Drug Administration (FDA) or the European Medicines Agency (EMA) to prevent or treat NAFLD/NASH (Ferguson & Finck, 2021; Mantovani & Dalbeni, 2021). Therefore, the first-line therapy is based on lifestyle modifications in diet, including the Mediterranean diet, low-fat diet, or low-carbohydrate diet, and increased physical activity to promote weight loss (David & Eapen, 2021). Weight loss associated with these interventions is associated with improvements in hepatic IR and liver fat accumulation (Carneros et al., 2020). Of note, a weight reduction of ≥ 10% leads to NASH resolution and fibrosis regression by at least one stage. Accordingly, the EASL, the European Association for the Study of Diabetes (EASD)and the European Association for the Study of Obesity (EASO), as well as the AASLD practice guidelines recommend that, in overweight/obese NAFLD patients, the first main goal is a weight loss of 5%-10%, known to produce improvements in steatosis and NASH resolution (EASL et al., 2016; Lonardo et al., 2021; Moore et al., 2020). To achieve this, guidelines recommend hypocaloric diets that induce an energy deficit of 500-1000 kcal/day and avoid alcohol, smoking, and fructose-containing drinks, along with a moderate-intensity aerobic exercise of 150-200 min/week (El-Agroudy et al., 2019). From the several diets tested in patients with NAFLD, the Mediterranean diet appears to be the one most capable of reducing liver fat and improving the metabolic profile, reducing the risk of T2DM and cardiovascular disease (Mantovani & Dalbeni, 2021). This diet is mainly characterized by a high intake of vegetables, monounsaturated and ω-3 fatty acids, with the total fat representing around 35% of the daily energy consumption (Lonardo et al., 2021; Mundi et al., 2020). In turn, exercise has been shown to improve hepatic insulin sensitivity and intrahepatic TG content even in the absence of weight loss (Carneros et al., 2020). However, not all patients commit at 100% to a healthy diet and regular exercise, and in some cohorts of patients, including older individuals, lifestyle modifications are not able to produce the same impact (Mantovani & Dalbeni, 2021).

Then, pharmacotherapies should be considered, especially for NASH patients with significant fibrosis, stage ≥ 2, and for patients with a high risk of fibrosis progression (EASL et al., 2016; Sumida & Yoneda, 2018). For a pharmacological agent to be considered beneficial for NAFLD/NASH, phase III clinical trials must reach one of these two endpoints: resolution of NASH without worsening of fibrosis; or improvement in fibrosis without worsening NASH. Due to the close association between NAFLD and metabolic features, many drugs already prescribed for metabolic syndrome conditions, such as T2DM, are in advanced clinical trials for NAFLD/NASH treatment (Ferguson & Finck, 2021). Pioglitazone, OCA, and Vitamin E are the only agents that, despite no approval, are recommended by the EASL-EASO-EASD and

the AASLD practice guidelines to be used in patients with NASH in “off-label” conditions (Mantovani & Dalbeni, 2021).

Pioglitazone is a thiazolidinedione insulin sensitizer already used to treat T2DM, that targets the nuclear receptor PPARγ. It seems to be beneficial for NAFLD, inducing resolution of NASH with improvements in liver fat content, insulin sensitivity, inflammation, and hepatocyte degeneration without worsening fibrosis (Ferguson & Finck, 2021). However, pioglitazone appears not to have a strong positive effect on fibrosis and leads to weight gain and bone fractures. Despite no official approval by most national medicines agencies, clinical guidelines recommend its use in patients with NASH with or without T2DM (David & Eapen, 2021).

OCA is a synthetic activator of FXR, clinically approved for treatment of primary biliary cholangitis and currently in phase III clinical trials for NASH (Sumida & Yoneda, 2018). OCA is known to regulate lipid and bile acids metabolism, modulating an anti-inflammatory and anti-fibrotic response. In phase IIb trials, OCA administration improved insulin sensitivity, liver fibrosis, inflammation, body weight loss, and NASH histological features in NAFLD patients. However, there are concerns about the worse lipid profile due to increased low-density lipoprotein (LDL) cholesterol levels, decreased high-density lipoprotein (HDL) cholesterol and triglycerides levels, especially in treatments at higher doses (Abenavoli et al., 2018; Malnick et al., 2020).

Finally, vitamin E, a potent antioxidant, showed significant improvements in serum liver enzymes and NASH histological features, including steatosis, inflammation, and hepatocyte ballooning, in a clinical trial used at a dose of 800 U/day. However, high vitamin E dosages might lead to hemorrhagic stroke or prostate cancer. As such, and due to insufficient investigation in NAFLD patients with T2DM, this antioxidant is only recommended to use in NASH non-diabetic patients (David & Eapen, 2021; Sumida & Yoneda, 2018).

Additional potential pharmacological approaches for NAFLD are under investigation, including metformin, glucagon-like peptide-1 (GLP-1) agonists, sodium-glucose co-transporter-2 (SGLT-2) inhibitors, PPARα-PPARγ-peroxisome proliferator-activated receptor delta (PPARδ) activators, thyroid hormone receptor beta (THRβ) agonists, and more (Table 1.2.) (David & Eapen, 2021).

Because targeting a single signalling pathway might not be effective to improve all NAFLD/NASH histological features and metabolic conditions, the development of combinational therapies that target the multiple pathways involved in NASH pathogenesis has been surging (Friedman et al., 2018). In this regard, miRNAs are attractive therapeutic options, due to their ability to regulate different genes. However, its application still presents some challenges, such as off-targeting effects and low serum stability. Currently, there are no miRNA-based therapies for NAFLD in clinical trials (Gjorgjieva et al., 2019). Nevertheless, several miRNA mimics and anti-miRNAs are in phase I or II trials for HCV infection, cancers,

and cardiovascular diseases (Su et al., 2018). For example, miravirsen, a miR-122 inhibitor, is in phase II clinical trials for patients with HCV-infection, being able to reduce viral RNA (Gjorgjieva et al., 2019). Also, MRG-201 (miRagen Therapeutics) is a miR-29 mimic that inhibits the expression of collagen and fibrotic proteins in phase I clinical trial for systemic sclerosis. If successful, it might become useful in other fibrotic conditions, such as liver fibrosis and NASH.

Table 1.2. | NAFLD therapy procedures/agents and their characteristics and recommendations according to EASL-EASD-EASO and AASLD guidelines. BMI, body mass index; FXR, farnesoid X receptor; GLP-1, glucagon-like peptide-1; LDL, low-density lipoprotein; NAS, NAFLD activity score; NAFLD, non-alcoholic fatty liver disease; NASH, non-alcoholic steatohepatitis; OCA, obeticholic acid; PPARγ, peroxisome proliferator-activated receptor gamma; SGLT-2, sodium-glucose co-transporter-2; T2DM, type 2 diabetes mellitus. Adapted from (David & Eapen, 2021; Mantovani & Dalbeni, 2021).

Therapy	Mechanism of action	Primary Endpoint	Side Effects	Recommendations
Diet	-	7%-10% total weight loss Improvements in steatosis and NASH resolution	-	Hypocaloric diets containing a 500-1000 kcal/day deficit with preferences to a Mediterranean diet, low-fat diet, or low-carbohydrate diet. Limit alcohol consumption and smoking
Excercise	-	7%-10% total weight loss Improvements in steatosis and NASH resolution	-	Moderate-intensity aerobic exercise of 150-200 min/week, in 3-5 sessions
Pioglitazone	PPARγ agonist	Improvement in NAS >2 without fibrosis worsening	Weight gain (2%-4%) Bone fractures Bladder cancer	Not yet approved outside T2DM, but recommended in patients with NASH with/without T2DM
OCA	FXR synthetic ligand	Resolution of NASH without worsening of fibrosis Improvement of fibrosis without worsening of NASH	Pruritus Increased LDL and cholesterol levels	Might be considered in NASH patients
Vitamin E	Antioxidant	Improvement in NAS >2 without fibrosis worsening	Hemorrhagic stroke Prostate cancer Headache Blurred vision	Might be considered in patients with NASH without T2DM

Metformin	AMPK-dependent	Small beneficial effects on liver steatosis and inflammation, and no effects on liver fibrosis and NASH resolution	Diarrhea Nausea Vomiting	Not recommended for NAFLD treatment
GLP-1 (liraglutide and semaglutide)	GLP-1 receptor agonists	Resolution of NASH with no effects on liver fibrosis Improvement of liver steatosis and hepatocyte ballooning	Loss of appetite Nausea Diarrhea	Premature to consider in NASH patients
SGLT-2 (dapagliflozin, empagliflozin...)	SGLT-2 inhibitors	Improvement of serum liver enzymes and liver fat content	Genitourinary infections Diabetic ketoacidosis Hypotension	Premature to consider in NASH patients
Bariatric Surgery	Restrict the amount of food the stomach can hold and/or promote the malabsorption of nutrients	Weight loss Resolution of NASH with improvements in fibrosis	Worsening of NAFLD features in some patients	Performed in patients with T2DM or severe obesity (BMI >35 kg/m^2)
AntagomiR-103/107	-	-	-	Interrupted in 2017

Chapter 2 | Objectives

The research conducted under this thesis was guided by the hypothesis that miR-222-3p plays an active, pathogenic role in NAFLD progression, at least in part, through direct modulation of *Mfn2*. Three main objectives were designed to test our hypothesis. First, we sought to validate an *in vivo* diet-induced NAFLD model, based on the MCD diet. Next, we aimed to elucidate whether miR-222-3p activation represents a key, primary event in NAFLD *in vivo* and to investigate whether targeting miR-222-3p could ameliorate disease progression. Finally, we aimed to unravel the impact of *Mfn2* in mediating the beneficial effects of the miR-222-3p inhibition.

Specifically, the main objectives in this thesis were to:

1. Characterize and validate a diet-induced NAFLD mouse model, based on the MCD diet combined with HFD supplemented with 0.1% L-methionine.
2. Elucidate whether miR-222-3p activation represents a key, primary event in an *in vivo* experimental NAFLD model and determine whether targeting miR-222-3p, through antagomiR-222-3p treatment, could ameliorate disease progression.
3. Unravel the role of *Mfn2* in mediating the ameliorating effects of miR-222-3p silencing, using liver-specific *Mfn2* KO mice.

Chapter 3 | Materials and Methods

3.1. NAFLD animal models and antagomiR treatment

C57BL6 mice were provided by Dr. António Zorzano (Complex Metabolic Diseases and Mitochondria, IRB, Barcelona, Spain). 10-week old C57BL6 male mice were fed either a control diet (n=19) or a MCD diet combined with a HFD and supplemented with 0.1% L-methionine on drinking water (n=21) for 3 weeks. In parallel, to investigate the therapeutic effects of silencing miR-222-3p, control and MCD-fed mice received 3 subcutaneous injections once a day for 3 consecutive days of either antagomiR-222-3p at 16 mg/kg body weight (n=9+10) (Qiagen, Hilden, Germany) or phosphate buffer saline (PBS) (n=10+11), prior to starting the diets (Figure 3.1). To study if any potential therapeutic effects are dependent on *Mfn2*, liver-specific *Mfn2* KO (Mfn2 KO) mice were generated after crossing ALB-Cre mice with *Mfn2*$^{loxp/loxp}$ mice (Hernández-Alvarez et al., 2019). Mfn2 KO mice were fed either a control diet (n=16) or a MCD diet (n=20) and treated with antagomiR-222-3p (n=8+10) or PBS (n=8+10), as control (Figure 3.1). At the indicated timepoints, animals were fasted for 4 hours, anesthetized using isoflurane, and then sacrificed by cervical dislocation. The left lateral liver lobe was removed, rinsed in normal saline, and immediately flash-frozen in liquid nitrogen for RNA and protein extraction. All animal experiments were carried out with the permission of the local animal ethical committee in accordance with the EU Directive (2010/63/EU), Portuguese law (DL 113/2013) and all relevant legislations. The experimental protocol was approved by Direcção Geral de Alimentação e Veterinária, Portugal. Animals received humane care in a temperature-controlled environment with a 12h light-dark cycle, complying with the Institute's guidelines, and as outlined in the "Guide for the Care and Use of Laboratory Animals" prepared by the National Academy of Sciences and published by the National Institutes of Health (NIH publication 86-23 revised 1985). All experiments were performed by an investigator accredited for directing animal experiments (FELASA level C).

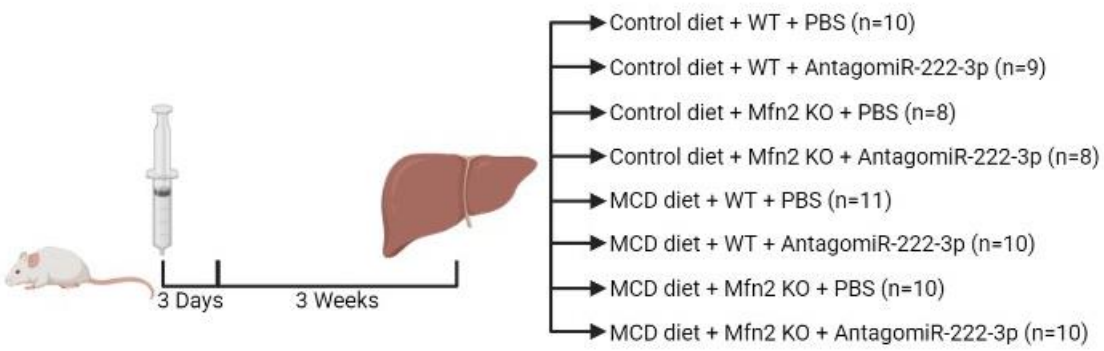

Figure 3.1. | Schematic overview of the animal model. MCD, methionine and choline-deficient; Mfn2 KO, liver-specific mitofusin 2 knock-out; PBS, phosphate buffer saline; WT, wild-type.

3.2. RNA extraction and RT-qPCR

Total RNA was extracted using TRIzol™ reagent (Thermo Fisher Scientific, Waltham, MA, USA) according to the manufacturer's instructions. RNA was eluted in 100 µL of RNase-free water and quantified using the Qubit™ RNA BR Assay Kit (Thermo Fisher Scientific, Waltham, MA, USA). Then, 1 µg of RNA was reverse transcribed with random hexamers by reverse transcription-polymerase chain reaction (RT-PCR) using NZY Reverse Transcriptase (Nzytech, Lisboa, Portugal), following the protocol recommended by the manufacturer, optimized for using 0.5 µL of NZY Reverse Transcriptase. The incubation steps were run on an Applied Biosystems 7300 Real-Time PCR System (Applied Biosystems, Thermo Fisher Scientific) using the conditions described in Table 3.1. cDNA was diluted in 20 µL of nuclease-free water (1:2). Real-Time PCR (qPCR) was performed using 2x Power SYBR Green PCR Master Mix (Thermo Fisher Scientific) in a QuantStudio™ 7 Flex Real-Time PCR System (Applied Biosystems, Thermo Fisher Scientific) following the program described in Table 3.1. For each gene, two duplicate reactions *per* sample were performed, with a total volume of 5 µL each, consisting of 2.5 µL of 2x Power SYBR Green PCR Master Mix, 2 µL of cDNA, 0.6 µM of each primer (Table 3.2), and nuclease-free water. Gene expression levels were quantified based on its standard curve and normalized to the level of hypoxanthine-guanine phosphoribosyltransferase (HPRT) and expressed as fold change from controls. To quantify miR-222-3p expression, TaqMan® Small RNA Assays (Applied Biosystems, Thermo Fisher Scientific) were used accordingly to manufacturer's specifications in a QuantStudio™ 7 Flex Real-Time PCR System (Applied Biosystems, Thermo Fisher Scientific). The incubation steps were followed as described in Table 3.1. The relative amount of miR-222-3p was normalized with U6 small nuclear RNA (snRNA), determined by the threshold cycle ($2^{-\Delta\Delta CT}$) method, where $\Delta\Delta CT = (C_{TmiR\text{-}222\text{-}3p} - C_{TU6})$ sample - $(C_{TmiR\text{-}222\text{-}3p} - C_{TU6})$ calibrator.

Table 3.1. | Incubation steps performed in RT-qPCR protocols. RT, reverse transcription; qPCR, real-time polymerase chain reaction.

Protocol	Step	Temperature (°C)	Time
RT (SYBR Green)	1	25	10 min
	2	50	50 min
	3	85	5 min
qPCR (SYBR Green)	1	95	2 min
	2 (×40 cycles)	95	5 sec
		60	30 sec
	3	95	15 sec
	4	60	1 min
	5	95	15 sec

RT (TaqMan)	1	16	30 min
	2	42	30 min
	3	85	5 min
qPCR (TaqMan)	1	95	10 min
	2 (×40 cycles)	95	15 sec
		60	1 min

Table 3.2. | Primer sequences used in qPCR. *CD36*, fatty acid translocase; *CDKN1B*, cyclin-dependent kinase inhibitor 1B; *Clec4f*, c-type lectin domain family member f; *F4/80*, adhesion G protein-coupled receptor; *HO-1*, heme oxygenase-1; *IL-1β*, interleukin-1 beta; ; *IL-8*, interleukin-8; *Mfn2*, mitofusin 2; *NLRP3*, nod-like receptor protein 3; *PPARγ*, peroxisome proliferator-activated receptor gamma; *TGF-β*, transforming growth factor-beta; *TLR4*, toll-like receptor 4; *TNF-α*, tumor necrosis factor-alpha; *α-SMA*, alpha-smooth muscle actin.

Gene	Primer Forward	Primer Reverse
CDKN1B	5'-ATG TTT CAG ACG GTT CCC CG-3'	5'-CTT AAT TCG GAG CTG TTT ACG TCT G-3'
Mfn2	5'-CAG AGC AGA GCC AAA CTG CT-3'	5'-AAC ATG TTG AGT TCG CTG TCC-3'
IL-8	5'-GCT ACG AAC TGC CTG ACG G-3'	5'-GCT GTT ATA GGT GGT TTC GTG GA-3'
IL-1β	5'-TGC CAC CTT TTG ACA GTG ATG-3	5'-TGA TGT GCT GCT GCG AGA TT-3'
TNF-α	5'-AGG CAC TCC CCC AAA AGA TG-3'	5'-TGA GGG TCT GGG CCA TAG AA-3'
TLR4	5'-TCC CTG CAT AGA GGT AGT TCC TA-3'	5'-CTT CAA GGG GTT GAA GCT CAG-3'
NLRP3	5'-AGA GCC TAC AGT TGG GTG AAA TG-3'	5'-CCA CGC TAC CAG GAA ATC TC-3'
TGF-β	5´-CTG CTG ACC CCC ACT GAT AC-3'	5'-GTG AGC GCT GAA TCG AAA GC-3'
Collagen 1α1	5'-CTG ACT GGA AGA GCG GAG AG-3'	5'-GAC GGC TGA GTA GGG AAC AC-3'
α-SMA	5'-CTG CTG ACC CCC ACT GAT AC-3'	5'-GTC AGC GCT GAA TCG AAA GC-3'
HO-1	5'-CGG GCC AGC AAC AAA GTG-3'	5'-AGT GTA AGG ACC CAT CGG AGA A-3'
Clec4f	5'-GAGGCCGAGCTGAACAGAG-3'	5'-TGTGAAGCCACCACAAAAAGAG-3'
F4/80	5'-GCATCATGGCATACCTGTTC-3'	5'-GAGCTAAGGTCAGTCTTCCT-3'
Albumin	5'-TGCTTTTTCCAGGGGTGTGTT-3'	5'-TTACTTCCTGCACTAATTTGGCA-3'
CD36	5'-GTCTATCTACGCTGTGTTCG-3'	5'-ACAGGCTTTCCTTCTTTGC-3'
PPARγ	5'-CTCACAATGCCATCAGGT-3'	5'-GCTGGTCGATATCACTGG-3'

3.3. Protein extraction

Liver tissue was homogenized using a motor-driven tissue homogenizer in ice-cold lysis buffer (10 mM Tris-HCl, pH 7.6, 5 mM MgCl2, 1.5 mM potassium acetate, 1% Nonidet P-40), 1× Halt Protease and Phosphatase Inhibitor Cocktail (Pierce, Thermo Fisher Scientific) and 2 mM Dithiothreitol (DTT). After sonication, to remove cell debris, the homogenate was centrifuged at 3,200 × g for 10 min at 4 ºC. Then, the supernatant was collected and stored at

-80 ºC. Total Protein concentration was determined using the Bio-Rad protein assay kit (Bio-Rad Laboratories, Hercules, CA, USA), following the manufacturer's instructions.

3.4. Immunoblot analysis

Forty µg of total protein extract was separated on a 10% or 12% sodium dodecyl sulfate-polyacrylamide gel electrophoresis (SDS-PAGE) and transferred onto a nitrocellulose membrane. The membrane was blocked with a 5% milk solution for 30 min and incubated overnight at 4 ºC with primary mouse monoclonal antibodies against MFN2 (1:1000; ab56889, Abcam PLC, Cambridge, United Kingdom), p27 (1:200; sc-1641, Santa Cruz Biotechnology, Dallas, Texas, USA), PTEN (1:1000; sc-7974, Santa Cruz Biotechnology) and β-actin (1:40000 A5441, Sigma-Aldrich Co, St. Louis, MO, USA), used as a loading control. Membranes were then incubated with secondary anti-mouse antibodies conjugated with horseradish peroxidase (1:5000, Bio-Rad Laboratories) for 2h. Finally, membranes were processed for protein detection using the Immobilon Western Chemiluminescent HRP Substrate (Sigma-Aldrich Co.) and developed in a ChemiDoc XRS+ System (Bio-Rad Laboratories) or an iBright™ FL1500 Imaging System (Thermo Fisher Scientific). Then, data were analysed using the Image Lab™ analysis software and iBright™ Analysis Software respectively.

3.5. Total ROS levels

To quantitate intracellular ROS levels, we used the nonfluorescent cell-permeant 2', 7'-dichlorodihydrofluorescein diacetate (H_2DCFDA, Sigma-Aldrich Co.), that is converted to fluorescent 2', 7'-dichlorofluorescein (DCF) by ROS. 10 mg of liver tissue was homogenized in 500 µL of ice-cold PBS followed by centrifugation at 10,200 × g for 5 min at 4 ºC to remove insoluble particles. The supernatant was recovered and 50 µL of each sample was incubated with an H_2DCFA probe at a final concentration of 10 µM for 15 min at room temperature (RT), protected from light. Results were normalized to the total protein of each sample. Fluorescence (Ex/Em: 492-495/517-527 nm) was measured using the GloMax-Multi+ Detection System (Promega Corporation, Madison, WI, USA).

3.6. Quantification of free fatty acids and triglycerides

Thirty mg of liver tissue were used to quantify the amount of TG by measuring the oxidized glycerol converted from TG using the Triglyceride Quantification Kit (MAK266, Sigma-Aldrich Co.) according to the manufacturer's instructions. The concentration of fatty acids (C8 and longer) was determined in 10 mg of liver tissue using the Free Fatty Acid Quantitation Kit (MAK044, Sigma Aldrich Co.) following the manufacturer's protocol. Colorimetric

measurements in both protocols were performed using a Varioskan LUX Multimode Microplate Reader (Thermo Fisher Scientific) and results normalized to the starting liver weight.

3.7. Statistical analysis

Data were analysed using GraphPad Prism 5 software (GraphPad Software, Inc., San Diego, CA, USA). Data were tested for normal Gaussian distribution through the Shapiro-Wilk and Kolmogorov-Smirnov normality tests. In comparison between two groups, data was statistically analysed using the Student's t-test. Between three or more groups was used the one-way analysis of variance (ANOVA) with Tukey's post hoc test or Kruskal-Wallis non-parametric ANOVA with Dunn's post hoc test for data following a Gaussian distribution or a non-Gaussian distribution, respectively. All data are presented as mean ± standard error of the mean (S.E.M). Values of at least $p < 0.05$ were considered statistically significant.

Chapter 4 | Results

4.1. MiR-222-3p is increased in the liver of MCD-fed mice and the expression of direct targets of miR-222-3p increases upon antagomiR-222-3p treatment

Recent studies reported increased expression of the miR-221/222 cluster in the liver of NASH patients and mouse models of NAFLD (Jiang et al., 2018). In parallel, our group has found that liver miR-222-3p expression levels are significantly increased in four different dietary murine models of NAFLD in comparison to the respective controls (unpublished results). So, in the present study, we first sought to evaluate the levels of liver miR-222-3p in mice fed a modified MCD diet. In accordance with previous results, we observed that miR-222-3p expression was significantly upregulated in MCD-fed wild-type (WT) mice compared with controls ($p < 0.001$) (Figure 4.1A).

Subsequently, we sought to validate miR-222-3p inhibition upon antagomiR-222-3p treatment by analysing expression levels of miR-222-3p direct targets *CDKN1B* (p27) and PTEN. *CDKN1B* mRNA expression and p27 protein levels were increased in the livers of MCD-fed mice treated with antagomiR-222-3p compared to control-injected MCD-fed mice, confirming miR-222-3p inhibition (Figure 4.1B). In addition, protein levels of PTEN, another well-described direct target of miR-222-3p, were also upregulated in mice fed the MCD diet and treated with antagomiR-222-3p (Figure 4.1C).

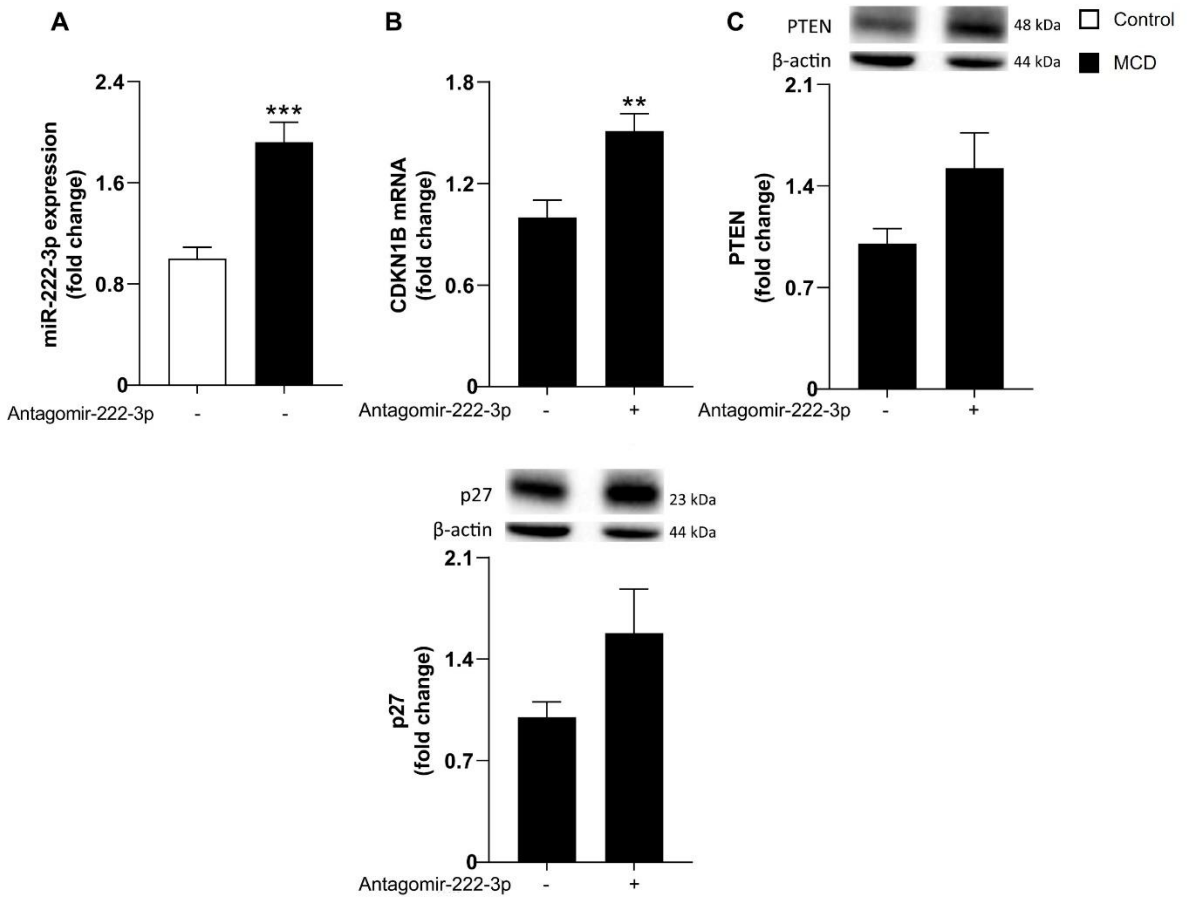

Figure 4.1: Liver miR-222-3p expression is increased in MCD-fed mice and targets *CDKN1B* (p27) and PTEN. 10-week old C57BL/6 male mice were fed either a control diet (n=10; white bars) or a MCD diet (n=21; black bars) for 3 weeks. MCD-fed mice were treated subcutaneously with PBS (n=11) or antagomiR-222-3p (n=10), as described in Material and Methods. **A.** RT-qPCR analysis of miR-222-3p. **B.** RT-qPCR analysis of *CDKN1B* and immunoblotting of p27. **C.** Immunoblotting of PTEN. Blots were normalized to endogenous β-actin. Data are expressed as mean ± S.E.M fold change. $^{**}p < 0.01$ and $^{***}p < 0.001$.

4.2. *Mfn2* is decreased in the liver of MCD-fed mice and increases upon antagomir-222-3p treatment

In a study that our group collaborated on, *Mfn2* was described to be significantly downregulated in a HFD-induced NASH mouse model (Hernández-Alvarez et al., 2019). Following this, our laboratory elucidated the role of *Mfn2* in several other NASH mouse models and showed that MFN2 protein expression was significantly downregulated in the liver of all of them (unpublished results). Herein, our results show that MFN2 protein levels are decreased in MCD-fed mice (Figure 4.2A). Of note, *Mfn2* mRNA levels were not as significantly decreased, suggesting that *Mfn2* might undergo post-transcriptional modifications, namely by miRNAs (Figure 4.2B).

Noteworthy, our group has previously validated that miR-222-3p directly targets *Mfn2 in vitro* (unpublished results). The results presented in this Thesis support this interaction to occur

also *in vivo*, as the decreased MFN2 protein levels in MCD-fed WT mice (Figure 4.2) negatively correlate to corresponding miR-222-3p expression levels (Figure 4.1A). Interestingly, MCD-fed WT mice treated with antagomiR-222-3p displayed increased levels of MFN2 protein but not *Mfn2* mRNA, comparing with mice injected with PBS only (Figure 4.2), suggesting that *Mfn2* is post-transcriptionally regulated, at least in part, by the direct interaction with miR-222-3p and consequently confirming once again the effectiveness of the antagomiR-222-3p. Last but not least, and as expected, Mfn2 KO mice displayed minimal *Mfn2* mRNA and protein expression levels (at least $p < 0.01$ versus corresponding WT controls). The residual *Mfn2* expression might be due to *Mfn2* still being expressed in liver cells other than hepatocytes.

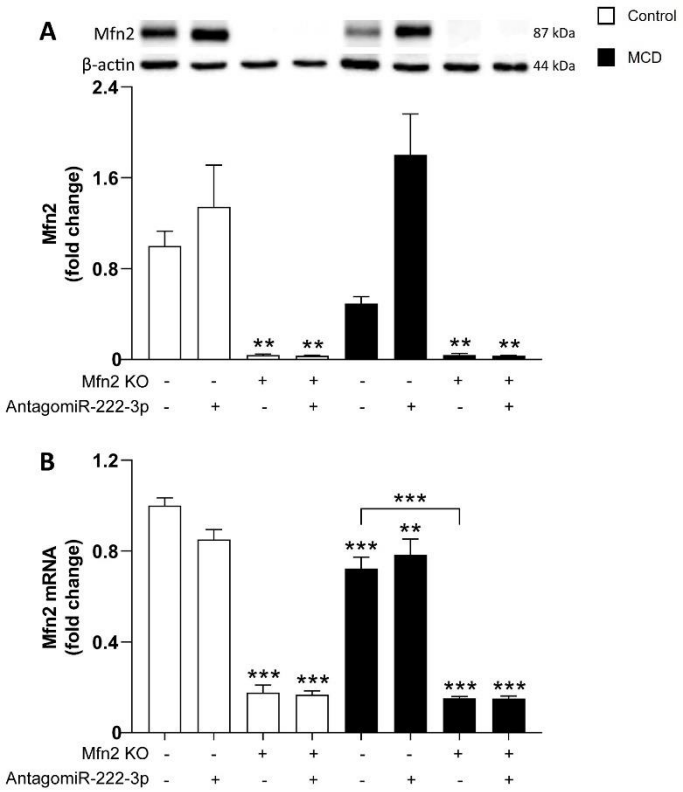

Figure 4.2: Liver *Mfn2* expression is inhibited in MCD-fed mice and increases upon antagomiR-222-3p treatment. 10-week old C57BL/6 male WT or Mfn2 KO mice were fed either a control diet (n=35; white bars) or a MCD diet (n=41; black bars) for 3 weeks. Control and MCD-fed mice were treated subcutaneously with PBS (n=10+8+11+10) or antagomiR-222-3p (n=9+8+10+10) as described in Material and Methods. **A.** Immunoblotting of MFN2. Blots were normalized to endogenous β-actin. **B.** RT-qPCR analysis of *Mfn2*. Data are expressed as mean ± S.E.M fold change. $^{**}p < 0.01$ and $^{***}p < 0.001$.

4.3. AntagomiR-222-3p treatment counteracts MCD-induced inflammation

The MCD diet animal model of NAFLD has been extensively studied, including by us, to induce the development of different degrees of NASH histopathological features, including steatosis, fibrosis, and inflammation (Rodrigues et al., 2017; Simão et al., 2019) (unpublished

results). In this study, MCD diet-fed WT mice displayed significant increases in hepatic pro-inflammatory cytokines mRNA expression, including *IL-8*, *IL-1β*, *TNF-α*, *TLR4*, and *NLRP3* ($p < 0.001$ comparing with control-fed WT, except for *IL-8*). In turn, miR-222-3p inhibition counteracted the MCD-induced inflammation, resulting in a significant decrease of pro-inflammatory cytokines hepatic expression (Figure 4.3). Unexpectedly, miR-222-3p inhibition only slightly less significantly prevented the increase of pro-inflammatory cytokines in MCD-fed Mfn2 KO mice, in comparison to the control-injected MCD-fed Mfn2 KO mice. Overall, these results indicate that miR-222-3p plays a role in NASH progression, more specifically in promoting hepatic inflammation, but in a broad view, independently of *Mfn2* liver expression.

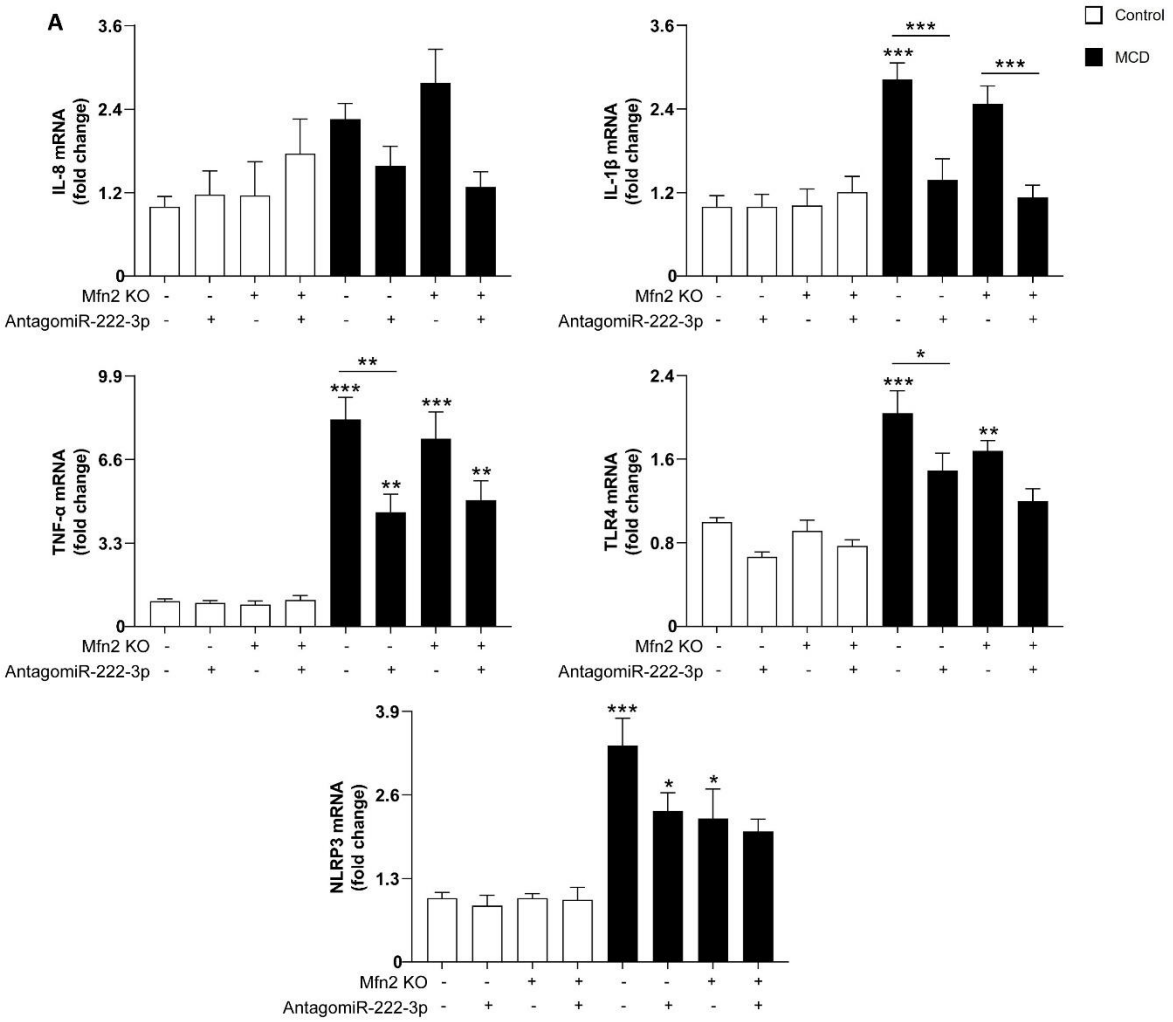

Figure 4.3: MiR-222-3p inhibition ameliorates MCD-induced inflammation. RT-qPCR analysis of *IL-8*, *IL-1β*, *TNF-α*, *TLR4* and *NLRP3*. Data are expressed as mean ± S.E.M fold change. *$p < 0.05$ **$p < 0.01$ and ***$p < 0.001$.

4.4. AntagomiR-222-3p treatment counteracts MCD-induced fibrosis

Like the inflammatory mRNA profile, MCD diet-fed WT mice also exhibited significantly increased expression levels of fibrosis markers *TGF-β*, *collagen-1α1*, and *α-SMA* (at least $p < 0.05$). Remarkably, mice treated with antagomiR-222-3p ameliorated MCD-induced fibrosis, as reflected by a significant decrease in the expression of all pro-fibrogenic factors ($p < 0.01$ comparing with MCD-fed WT, except for *α-SMA*) (Figure 4.4). Mfn2 KO mice fed the MCD diet and treated with antagomiR-222-3p also show decreased expression levels of hepatic fibrosis signals compared to their respective control-injected mice, again, only slightly less when compared with WT animals in the same conditions, suggesting that miR-222-3p also contributes to the development of fibrosis during NAFLD progression in mice, but not through a *Mfn2*-dependent manner.

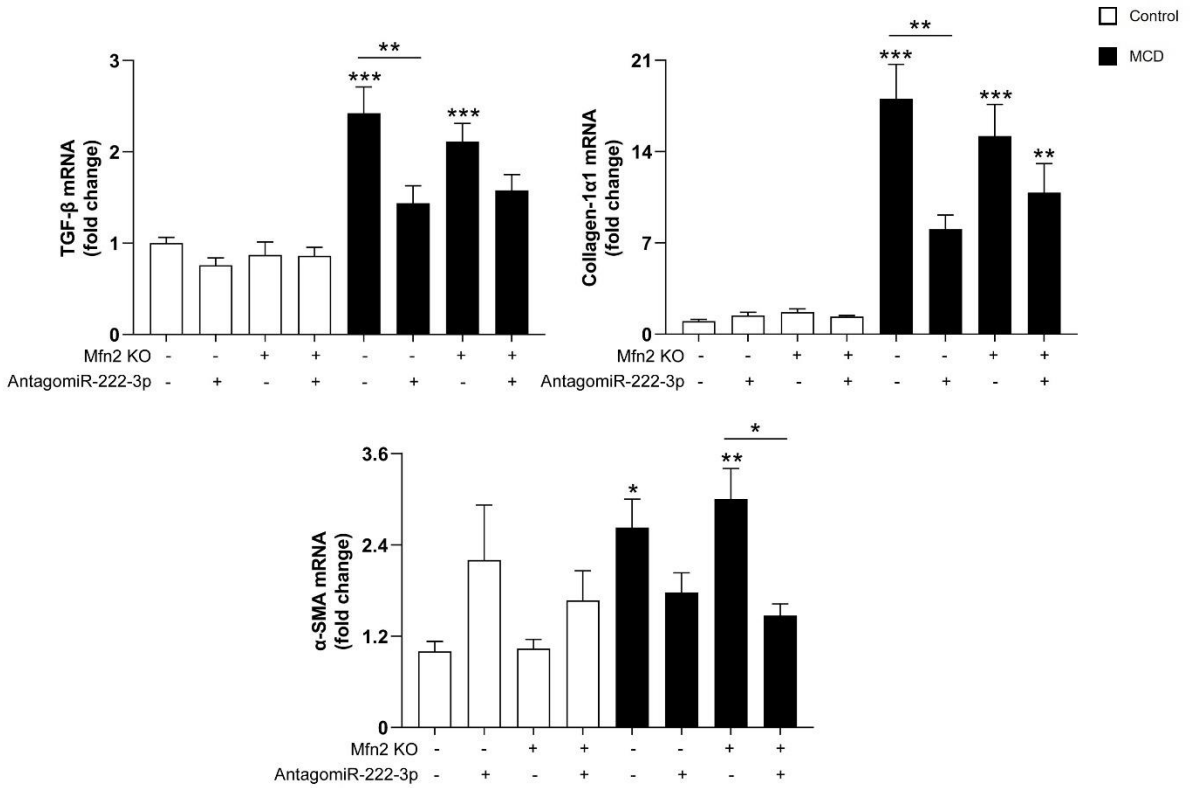

Figure 4.4: MiR-222-3p inhibition ameliorates MCD-induced fibrosis. RT-qPCR analysis of *TGF-β*, *collagen-1α1* and *α-SMA*. Data are expressed as mean ± S.E.M fold change. *$p < 0.05$ **$p < 0.01$ and ***$p < 0.001$.

4.5. AntagomiR-222-3p treatment counteracts MCD-induced oxidative stress

In agreement with previous results, ROS levels were also significantly elevated in MCD-fed WT mice, compared with control diet-fed mice ($p < 0.01$) (Figure 4.5A). In parallel, ROS regulator heme oxygenase-1 (*HO-1*) mRNA expression was also significantly upregulated in mice fed the MCD diet ($p < 0.01$) (Figure 4.5B). MCD-fed WT mice treated with antagomiR-

222-3p exhibited significantly decreased ROS production and *HO-1* expression, compared to control-injected MCD-fed WT mice, returning to values of the same magnitude as control diet mice (at least $p < 0.05$) (Figure 4.5).

Liver Mfn2 KO mice have been reported to develop ER stress and ROS production in the mitochondria (Muñoz et al., 2013; Sebastian et al., 2012). Our results showed that, under the control diet, liver Mfn2 KO mice presented with a moderate increase in ROS production. However, no augmented production was observed in MCD-fed mice. In fact, ROS and *HO-1* mRNA levels were slightly reduced in MCD-fed Mfn2 KO mice compared with MCD-fed WT mice. This may, at least partially, explain why antagomiR-222-3p-mediated inhibition of ROS and *HO-1* mRNA levels in Mfn2 KO mice is not statistically significant, contrary to what is observed in WT mice, without meaning that *Mfn2* is involved in antagomiR-222-3p-dependent protective effects. More studies will be needed to elucidate these findings.

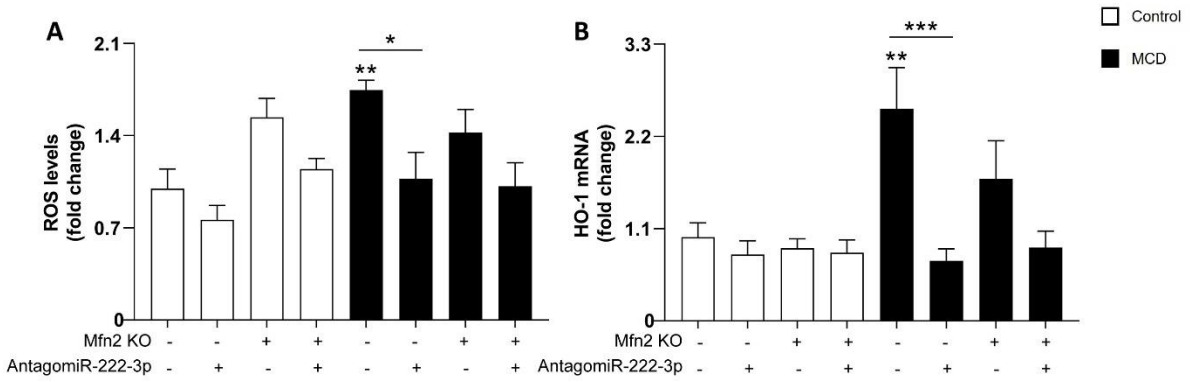

Figure 4.5: MiR-222-3p inhibition ameliorates MCD-induced oxidative stress. A. ROS levels. **B.** RT-qPCR analysis of *HO-1*. Data are expressed as mean ± S.E.M fold change. *$p < 0.05$ **$p < 0.01$ and ***$p < 0.001$.

4.6. AntagomiR-222-3p treatment counteracts MCD-induced triglyceride accumulation

Accumulation of TGs and FFAs in the liver is considered one of the major early triggers of NAFLD pathogenesis resulting in oxidative stress and hepatic inflammation (Buzzetti et al., 2016). Our results show that both WT and Mfn2 KO mice fed the MCD-diet present significantly elevated levels of hepatic TGs compared to respective controls ($p < 0.001$) (Figure 4.6A). MiR-222-3p inhibition significantly ameliorated MCD-induced TG hepatic concentration in both genotypes (at least $p < 0.05$). Regarding FFA concentration, no major alterations were observed across all experimental groups (Figure 4.6B).

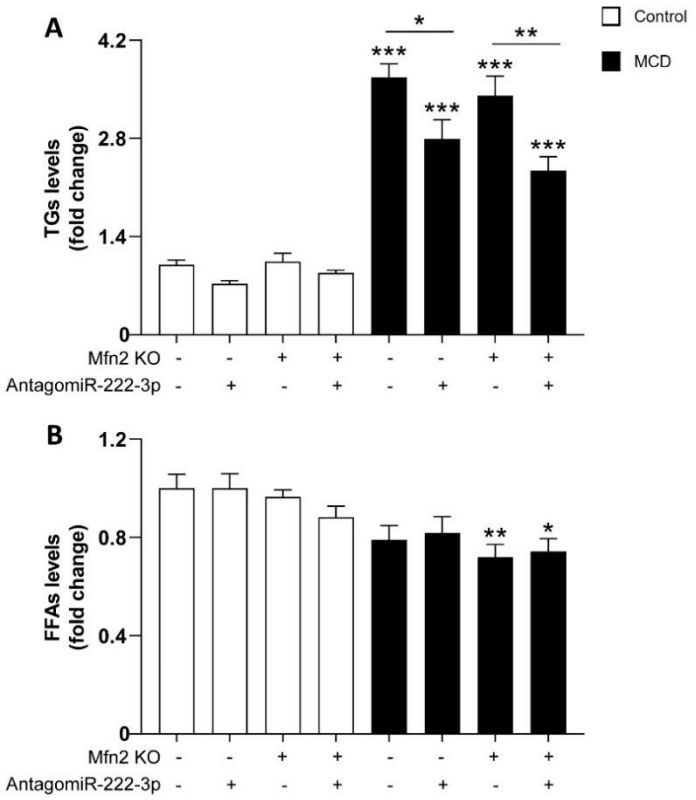

Figure 4.6: MiR-222-3p inhibition slightly ameliorates MCD-induced triglyceride accumulation. A. Liver TG quantification. **B.** Liver FFA quantification. Data are expressed as mean ± S.E.M fold change. *$p < 0.05$ **$p < 0.01$ and ***$p < 0.001$.

4.7. AntagomiR-222-3p treatment counteracts MCD-induced activation of inflammatory cells

During NASH development, inflammatory cells are recruited and activated in the liver (Cobbina & Akhlaghi, 2017). Here, c-type lectin domain family 4 member f (*Clec4f*) and adhesion G protein-coupled receptor (*F4/80*), both markers of macrophages, more specifically KCs, showed to be differently expressed. Despite a increase in MCD-fed mice, *Clec4f* mRNA levels were significantly inhibited upon treatment with antagomiR-222-3p ($p < 0.001$) (Figure 4.7A). *F4/80* mRNA expression significantly increased in MCD-fed mice, comparing with control diet-fed animals ($p < 0.001$), with miR-222-3p inhibition resulting in a significant suppression of *Clec4f* expression to values similar to those of control-fed WT mice ($p < 0.001$) (Figure 4.7B). Mfn2 KO mice exhibited similar expression patterns to those of MCD-fed WT mice.

Albumin is used as a hepatocyte-specific marker (Motiño et al., 2019). In MCD-fed mice, *albumin* expression was significantly reduced in in both WT and Mfn2 KO animals (at least $p < 0.05$), whereas antagomiR-222-3p treatment did not induce any major alterations in comparison to control-injected mice. In addition, control-fed Mfn2 KO mice exhibited a

decrease in the amount of hepatocytes expressing *albumin* (Figure 4.7C). Furthermore, we analysed the ratio of *F4/80* mRNA expression over the mRNA expression of *albumin*. This way, we were able to predict a fold change variation of the amount of KCs in relation to the amount of hepatocytes in the liver. In MCD-fed WT mice, the *F4/80*/*albumin* ratio significantly increased by more than 5-fold in comparison to control diet-fed WT mice ($p < 0.001$), suggesting that in MCD-fed mice there were over 5 times more KCs activated *per* hepatocyte than in control mice. MiR-222-3p inhibition decreased this proportion by >2.5-fold, compared to the control-injected MCD-fed mice ($p < 0.001$). Curiously, Mfn2 KO mice fed the MCD diet showed a smaller increase of the *F4/80*/*albumin* ration, compared with MCD diet-fed WT mice, with the antagomiR-222-3p treatment also significantly decreasing the proportion of KCs to hepatocytes by >2-fold ($p < 0.01$) (Figure 4.7D). Altogether, congruent with pro-inflammatory cytokines data, the activation of liver immune cells, again, attribute a key role to miR-222-3p function in NAFLD pathogenesis but fails to assign an important role to *Mfn2* in antagomiR-222-3p mediated signalling.

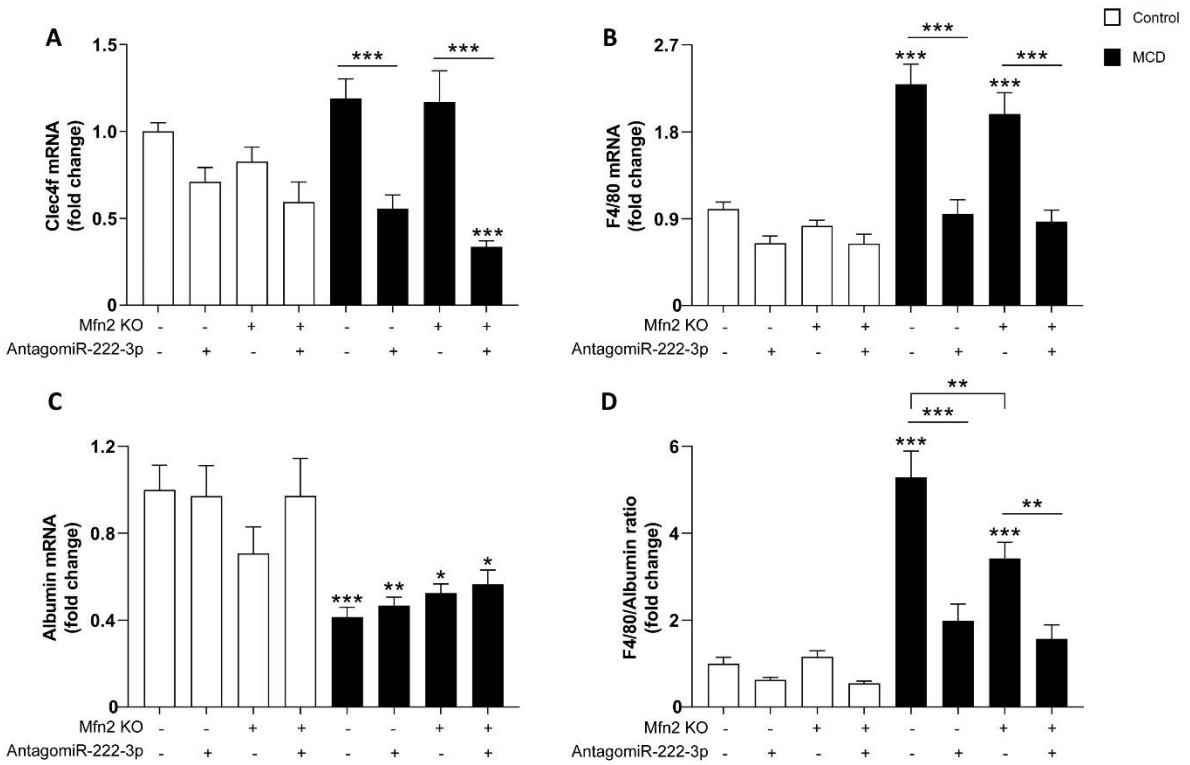

Figure 4.7: MiR-222-3p inhibition ameliorates MCD-induced inflammatory cells activation. A. RT-qPCR analysis of *Clec4f*. **B.** RT-qPCR analysis of *F4/80*. **C.** RT-qPCR analysis of *Albumin*. **D.** *F4/80/albumin* ratio. Data are expressed as mean ± S.E.M fold change. *$p < 0.05$ **$p < 0.01$ and ***$p < 0.001$.

4.8. AntagomiR-222-3p treatment counteracts MCD-induced alterations in key lipid metabolism-related genes

Hepatic *CD36* and *PPARγ* expression directly correlate with NAFLD progression, as its overexpression leads to dysregulated lipid metabolism through promotion of lipid uptake by hepatocytes and DNL (Cordoba-Chacon, 2020). Our results showed that MCD diet-induced *CD36* and *PPARγ* mRNA expression was completely reverted by antagomir-222-3p (at least $p < 0.05$) (Figure 4.8). Noteworthy, in Mfn2 KO animals, mRNA levels of these genes were similarly (*CD36*) or more strongly (*PPARγ*) induced (at least $p < 0.01$), and treatment with antagomir-222-3p less efficiently prevented these increases, comparing with MCD-fed WT mice. Overall, these results suggest that miR-222-3p plays a detrimental role in modulating liver lipid metabolism signalling pathways during NASH progression, at least in part, through targeting of *Mfn2* in hepatocytes.

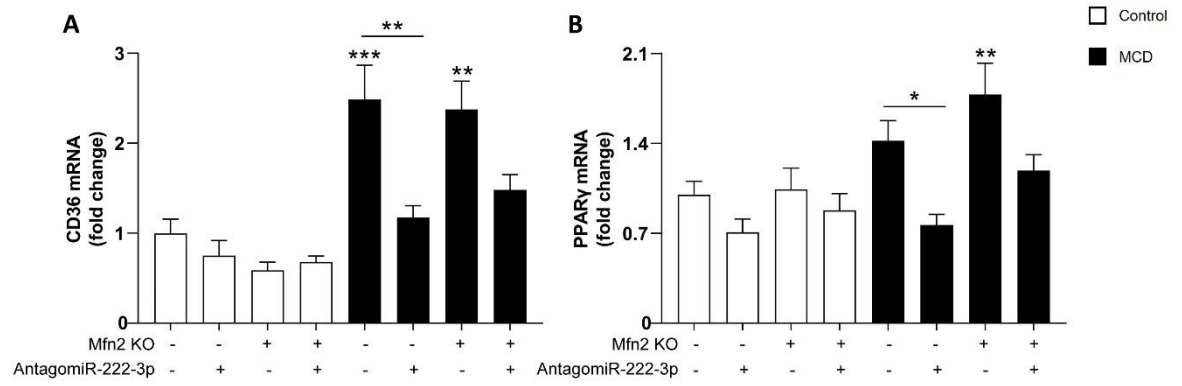

Figure 4.8: MiR-222-3p inhibition ameliorates MCD-induced *CD36* and *PPARγ* mRNA expression. A. RT-qPCR analysis of *CD36*. **B.** RT-qPCR analysis of *PPARγ*. Data are expressed as mean ± S.E.M fold change. *$p < 0.05$ **$p < 0.01$ and ***$p < 0.001$.

Chapter 5 | Discussion

MiRNAs have been extensively studied in the last decade for their role in NAFLD pathogenesis, with changes in the liver miRNA signature contributing to altered inflammation, fibrosis, oxidative stress, and lipid metabolism (Szabo & Csak, 2016). MiR-222-3p has been found to be significantly upregulated in the livers of *ob/ob* mice, mice fed a HF and sucrose diet, as well as in the liver of NASH patients (Cheung et al., 2008; J.-J. Wang et al., 2019). Further, our group has additionally described augmented miR-222-3p expression in the liver of NAFLD patients and several different diet-induced NASH mice models (unpublished results). In agreement, our current results showed that mice fed a MCD diet exhibit considerably higher miR-222-3p liver expression levels. Furthermore, miR-222-3p has been described to have a wide range of roles by targeting a variety of genes, including *CDKN1B*

(p27) and *PTEN* (Garofalo et al., 2009; X. Wang et al., 2019). In this regard, we observed that inhibiting miR-222-3p in mice fed a MCD diet led to enhanced *CDKN1B* gene expression, as well as p27 and PTEN protein levels, confirming the activity of antagomiR-222-3p in suppressing the expression of miR-222-3p targets.

Mitochondrial dysfunction constitutes a key trigger of impaired oxidative stress and lipid metabolism. Indeed, in NAFLD patients, mitochondria within hepatocytes present an aberrant phenotype, being swollen and enlarged in number and size (Longo et al., 2021). As a result, NAFLD progression has been linked to deregulation of proteins involved in mitochondrial dynamics processes (López-Lluch et al., 2008). In particular, MFN2 is recognized to play a role in NAFLD progression. Indeed, we recently showed that *Mfn2* expression is reduced in the liver of patients and several diet-induced mice models with NASH (Hernández-Alvarez et al., 2019). In this study, consistent with the previous results, we show that *Mfn2* is downregulated in the liver of MCD-fed mice. Interestingly, our group recently identified miR-222-3p as the most upregulated miRNA in the liver of a dietary NASH mouse model and, through *in silico* analysis, discovered that it could potentially bind to the 3'UTR of both mouse and human *Mfn2*. Subsequent *in vitro* studies validated *Mfn2* as a direct target of miR-222-3p (unpublished results). In this regard, our current results showed that *Mfn2* downregulation in MCD-fed WT mice negatively correlated with miR-222-3p expression, supporting the notion that *Mfn2* expression could be, at least in part, directly modulated by miR-222-3p *in vivo* as well. Giving further strength to this theory, inhibition of miR-222-3p, using antagomir-222-3p, led to significant increases in MFN2 protein levels. In addition, MFN2 protein levels appeared to be more affected in comparison with mRNA levels, supporting the post-transcriptional regulation of *Mfn2* by miR-222-3p.

Cytokines are known to play a major role in inflammatory processes during NAFLD pathogenesis (Tilg, 2010). For example, expression levels of different pro-inflammatory cytokines, such as IL-8 and TNF-α, show a strong correlation with the severity of NAFLD. In addition, the NLRP3 inflammasome has been shown to be increasingly activated during human NASH progression (du Plessis et al., 2016; Parthasarathy et al., 2020). Accordingly, our results show that MCD-fed mice display a significant increase in pro-inflammatory cytokines *IL-8*, *IL-1β*, *TNF-α*, *TLR4*, and *NLRP3* gene expression. In contrast, MCD-fed mice treated with antagomiR-222-3p display reduced levels of all these inflammatory cytokines and mediators. Of note, a recent study suggested that silencing of miR-222-3p in a mouse model of NASH was capable of reducing inflammation, most likely via relieved repression of TIMP3 (Jiang et al., 2018). Using Mfn2 KO mice under a normal chow diet, Hernandez-Alvarez *et al.*, showed that these mice develop NASH-like features over time, including hepatic inflammation associated with a significant increase in hepatic pro-inflammatory cytokines gene expression, including *IL-1β* and *TNF-α* (Hernández-Alvarez et al., 2019). However, contrary to their

findings, in this study, chow-fed Mfn2 KO mice presented with similar pro-inflammatory cytokine expression levels to WT mice. Because our previous and current results suggested that *Mfn2* was a direct target of miR-222-3p in liver cells, we hypothesized that some of the protective effects of antagomiR-222-3p on NASH histopathological and metabolic features, induced by the MCD diet, would be reduced in Mfn2 KO mice. However, MCD-fed Mfn2 KO mice treated with antagomiR-222-3p continued to exhibit a considerable reduction in pro-inflammatory cytokines. Exceptionally, *NLRP3* was the only gene whose expression remained unaffected compared to control-injected mice. Interestingly, it was reported that MFN2 binds to NLRP3, enhances its recruitment to mitochondria, and is necessary for full NLRP3 inflammasome activation in macrophages, which might explain the lower *NLRP3* inflammasome activation in Mfn2 KO mice (Ichinohe et al., 2013; Sutterwala et al., 2014; Xu et al., 2020). Because of this, the potential benefits of antagomiR-222-3p in Mfn2 KO mice could be limited, since *NLRP3* expression is not as increased as in WT mice. However, since these findings were reported using RNA viruses and infection with *Mycobacterium tuberculosis*, more research is needed to determine whether the same pathway occurs during NAFLD pathogenesis *in vivo* (Ichinohe et al., 2013; Xu et al., 2020).

During the course of NAFLD, pro-inflammatory cytokines released by inflammatory cells activate HSCs, which change into myofibroblast-like cells and produce pro-fibrogenic cytokines that promote hepatic fibrosis. These include TGF-β, collagen-1α1, and α-SMA, among others (Ogawa et al., 2012; Prasun et al., 2021; Rada et al., 2020). Furthermore, enhanced fibrogenic response and fibrosis are also observed in NASH patients and diet-induced NASH mouse models (Luo et al., 2016; L. Yang et al., 2014). Here, we show that MCD-fed mice developed fibrosis, as evidenced by significantly increased expression of pro-fibrotic genes TGF-β, *α-SMA*, and most notably *collagen-1α1*. MiR-222-3p has been found to stimulate HSCs through AKT activation (Shen et al., 2014). In addition, miR-222-3p expression was found to positively correlate with the expression of fibrogenic genes in human fibrotic livers (Ogawa et al., 2012). In agreement, our results showed that antagomiR-222-3p prevented MCD-induced expression of pro-fibrotic genes. Interestingly, according to Hernandez-Alvarez *et al.*, *Mfn2* ablation alone resulted in the development of liver fibrosis, due to a modest increase in genes encoding fibrotic markers (Hernández-Alvarez et al., 2019). However, while we found a similar increase in *collagen-1α1* expression in Mfn2 KO mice in our study, this increase is too small compared to the increase in MCD-fed mice to conclude that fibrosis has already developed. Nonetheless, it suggests that *Mfn2* deficiency may play a role in triggering the development of fibrosis. Interestingly, NLRP3 activation has been linked to HSC activation and collagen deposition in the liver, resulting in severe fibrosis (Wree, McGeough, et al., 2014). Of note, *NLRP3*-deficient animals are protected from CDAA-induced liver fibrosis, indicating that NLRP3 inflammasome activation is a key contributor to liver fibrosis during NASH progression (Wree, Eguchi, et al.,

2014). The lower expression of pro-fibrotic markers in Mfn2 KO MCD-fed mice compared to MCD-fed mice may relate with a lower NLRP3 inflammasome activation, supporting this *NLRP3*-dependent function in fibrosis. Consequently, treatment of MCD-fed Mfn2 KO mice with antagomiR-222-3p appears to elicit a smaller protective impact against fibrosis, compared to its effect in MCD-fed WT mice.

Excessive generation of ROS has been identified as an early trigger of NAFLD development (Wei et al., 2008). In parallel, hepatic induction of *HO-1* is known to be related to increased ROS production. Interestingly, *HO-1* expression appears to be a protective mechanism against oxidative stress and lipid peroxidation. Li *et al.*, found that in parallel to increased ROS levels, *HO-1* expression was significantly elevated in diet-induced NASH, and demonstrated that HO-1 displays hepatoprotective effects by attenuating ROS levels during NASH progression (D. Li et al., 2020; Malaguarnera et al., 2009). In agreement, our results showed that MCD-fed mice exhibited higher ROS production and *HO-1* expression in the liver, whereas antagomiR-222-3p treatment prevented these changes. *Mfn2* deficiency is known to enhance ROS production and, as a result, lead to mitochondrial dysfunction (Sebastian et al., 2012). In this regard, our findings unequivocally show that control-fed Mfn2 KO mice produce more ROS. Surprisingly, the same trend was not observed in MCD-fed mice. Further, antagomiR-222-3p-mediated inhibition of ROS and *HO-1* expression was not too different between MCD-fed Mfn2 KO and WT mice, suggesting that the protective effects of antagomiR-222-3p are mostly independent of *Mfn2*.

Early during NAFLD development, hepatocytes accumulate TGs and FFAs. For example, TG levels were shown to increase by 81% in mice fed a high-fat high-sucrose diet (Bassot et al., 2021). In agreement, our results showed that MCD-fed WT mice exhibited a more than 3.5-fold increase in hepatic TG levels, with treatment with antagomiR-222-3p partially preventing this increase. Similar results were observed in MCD-fed Mfn2 KO mice, suggesting that the amelioration in TGs accumulation by miR-222-3p inhibition does not seem to be Mfn2-dependent. It should be noted that TG synthesis and accumulation is not always harmful or hepatotoxic. In fact, TGs synthesis has been reported to be a beneficial mechanism to protect the liver from FFAs accumulation and lipotoxicity. In this regard, levels of FFAs remained constant across all experimental groups, suggesting TG production and accumulation in MCD-fed mice is preventing harmful FFA accumulation. More studies are needed to elucidate this hypothesis.

Chronic inflammation with recruitment and activation of inflammatory cells in the liver is a main event during NASH (Cobbina & Akhlaghi, 2017). The surface marker *F4/80* is seen on liver mononuclear cells and is used to identify KCs (Kinoshita et al., 2010; Lopez et al., 2011). Apart from *F4/80*, *Clec4f* appears to be one of the most precise KC markers (Guillot & Tacke, 2019). In MCD-fed mice, $CLEC4F^-$ KCs were shown to be recruited to the liver with some being

activated into CLEC4F^{+} (Remmerie et al., 2020). Our findings suggest that there is increased inflammatory cell activation in the liver of mice fed the MCD diet, whereas treatment with antagomiR-222-3p significantly reduces activation of inflammatory cells. Interestingly, control diet-fed mice treated with antagomiR-222-3p already displayed a slight decrease in the expression of *Clec4f* and *F4/80* markers, suggesting that miR-222-3p plays a major role in the activation of inflammatory cells, even in the absence of strong pro-inflammatory signals. *Albumin* is used as a hepatocyte-specific marker (Motiño et al., 2019). Because our results show that its expression is significantly reduced in MCD-fed mice, it may be hypothesized that hepatocyte ballooning and loss, for instance through apoptosis, has occurred in the livers of these mice. If so, miR-222-3p inhibition appears not to play a protective role in this cell loss, as it did not induce any changes in *albumin* expression. The *F4/80*/*albumin* expression ratio can be used to compare the amount of KCs to the amount of hepatocytes. (Lopez et al., 2011). By combining the considerable increase in KCs activation with the significant decrease in hepatocyte number, a significant rise in the amount of KCs *per* hepatocyte is found in MCD-fed mice. On the contrary, inhibition of miR-222-3p in MCD-fed mice resulted in a significant reduction in activated KCs *per* hepatocyte, mostly driven by a decrease in inflammatory cell activation and not so much by increased healthy hepatocytes. Similar results were obtained in Mfn2 KO mice, again suggesting that the protective role of antagomir-222-3p on inflammation is mostly *Mfn2*-independent.

Hepatic CD36 and PPARγ upregulation has been directly linked to NAFLD progression, contributing to dysregulated lipid metabolism, by facilitating lipid uptake and oxidation (Cordoba-Chacon, 2020; Maréchal et al., 2018). As such, *CD36* expression directly correlates with hepatic TG content (Rada et al., 2020). Furthermore, it has been shown that hepatic *PPARγ* and *CD36* expression is elevated, primarily in KCs and hepatocytes, in diet-induced NASH models and NAFLD patients (Cordoba-Chacon, 2020; Pepino et al., 2014; Samovski & Abumrad, 2019). In agreement, we showed that, in MCD-fed mice, the *PPARγ-CD36* pathway is increased and that miR-222-3p inhibition prevents its augmented expression. *PPARγ-CD36* expression increases in Mfn2 KO MCD-fed mice, with *PPARγ* being even more expressed than in MCD-fed mice in the presence of *Mfn2*. Recent studies have revealed that MFN2 may suppress *PPARγ*, which could explain this result (Mancini et al., 2019). In Mfn2 KO mice fed a MCD diet, suppression of miR-222-3p resulted in reduced expression levels of *PPARγ-CD36*, which was consistent with the prior results.

Overall, inhibition of miR-222-3p ameliorated MCD-induced NASH-like features even in Mfn2 KO mice, implying that antagomiR-222-3p protective effects are not, at least fully, dependent on hepatocyte-specific *Mfn2*. In fact, *Mfn2* expressed from liver cells other than hepatocytes, such as HSCs and macrophages, may have a greater role in the antagomiR-222-3p-mediated protective effects. For example, a recent study has revealed that MFN2 in HSCs

plays a vital role in inducing apoptosis, suppressing TGF-β/Smad signaling, and decreasing collagen type I, III, and IV production. Moreover, overexpression of HSCs-specific *Mfn2* significantly improved CCl4-induced liver fibrosis and reduced immune cell infiltration *in vivo* (H. Zhu et al., 2020). Furthermore, *Mfn2* is also highly expressed in macrophages, where it plays an important role in the immune response, particularly when exposed to a stressful environment, such as pro-inflammatory signals. *Mfn2*-deficiency in macrophages was shown to critically reduce ROS production and hinder protection from *Mycobacterium tuberculosis* infection or LPS-induced endotoxemia through reducing the transition of M1 macrophages to M2 macrophages, which results in increased TNF-α production (Lloberas et al., 2020).

Chapter 6 | Conclusion

In this work, we established that our MCD diet model combined with HFD and supplemented with 0.1% L-methionine on drinking water, induced NASH-like liver features in a short period of time, including inflammation, fibrosis, oxidative stress, TG accumulation, inflammatory cells activation, and dysregulated lipid metabolism. Still, further histopathological studies should be carried out to assess the degree of inflammation, fibrosis, and hepatocyte ballooning, by direct visualization, and correlate these findings with the biochemical and clinical manifestations found in this study.

This study also demonstrated that miR-222-3p inhibition significantly ameliorates diet-induced inflammation, fibrosis, oxidative stress, and lipid metabolism. Our findings strongly highlight the targeting of miR-222-3p as a promising therapeutic strategy for preventing NAFLD/NASH progression. Still, several complementary studies are needed to analyse the expression of genes involved in TG synthesis, such as diacylglycerol-acyltransferases (*DGATs*) and 1-acylglycerol-3-phosphate O-acyltransferases (*AGPATs*), to confirm the number of KCs activated in relation to healthy hepatocytes using immunohistochemistry, and to determine whether miR-222-3p exerts anti-apoptotic functions *in vivo*.

Finally, unexpectedly, hepatocyte-specific *Mfn2* expression failed to be required for miR-222-3p-mediated beneficial effects. Instead, even in the absence of *Mfn2*, inhibition of miR-222-3p improved NASH-like features, almost always in the same order of magnitude. Therefore, future research should focus on the role of *Mfn2* expression in other liver cells besides hepatocytes, such as HSCs and macrophages, to better understand the role of the miR-222-3p:*Mfn2* pathway in NAFLD pathogenesis, as well as miR-222-3p-dependent:*Mfn2*-independent pathways that may contribute to improvement of experimental NASH.

Altogether, the results obtained in this thesis indicate that activation of miR-222-3p is a critical factor in NAFLD/NASH pathogenesis, leading to inflammation, fibrosis, and oxidative stress development with TG accumulation, inflammatory cell activation, and dysregulated lipid

metabolism. In fact, although not being dependent on hepatocyte *Mfn2* expression, inhibiting miR-222-3p counteracts all the diet-induced NASH-like features. As such, targeting miR-222-3p may represent an appealing prospective therapeutic approach for treating NAFLD.

Chapter 7 | References

Abenavoli, L., Falalyeyeva, T., Boccuto, L., Tsyryuk, O., & Kobyliak, N. (2018). Obeticholic Acid: A New Era in the Treatment of Nonalcoholic Fatty Liver Disease. *Pharmaceuticals*, *11*(4), 104.

Altajar, S., & Baffy, G. (2020). Skeletal Muscle Dysfunction in the Development and Progression of Nonalcoholic Fatty Liver Disease. *Journal of Clinical and Translational Hepatology*, *8*(4), 1–10.

Archer, S. L. (2013). Mitochondrial Dynamics — Mitochondrial Fission and Fusion in Human Diseases. *New England Journal of Medicine*, *369*(23), 2236–2251.

Armutcu, F. (2019). Organ crosstalk: the potent roles of inflammation and fibrotic changes in the course of organ interactions. *Inflammation Research*, *68*(10), 825–839.

Asrani, S. K., Devarbhavi, H., Eaton, J., & Kamath, P. S. (2019). Burden of liver diseases in the world. *Journal of Hepatology*, *70*(1), 151–171.

Bach, D., Naon, D., Pich, S., Soriano, F. X., Vega, N., Rieusset, J., Laville, M., Guillet, C., Boirie, Y., Wallberg-Henriksson, H., Manco, M., Calvani, M., Castagneto, M., Palacin, M., Mingrone, G., Zierath, J. R., Vidal, H., & Zorzano, A. (2005). Expression of Mfn2, the Charcot-Marie-Tooth Neuropathy Type 2A Gene, in Human Skeletal Muscle: Effects of Type 2 Diabetes, Obesity, Weight Loss, and the Regulatory Role of Tumor Necrosis Factor and Interleukin-6. *Diabetes*, *54*(9), 2685–2693.

Bach, Daniel, Pich, S., Soriano, F. X., Vega, N., Baumgartner, B., Oriola, J., Daugaard, J. R., Lloberas, J., Camps, M., Zierath, J. R., Rabasa-Lhoret, R., Wallberg-Henriksson, H., Laville, M., Palacín, M., Vidal, H., Rivera, F., Brand, M., & Zorzano, A. (2003). Mitofusin-2 Determines Mitochondrial Network Architecture and Mitochondrial Metabolism. *Journal of Biological Chemistry*, *278*(19), 17190–17197.

Bassot, A., Prip-Buus, C., Alves, A., Berdeaux, O., Perrier, J., Lenoir, V., Ji-Cao, J., Berger, M.-A., Loizon, E., Cabaret, S., Panthu, B., Rieusset, J., & Morio, B. (2021). Loss and gain of function of Grp75 or mitofusin 2 distinctly alter cholesterol metabolism, but all promote triglyceride accumulation in hepatocytes. *Biochimica et Biophysica Acta (BBA) - Molecular and Cell Biology of Lipids*, *1866*(12), 159030.

Bedossa, P., Poitou, C., Veyrie, N., Bouillot, J.-L., Basdevant, A., Paradis, V., Tordjman, J., & Clement, K. (2012). Histopathological algorithm and scoring system for evaluation of liver lesions in morbidly obese patients. *Hepatology*, *56*(5), 1751–1759.

Brunt, E. M., Janney, C. G., Di Bisceglie, A. M., Neuschwander-Tetri, B. A., & Bacon, B. R. (1999). Nonalcoholic Steatohepatitis: A Proposal for Grading and Staging The Histological Lesions. *American Journal of Gastroenterology*, *94*(9), 2467–2474.

Bucha, S., Mukhopadhyay, D., & Bhattacharyya, N. P. (2015). Regulation of mitochondrial morphology and cell cycle by microRNA-214 targeting Mitofusin2. *Biochemical and Biophysical Research Communications*, *465*(4), 797–802.

Buzzetti, E., Pinzani, M., & Tsochatzis, E. A. (2016). The multiple-hit pathogenesis of non-alcoholic fatty liver disease (NAFLD). *Metabolism*, *65*(8), 1038–1048.

Cai, C., Song, X., Chen, Y., Chen, X., & Yu, C. (2020). Relationship between relative skeletal muscle mass and nonalcoholic fatty liver disease: a systematic review and meta-analysis. *Hepatology International*, *14*(1), 115–126.

Carneros, D., López-Lluch, G., & Bustos, M. (2020). Physiopathology of Lifestyle Interventions in Non-Alcoholic Fatty Liver Disease (NAFLD). *Nutrients*, *12*(11), 3472.

Castera, L., Vilgrain, V., & Angulo, P. (2013). Noninvasive evaluation of NAFLD. *Nature Reviews Gastroenterology & Hepatology*, *10*(11), 666–675.

Cha, J.-Y., Kim, D.-H., & Chun, K.-H. (2018). The role of hepatic macrophages in nonalcoholic fatty liver disease and nonalcoholic steatohepatitis. *Laboratory Animal Research*, *34*(4), 133.

Chakravarthy, M. V., Siddiqui, M. S., Forsgren, M. F., & Sanyal, A. J. (2020). Harnessing Muscle–Liver Crosstalk to Treat Nonalcoholic Steatohepatitis. *Frontiers in Endocrinology*, *11*, 1.

Chandhok, G., Lazarou, M., & Neumann, B. (2018). Structure, function, and regulation of mitofusin-2 in health and disease. *Biological Reviews*, *93*(2), 933–949.

Cheung, O., Puri, P., Eicken, C., Contos, M. J., Mirshahi, F., Maher, J. W., Kellum, J. M., Min, H., Luketic, V. A., & Sanyal, A. J. (2008). Nonalcoholic steatohepatitis is associated with altered hepatic MicroRNA expression. *Hepatology*, *48*(6), 1810–1820.

Cobbina, E., & Akhlaghi, F. (2017). Non-alcoholic fatty liver disease (NAFLD) – pathogenesis, classification, and effect on drug metabolizing enzymes and transporters. *Drug Metabolism Reviews*, *49*(2), 197–211.

Cordoba-Chacon, J. (2020). Loss of Hepatocyte-Specific PPAR γ Expression Ameliorates Early Events of Steatohepatitis in Mice Fed the Methionine and Choline-Deficient Diet. *PPAR Research*, *2020*, 1–13.

Cotter, T. G., Dong, L., Holmen, J., Gilroy, R., Krong, J., & Charlton, M. (2020). Nonalcoholic fatty liver disease: impact on healthcare resource utilization, liver transplantation and mortality in a large, integrated healthcare system. *Journal of Gastroenterology*, *55*(7), 722–730.

David, D., & Eapen, C. E. (2021). What Are the Current Pharmacological Therapies for

Nonalcoholic Fatty Liver Disease? *Journal of Clinical and Experimental Hepatology*, *11*(2), 232–238.

Day, C. P., & James, O. F. W. (1998). Steatohepatitis: A tale of two “hits”? *Gastroenterology*, *114*(4), 842–845.

de Conti, A., Ortega, J. F., Tryndyak, V., Dreval, K., Moreno, F. S., Rusyn, I., Beland, F. A., & Pogribny, I. P. (2017). MicroRNA deregulation in nonalcoholic steatohepatitis-associated liver carcinogenesis. *Oncotarget*, *8*(51), 88517–88528.

Denk, H., Abuja, P. M., & Zatloukal, K. (2019). Animal models of NAFLD from the pathologist’s point of view. *Biochimica et Biophysica Acta (BBA) - Molecular Basis of Disease*, *1865*(5), 929–942.

Dong, R., Zheng, Y., Chen, G., Zhao, R., Zhou, Z., & Zheng, S. (2015). miR-222 Overexpression May Contribute to Liver Fibrosis in Biliary Atresia by Targeting PPP2R2A. *Journal of Pediatric Gastroenterology & Nutrition*, *60*(1), 84–90.

Dongiovanni, P., Meroni, M., Longo, M., Fargion, S., & Fracanzani, A. (2018). miRNA Signature in NAFLD: A Turning Point for a Non-Invasive Diagnosis. *International Journal of Molecular Sciences*, *19*(12), 3966.

du Plessis, J., Korf, H., van Pelt, J., Windmolders, P., Vander Elst, I., Verrijken, A., Hubens, G., Van Gaal, L., Cassiman, D., Nevens, F., Francque, S., & van der Merwe, S. (2016). Pro-Inflammatory Cytokines but Not Endotoxin-Related Parameters Associate with Disease Severity in Patients with NAFLD. *PLOS ONE*, *11*(12), e0166048.

EASL, EASD, & EASO. (2016). EASL–EASD–EASO Clinical Practice Guidelines for the management of non-alcoholic fatty liver disease. *Journal of Hepatology*, *64*(6), 1388–1402.

El-Agroudy, N. N., Kurzbach, A., Rodionov, R. N., O’Sullivan, J., Roden, M., Birkenfeld, A. L., & Pesta, D. H. (2019). Are Lifestyle Therapies Effective for NAFLD Treatment? *Trends in Endocrinology & Metabolism*, *30*(10), 701–709.

Estes, C., Razavi, H., Loomba, R., Younossi, Z., & Sanyal, A. J. (2018). Modeling the Epidemic of Nonalcoholic Fatty Liver Disease Demonstrates an Exponential Increase in Burden of Disease. *Hepatology*, *67*(1), 123–133.

Fang, Y.-L., Chen, H., Wang, C.-L., & Liang, L. (2018). Pathogenesis of non-alcoholic fatty liver disease in children and adolescence: From “two hit theory” to “multiple hit model.” *World Journal of Gastroenterology*, *24*(27), 2974–2983.

Ferguson, D., & Finck, B. N. (2021). Emerging therapeutic approaches for the treatment of NAFLD and type 2 diabetes mellitus. *Nature Reviews Endocrinology*, *17*(8), 484–495.

Fornari, F., Gramantieri, L., Ferracin, M., Veronese, A., Sabbioni, S., Calin, G. A., Grazi, G. L., Giovannini, C., Croce, C. M., Bolondi, L., & Negrini, M. (2008). MiR-221 controls CDKN1C/p57 and CDKN1B/p27 expression in human hepatocellular carcinoma.

Oncogene, *27*(43), 5651–5661.

Fouad, Y., Waked, I., Bollipo, S., Gomaa, A., Ajlouni, Y., & Attia, D. (2020). What's in a name? Renaming 'NAFLD' to 'MAFLD.' *Liver International*, *40*(6), 1254–1261.

Friedman, S. L., Neuschwander-Tetri, B. A., Rinella, M., & Sanyal, A. J. (2018). Mechanisms of NAFLD development and therapeutic strategies. *Nature Medicine*, *24*(7), 908–922.

Gan, K.-X. (2013). Mitofusin-2 ameliorates high-fat diet-induced insulin resistance in liver of rats. *World Journal of Gastroenterology*, *19*(10), 1572.

Garofalo, M., Di Leva, G., Romano, G., Nuovo, G., Suh, S.-S., Ngankeu, A., Taccioli, C., Pichiorri, F., Alder, H., Secchiero, P., Gasparini, P., Gonelli, A., Costinean, S., Acunzo, M., Condorelli, G., & Croce, C. M. (2009). miR-221&222 Regulate TRAIL Resistance and Enhance Tumorigenicity through PTEN and TIMP3 Downregulation. *Cancer Cell*, *16*(6), 498–509.

Gatfield, D., Le Martelot, G., Vejnar, C. E., Gerlach, D., Schaad, O., Fleury-Olela, F., Ruskeepaa, A.-L., Oresic, M., Esau, C. C., Zdobnov, E. M., & Schibler, U. (2009). Integration of microRNA miR-122 in hepatic circadian gene expression. *Genes & Development*, *23*(11), 1313–1326.

Ge, X., Zheng, L., Wang, M., Du, Y., & Jiang, J. (2020). Prevalence trends in non-alcoholic fatty liver disease at the global, regional and national levels, 1990–2017: a population-based observational study. *BMJ Open*, *10*(8), e036663.

Gjorgjieva, M., Sobolewski, C., Dolicka, D., Correia de Sousa, M., & Foti, M. (2019). miRNAs and NAFLD: from pathophysiology to therapy. *Gut*, *68*(11), 2065–2079.

Guillot, A., & Tacke, F. (2019). Liver Macrophages: Old Dogmas and New Insights. *Hepatology Communications*, *3*(6), 730–743.

Guo, Y., Xiong, Y., Sheng, Q., Zhao, S., Wattacheril, J., & Flynn, C. R. (2016). A micro-RNA expression signature for human NAFLD progression. *Journal of Gastroenterology*, *51*(10), 1022–1030.

Ha, M., & Kim, V. N. (2014). Regulation of microRNA biogenesis. *Nature Reviews Molecular Cell Biology*, *15*(8), 509–524.

Hao, J., Zhang, C., Zhang, A., Wang, K., Jia, Z., Wang, G., Han, L., Kang, C., & Pu, P. (2012). miR-221/222 is the regulator of Cx43 expression in human glioblastoma cells. *Oncology Reports*, *27*(5), 1504–1510.

He, Z., Hu, C., & Jia, W. (2016). miRNAs in non-alcoholic fatty liver disease. *Frontiers of Medicine*, *10*(4), 389–396.

Hernández-Alvarez, M. I., Sebastián, D., Vives, S., Ivanova, S., Bartoccioni, P., Kakimoto, P., Plana, N., Veiga, S. R., Hernández, V., Vasconcelos, N., Peddinti, G., Adrover, A., Jové, M., Pamplona, R., Gordaliza-Alaguero, I., Calvo, E., Cabré, N., Castro, R., Kuzmanic, A., … Zorzano, A. (2019). Deficient Endoplasmic Reticulum-Mitochondrial

Phosphatidylserine Transfer Causes Liver Disease. *Cell*, *177*(4), 881-895.e17.

Hernandez-Alvarez, M. I., Thabit, H., Burns, N., Shah, S., Brema, I., Hatunic, M., Finucane, F., Liesa, M., Chiellini, C., Naon, D., Zorzano, A., & Nolan, J. J. (2010). Subjects With Early-Onset Type 2 Diabetes Show Defective Activation of the Skeletal Muscle PGC-1 /Mitofusin-2 Regulatory Pathway in Response to Physical Activity. *Diabetes Care*, *33*(3), 645–651.

Huang, E., Peng, N., Xiao, F., Hu, D., Wang, X., & Lu, L. (2020). The Roles of Immune Cells in the Pathogenesis of Fibrosis. *International Journal of Molecular Sciences*, *21*(15), 5203.

Ichinohe, T., Yamazaki, T., Koshiba, T., & Yanagi, Y. (2013). Mitochondrial protein mitofusin 2 is required for NLRP3 inflammasome activation after RNA virus infection. *Proceedings of the National Academy of Sciences*, *110*(44), 17963–17968.

Im, Y. R., Hunter, H., Gracia Hahn, D., Duret, A., Cheah, Q., Dong, J., Fairey, M., Hjalmarsson, C., Li, A., Lim, H. K., McKeown, L., Mitrofan, C., Rao, R., Utukuri, M., Rowe, I. A., & Mann, J. P. (2021). A Systematic Review of Animal Models of NAFLD Finds High-Fat, High-Fructose Diets Most Closely Resemble Human NAFLD. *Hepatology*, *74*(4), 1884–1901.

Itagaki, H., Shimizu, K., Morikawa, S., Ogawa, K., & Ezaki, T. (2013). Morphological and functional characterization of non-alcoholic fatty liver disease induced by a methionine-choline-deficient diet in C57BL/6 mice. *International Journal of Clinical and Experimental Pathology*, *6*(12), 2683–2696.

Jahn, D., Kircher, S., Hermanns, H. M., & Geier, A. (2019). Animal models of NAFLD from a hepatologist's point of view. *Biochimica et Biophysica Acta (BBA) - Molecular Basis of Disease*, *1865*(5), 943–953.

James, S. L., Abate, D., Abate, K. H., Abay, S. M., Abbafati, C., Abbasi, N., Abbastabar, H., Abd-Allah, F., Abdela, J., Abdelalim, A., Abdollahpour, I., Abdulkader, R. S., Abebe, Z., Abera, S. F., Abil, O. Z., Abraha, H. N., Abu-Raddad, L. J., Abu-Rmeileh, N. M. E., Accrombessi, M. M. K., … Murray, C. J. L. (2018). Global, regional, and national incidence, prevalence, and years lived with disability for 354 diseases and injuries for 195 countries and territories, 1990–2017: a systematic analysis for the Global Burden of Disease Study 2017. *The Lancet*, *392*(10159), 1789–1858.

Jeong, G., Lim, Y.-H., Kim, N. J., Wee, G., & Kim, Y.-K. (2017). Knockout of miR-221 and miR-222 reveals common and specific targets for paralogous miRNAs. *RNA Biology*, *14*(2), 197–205.

Jiang, X., Jiang, L., Shan, A., Su, Y., Cheng, Y., Song, D., Ji, H., Ning, G., Wang, W., & Cao, Y. (2018). Targeting hepatic miR-221/222 for therapeutic intervention of nonalcoholic steatohepatitis in mice. *EBioMedicine*, *37*, 307–321.

Jornayvaz, F. R., & Shulman, G. I. (2010). Regulation of mitochondrial biogenesis. *Essays in Biochemistry*, *47*, 69–84.

Kazankov, K., Jørgensen, S. M. D., Thomsen, K. L., Møller, H. J., Vilstrup, H., George, J., Schuppan, D., & Grønbæk, H. (2019). The role of macrophages in nonalcoholic fatty liver disease and nonalcoholic steatohepatitis. *Nature Reviews Gastroenterology & Hepatology*, *16*(3), 145–159.

Kim, G., Lee, S., Lee, Y., Jun, J. E., Ahn, J., Bae, J. C., Jin, S., Hur, K. Y., Jee, J. H., Lee, M., & Kim, J. H. (2018). Relationship Between Relative Skeletal Muscle Mass and Nonalcoholic Fatty Liver Disease: A 7-Year Longitudinal Study. *Hepatology*, *68*(5), 1755–1768.

Kim, J.-Y., Lee, G.-N., Song, H. C., Park, Y.-M., Ahn, Y.-B., Han, K., & Ko, S.-H. (2020). Association between Fatty Liver Index and Periodontitis: the Korea National Health and Nutrition Examination Survey. *Scientific Reports 2020 10:1*, *10*(1), 1–7.

Kinoshita, M., Uchida, T., Sato, A., Nakashima, M., Nakashima, H., Shono, S., Habu, Y., Miyazaki, H., Hiroi, S., & Seki, S. (2010). Characterization of two F4/80-positive Kupffer cell subsets by their function and phenotype in mice. *Journal of Hepatology*, *53*(5), 903–910.

Koch, L. K., & Yeh, M. M. (2018). Nonalcoholic fatty liver disease (NAFLD): Diagnosis, pitfalls, and staging. *Annals of Diagnostic Pathology*, *37*, 83–90.

le Sage, C., Nagel, R., Egan, D. A., Schrier, M., Mesman, E., Mangiola, A., Anile, C., Maira, G., Mercatelli, N., Ciafrè, S. A., Farace, M. G., & Agami, R. (2007). Regulation of the p27Kip1 tumor suppressor by miR-221 and miR-222 promotes cancer cell proliferation. *The EMBO Journal*, *26*(15), 3699–3708.

Li, D., Zhao, D., Du, J., Dong, S., Aldhamin, Z., Yuan, X., Li, W., Du, H., Zhao, W., Cui, L., Liu, L., Fu, N., & Nan, Y. (2020). Heme oxygenase-1 alleviated non-alcoholic fatty liver disease via suppressing ROS-dependent endoplasmic reticulum stress. *Life Sciences*, *253*, 117678.

Li, P., Jiao, J., Gao, G., & Prabhakar, B. S. (2012). Control of mitochondrial activity by miRNAs. *Journal of Cellular Biochemistry*, *113*(4), 1104–1110.

Li, R., Toan, S., & Zhou, H. (2020). Role of mitochondrial quality control in the pathogenesis of nonalcoholic fatty liver disease. *Aging*, *12*(7), 6467–6485.

Lindenmeyer, C. C., & McCullough, A. J. (2018). The Natural History of Nonalcoholic Fatty Liver Disease—An Evolving View. *Clinics in Liver Disease*, *22*(1), 11–21.

Liu, C.-H., Ampuero, J., Gil-Gómez, A., Montero-Vallejo, R., Rojas, Á., Muñoz-Hernández, R., Gallego-Durán, R., & Romero-Gómez, M. (2018). miRNAs in patients with non-alcoholic fatty liver disease: A systematic review and meta-analysis. *Journal of Hepatology*, *69*(6), 1335–1348.

Liu, Z., Sun, J., Liu, B., Zhao, M., Xing, E., & Dang, C. (2018). miRNA-222 promotes liver cancer cell proliferation, migration and invasion and inhibits apoptosis by targeting BBC3. *International Journal of Molecular Medicine*, *42*(1), 141–148.

Lloberas, J., Muñoz, J. P., Hernández-Álvarez, M. I., Cardona, P.-J., Zorzano, A., & Celada, A. (2020). Macrophage mitochondrial MFN2 (mitofusin 2) links immune stress and immune response through reactive oxygen species (ROS) production. *Autophagy*, *16*(12), 2307–2309.

Lonardo, A., Arab, J. P., & Arrese, M. (2021). Perspectives on Precision Medicine Approaches to NAFLD Diagnosis and Management. *Advances in Therapy*, *38*(5), 2130–2158.

Longo, M., Meroni, M., Paolini, E., Macchi, C., & Dongiovanni, P. (2021). Mitochondrial dynamics and nonalcoholic fatty liver disease (NAFLD): new perspectives for a fairy-tale ending? *Metabolism*, *117*, 154708.

López-Lluch, G., Irusta, P. M., Navas, P., & de Cabo, R. (2008). Mitochondrial biogenesis and healthy aging. *Experimental Gerontology*, *43*(9), 813–819.

López-Riera, M., Conde, I., Quintas, G., Pedrola, L., Zaragoza, Á., Perez-Rojas, J., Salcedo, M., Benlloch, S., Castell, J. V., & Jover, R. (2018). Non-invasive prediction of NAFLD severity: a comprehensive, independent validation of previously postulated serum microRNA biomarkers. *Scientific Reports*, *8*(1), 10606.

Lopez, B. G., Tsai, M. S., Baratta, J. L., Longmuir, K. J., & Robertson, R. T. (2011). Characterization of Kupffer cells in livers of developing mice. *Comparative Hepatology*, *10*(1), 2.

Loyer, X., Paradis, V., Hénique, C., Vion, A.-C., Colnot, N., Guerin, C. L., Devue, C., On, S., Scetbun, J., Romain, M., Paul, J.-L., Rothenberg, M. E., Marcellin, P., Durand, F., Bedossa, P., Prip-Buus, C., Baugé, E., Staels, B., Boulanger, C. M., … Rautou, P.-E. (2016). Liver microRNA-21 is overexpressed in non-alcoholic steatohepatitis and contributes to the disease in experimental models by inhibiting PPARα expression. *Gut*, *65*(11), 1882–1894.

Luo, Y., Burrington, C. M., Graff, E. C., Zhang, J., Judd, R. L., Suksaranjit, P., Kaewpoowat, Q., Davenport, S. K., O'Neill, A. M., & Greene, M. W. (2016). Metabolic phenotype and adipose and liver features in a high-fat Western diet-induced mouse model of obesity-linked NAFLD. *American Journal of Physiology-Endocrinology and Metabolism*, *310*(6), E418–E439.

Malaguarnera, M., Di Rosa, M., Nicoletti, F., & Malaguarnera, L. (2009). Molecular mechanisms involved in NAFLD progression. *Journal of Molecular Medicine*, *87*(7), 679–695.

Malnick, S., Mildiner, S., & Neuman, M. G. (2020). Obeticholic acid for treatment of NAFLD—

A drug in search of a disease. *GastroHep*, *2*(3), 133–137.

Mancini, G., Pirruccio, K., Yang, X., Blüher, M., Rodeheffer, M., & Horvath, T. L. (2019). Mitofusin 2 in Mature Adipocytes Controls Adiposity and Body Weight. *Cell Reports*, *26*(11), 2849-2858.e4.

Mantena, S. K., King, A. L., Andringa, K. K., Eccleston, H. B., & Bailey, S. M. (2008). Mitochondrial dysfunction and oxidative stress in the pathogenesis of alcohol- and obesity-induced fatty liver diseases. *Free Radical Biology and Medicine*, *44*(7), 1259–1272.

Mantovani, A., & Dalbeni, A. (2021). Treatments for NAFLD: State of Art. *International Journal of Molecular Sciences*, *22*(5), 2350.

Maréchal, L., Laviolette, M., Rodrigue-Way, A., Sow, B., Brochu, M., Caron, V., & Tremblay, A. (2018). The CD36-PPARγ Pathway in Metabolic Disorders. *International Journal of Molecular Sciences*, *19*(5), 1529.

Michlewski, G., & Cáceres, J. F. (2019). Post-transcriptional control of miRNA biogenesis. *RNA*, *25*(1), 1–16.

Mingrone, G., Manco, M., Calvani, M., Castagneto, M., Naon, D., & Zorzano, A. (2005). Could the low level of expression of the gene encoding skeletal muscle mitofusin-2 account for the metabolic inflexibility of obesity? *Diabetologia*, *48*(10), 2108–2114.

Moon, A. M., Singal, A. G., & Tapper, E. B. (2020). Contemporary Epidemiology of Chronic Liver Disease and Cirrhosis. *Clinical Gastroenterology and Hepatology*, *18*(12), 2650–2666.

Moore, M. P., Cunningham, R. P., Dashek, R. J., Mucinski, J. M., & Rector, R. S. (2020). A Fad too Far? Dietary Strategies for the Prevention and Treatment of NAFLD. *Obesity*, *28*(10), 1843–1852.

Motiño, O., Francés, D. E., Casanova, N., Fuertes-Agudo, M., Cucarella, C., Flores, J. M., Vallejo-Cremades, M. T., Olmedilla, L., Pérez Peña, J., Bañares, R., Boscá, L., Casado, M., & Martín-Sanz, P. (2019). Protective Role of Hepatocyte Cyclooxygenase-2 Expression Against Liver Ischemia-Reperfusion Injury in Mice. *Hepatology*, *70*(2), 650–665.

Mundi, M. S., Velapati, S., Patel, J., Kellogg, T. A., Abu Dayyeh, B. K., & Hurt, R. T. (2020). Evolution of NAFLD and Its Management. *Nutrition in Clinical Practice*, *35*(1), 72–84.

Muñoz, J. P., Ivanova, S., Sánchez-Wandelmer, J., Martínez-Cristóbal, P., Noguera, E., Sancho, A., Díaz-Ramos, A., Hernández-Alvarez, M. I., Sebastián, D., Mauvezin, C., Palacín, M., & Zorzano, A. (2013). Mfn2 modulates the UPR and mitochondrial function via repression of PERK. *The EMBO Journal*, *32*(17), 2348–2361.

Murchison, E. P., & Hannon, G. J. (2004). miRNAs on the move: miRNA biogenesis and the RNAi machinery. *Current Opinion in Cell Biology*, *16*(3), 223–229.

Nassir, F., Rector, R. S., Hammoud, G. M., & Ibdah, J. A. (2015). Pathogenesis and Prevention of Hepatic Steatosis. *Gastroenterology & Hepatology*, *11*(3), 167.

Ogawa, T., Enomoto, M., Fujii, H., Sekiya, Y., Yoshizato, K., Ikeda, K., & Kawada, N. (2012). MicroRNA-221/222 upregulation indicates the activation of stellate cells and the progression of liver fibrosis. *Gut*, *61*(11), 1600–1609.

Paik, J. M., Golabi, P., Younossi, Y., Mishra, A., & Younossi, Z. M. (2020). Changes in the Global Burden of Chronic Liver Diseases From 2012 to 2017: The Growing Impact of NAFLD. *Hepatology*, *72*(5), 1605–1616.

Parthasarathy, G., Revelo, X., & Malhi, H. (2020). Pathogenesis of Nonalcoholic Steatohepatitis: An Overview. *Hepatology Communications*, *4*(4), 478–492.

Pepino, M. Y., Kuda, O., Samovski, D., & Abumrad, N. A. (2014). Structure-Function of CD36 and Importance of Fatty Acid Signal Transduction in Fat Metabolism. *Annual Review of Nutrition*, *34*(1), 281–303.

Picca, A., Lezza, A., Leeuwenburgh, C., Pesce, V., Calvani, R., Landi, F., Bernabei, R., & Marzetti, E. (2017). Fueling Inflamm-Aging through Mitochondrial Dysfunction: Mechanisms and Molecular Targets. *International Journal of Molecular Sciences*, *18*(5), 933.

Pich, S., Bach, D., Briones, P., Liesa, M., Camps, M., Testar, X., Palacín, M., & Zorzano, A. (2005). The Charcot–Marie–Tooth type 2A gene product, Mfn2, up-regulates fuel oxidation through expression of OXPHOS system. *Human Molecular Genetics*, *14*(11), 1405–1415.

Pimpin, L., Cortez-Pinto, H., Negro, F., Corbould, E., Lazarus, J. V., Webber, L., & Sheron, N. (2018). Burden of liver disease in Europe: Epidemiology and analysis of risk factors to identify prevention policies. *Journal of Hepatology*, *69*(3), 718–735.

Pirola, C. J., Fernández Gianotti, T., Castaño, G. O., Mallardi, P., San Martino, J., Mora Gonzalez Lopez Ledesma, M., Flichman, D., Mirshahi, F., Sanyal, A. J., & Sookoian, S. (2015). Circulating microRNA signature in non-alcoholic fatty liver disease: from serum non-coding RNAs to liver histology and disease pathogenesis. *Gut*, *64*(5), 800–812.

Popov, L. (2020). Mitochondrial biogenesis: An update. *Journal of Cellular and Molecular Medicine*, *24*(9), 4892–4899.

Prasun, P., Ginevic, I., & Oishi, K. (2021). Mitochondrial dysfunction in nonalcoholic fatty liver disease and alcohol related liver disease. *Translational Gastroenterology and Hepatology*, *6*, 4–4.

Rada, P., González-Rodríguez, Á., García-Monzón, C., & Valverde, Á. M. (2020). Understanding lipotoxicity in NAFLD pathogenesis: is CD36 a key driver? *Cell Death & Disease*, *11*(9), 802.

Remmerie, A., Martens, L., & Scott, C. L. (2020). Macrophage Subsets in Obesity, Aligning

the Liver and Adipose Tissue. *Frontiers in Endocrinology*, *11*.

Rodrigues, P. M., Afonso, M. B., Simão, A. L., Carvalho, C. C., Trindade, A., Duarte, A., Borralho, P. M., Machado, M. V, Cortez-Pinto, H., Rodrigues, C. M., & Castro, R. E. (2017). Erratum: miR-21 ablation and obeticholic acid ameliorate nonalcoholic steatohepatitis in mice. *Cell Death & Disease*, *8*(5), e2825–e2825.

Samovski, D., & Abumrad, N. A. (2019). Regulation of lipophagy in NAFLD by cellular metabolism and CD36. *Journal of Lipid Research*, *60*(4), 755–757.

Sanyal, A. J. (2011). NASH: A global health problem. *Hepatology Research*, *41*(7), 670–674.

Scarpulla, R. C., Vega, R. B., & Kelly, D. P. (2012). Transcriptional integration of mitochondrial biogenesis. *Trends in Endocrinology & Metabolism*, *23*(9), 459–466.

Sebastian, D., Hernandez-Alvarez, M. I., Segales, J., Sorianello, E., Munoz, J. P., Sala, D., Waget, A., Liesa, M., Paz, J. C., Gopalacharyulu, P., Oresic, M., Pich, S., Burcelin, R., Palacin, M., & Zorzano, A. (2012). Mitofusin 2 (Mfn2) links mitochondrial and endoplasmic reticulum function with insulin signaling and is essential for normal glucose homeostasis. *Proceedings of the National Academy of Sciences*, *109*(14), 5523–5528.

Segalés, J., Paz, J. C., Hernández-Alvarez, M. I., Sala, D., Muñoz, J. P., Noguera, E., Pich, S., Palacín, M., Enríquez, J. A., & Zorzano, A. (2013). A form of mitofusin 2 (Mfn2) lacking the transmembrane domains and the COOH-terminal end stimulates metabolism in muscle and liver cells. *American Journal of Physiology-Endocrinology and Metabolism*, *305*(10), E1208–E1221.

Shen, W., Dong, R., Chen, G., & Zheng, S. (2014). microRNA-222 modulates liver fibrosis in a murine model of biliary atresia. *Biochemical and Biophysical Research Communications*, *446*(1), 155–159.

Silva, J. M., Silva, M. J., Calinas, F., & Nogueira, P. J. (2021). Burden of Liver Cirrhosis in Portugal between 2010 and 2017. *GE - Portuguese Journal of Gastroenterology*, *28*(3), 153–161.

Simão, A. L., Afonso, M. B., Rodrigues, P. M., Gama-Carvalho, M., Machado, M. V., Cortez-Pinto, H., Rodrigues, C. M. P., & Castro, R. E. (2019). Skeletal muscle miR-34a/SIRT1:AMPK axis is activated in experimental and human non-alcoholic steatohepatitis. *Journal of Molecular Medicine*, *97*(8), 1113–1126.

Smiderle, C. A., Coral, G. P., De Carli, L. A., Mattos, A. A. de, Mattos, A. Z. de, & Tovo, C. V. (2021). Performace of triglyceride-glucose index on diagnosis and staging of NAFLD in obese patients. *Arquivos de Gastroenterologia*, *58*(2), 139–144.

Su, Q., Kumar, V., Sud, N., & Mahato, R. I. (2018). MicroRNAs in the pathogenesis and treatment of progressive liver injury in NAFLD and liver fibrosis. *Advanced Drug Delivery Reviews*, *129*, 54–63.

Sumida, Y., & Yoneda, M. (2018). Current and future pharmacological therapies for

NAFLD/NASH. *Journal of Gastroenterology*, *53*(3), 362–376.

Sutterwala, F. S., Haasken, S., & Cassel, S. L. (2014). Mechanism of NLRP3 inflammasome activation. *Annals of the New York Academy of Sciences*, *1319*(1), 82–95.

Szabo, G., & Csak, T. (2016). Role of MicroRNAs in NAFLD/NASH. *Digestive Diseases and Sciences*, *61*(5), 1314–1324.

Takahashi, Y. (2012). Animal models of nonalcoholic fatty liver disease/nonalcoholic steatohepatitis. *World Journal of Gastroenterology*, *18*(19), 2300.

Tan, Y., Ge, G., Pan, T., Wen, D., & Gan, J. (2014). A Pilot Study of Serum MicroRNAs Panel as Potential Biomarkers for Diagnosis of Nonalcoholic Fatty Liver Disease. *PLoS ONE*, *9*(8), e105192.

Tessitore, A., Cicciarelli, G., Del Vecchio, F., Gaggiano, A., Verzella, D., Fischietti, M., Mastroiaco, V., Vetuschi, A., Sferra, R., Barnabei, R., Capece, D., Zazzeroni, F., & Alesse, E. (2016). MicroRNA expression analysis in high fat diet-induced NAFLD-NASH-HCC progression: study on C57BL/6J mice. *BMC Cancer*, *16*(1), 3.

Tétreault, N., & De Guire, V. (2013). miRNAs: Their discovery, biogenesis and mechanism of action. *Clinical Biochemistry*, *46*(10–11), 842–845.

Tilg, H. (2010). The Role of Cytokines in Non-Alcoholic Fatty Liver Disease. *Digestive Diseases*, *28*(1), 179–185.

Tilg, H., & Moschen, A. R. (2010). Evolution of inflammation in nonalcoholic fatty liver disease: The multiple parallel hits hypothesis. *Hepatology*, *52*(5), 1836–1846.

van der Bliek, A. M., Shen, Q., & Kawajiri, S. (2013). Mechanisms of Mitochondrial Fission and Fusion. *Cold Spring Harbor Perspectives in Biology*, *5*(6), a011072–a011072.

Vinciguerra, M., Sgroi, A., Veyrat-Durebex, C., Rubbia-Brandt, L., Buhler, L. H., & Foti, M. (2009). Unsaturated fatty acids inhibit the expression of tumor suppressor phosphatase and tensin homolog (PTEN) via microRNA-21 up-regulation in hepatocytes. *Hepatology*, *49*(4), 1176–1184.

Vishnoi, A., & Rani, S. (2017). MiRNA Biogenesis and Regulation of Diseases: An Overview. In *Methods in molecular biology (Clifton, N.J.)* (Vol. 1509, pp. 1–10). Methods Mol Biol.

Wang, J.-J., Zhang, Y.-T., Tseng, Y. J., & Zhang, J. (2019). miR-222 targets ACOX1, promotes triglyceride accumulation in hepatocytes. *Hepatobiliary & Pancreatic Diseases International*, *18*(4), 360–365.

Wang, X., Liao, X., Huang, K., Zeng, X., Liu, Z., Zhou, X., Yu, T., Yang, C., Yu, L., Wang, Q., Han, C., Zhu, G., Ye, X., & Peng, T. (2019). Clustered microRNAs hsa-miR-221-3p/hsa-miR-222-3p and their targeted genes might be prognostic predictors for hepatocellular carcinoma. *Journal of Cancer*, *10*(11), 2520–2533.

Wang, Z., Wang, Z., Gao, L., Xiao, L., Yao, R., Du, B., Li, Y., Wu, L., Liang, C., Huang, Z., Li, P., & Zhang, Y. (2020). miR-222 inhibits cardiac fibrosis in diabetic mice heart via

regulating Wnt/β-catenin-mediated endothelium to mesenchymal transition. *Journal of Cellular Physiology*, *235*(3), 2149–2160.

Wei, Y., Rector, R. S., Thyfault, J. P., & Ibdah, J. A. (2008). Nonalcoholic fatty liver disease and mitochondrial dysfunction. *World Journal of Gastroenterology*, *14*(2), 193.

WHO. (2017). *Global hepatitis report, 2017*.

Wree, A., Eguchi, A., McGeough, M. D., Pena, C. A., Johnson, C. D., Canbay, A., Hoffman, H. M., & Feldstein, A. E. (2014). NLRP3 inflammasome activation results in hepatocyte pyroptosis, liver inflammation, and fibrosis in mice. *Hepatology*, *59*(3), 898–910.

Wree, A., McGeough, M. D., Peña, C. A., Schlattjan, M., Li, H., Inzaugarat, M. E., Messer, K., Canbay, A., Hoffman, H. M., & Feldstein, A. E. (2014). NLRP3 inflammasome activation is required for fibrosis development in NAFLD. *Journal of Molecular Medicine*, *92*(10), 1069–1082.

Xu, F., Qi, H., Li, J., Sun, L., Gong, J., Chen, Y., Shen, A., & Li, W. (2020). Mycobacterium tuberculosis infection up-regulates MFN2 expression to promote NLRP3 inflammasome formation. *Journal of Biological Chemistry*, *295*(51), 17684–17697.

Yang, L., Roh, Y. S., Song, J., Zhang, B., Liu, C., Loomba, R., & Seki, E. (2014). Transforming growth factor beta signaling in hepatocytes participates in steatohepatitis through regulation of cell death and lipid metabolism in mice. *Hepatology*, *59*(2), 483–495.

Yang, Y.-F., Wang, F., Xiao, J.-J., Song, Y., Zhao, Y.-Y., Cao, Y., Bei, Y.-H., & Yang, C.-Q. (2014). MiR-222 overexpression promotes proliferation of human hepatocellular carcinoma HepG2 cells by downregulating p27. *International Journal of Clinical and Experimental Medicine*, *7*(4), 893.

Youle, R. J., & van der Bliek, A. M. (2012). Mitochondrial Fission, Fusion, and Stress. *Science*, *337*(6098), 1062–1065.

Younossi, Z. M., Marchesini, G., Pinto-Cortez, H., & Petta, S. (2019). Epidemiology of Nonalcoholic Fatty Liver Disease and Nonalcoholic Steatohepatitis: Implications for Liver Transplantation. *Transplantation*, *103*(1), 22–27.

Zhang, X., Ji, X., Wang, Q., & Li, J. Z. (2018). New insight into inter-organ crosstalk contributing to the pathogenesis of non-alcoholic fatty liver disease (NAFLD). *Protein & Cell*, *9*(2), 164–177.

Zhang, Ying, Yang, L., Gao, Y.-F., Fan, Z.-M., Cai, X.-Y., Liu, M.-Y., Guo, X.-R., Gao, C.-L., & Xia, Z.-K. (2013). MicroRNA-106b induces mitochondrial dysfunction and insulin resistance in C2C12 myotubes by targeting mitofusin-2. *Molecular and Cellular Endocrinology*, *381*(1–2), 230–240.

Zhang, Yong, Jiang, L., Hu, W., Zheng, Q., & Xiang, W. (2011). Mitochondrial dysfunction during in vitro hepatocyte steatosis is reversed by omega-3 fatty acid–induced up-

regulation of mitofusin 2. *Metabolism*, *60*(6), 767–775.

Zhou, X., Zhang, L., Zheng, B., Yan, Y., Zhang, Y., Xie, H., Zhou, L., Zheng, S., & Wang, W. (2016). MicroRNA-761 is upregulated in hepatocellular carcinoma and regulates tumorigenesis by targeting Mitofusin-2. *Cancer Science*, *107*(4), 424–432.

Zhu, H., Shan, Y., Ge, K., Lu, J., Kong, W., & Jia, C. (2020). Specific Overexpression of Mitofusin-2 in Hepatic Stellate Cells Ameliorates Liver Fibrosis in Mice Model. *Human Gene Therapy*, *31*(1–2), 103–109.

Zhu, M., Wang, Q., Zhou, W., Liu, T., Yang, L., Zheng, P., Zhang, L., & Ji, G. (2018). Integrated analysis of hepatic mRNA and miRNA profiles identified molecular networks and potential biomarkers of NAFLD. *Scientific Reports*, *8*(1), 7628.

Zorzano, A. (2009). Regulation of mitofusin-2 expression in skeletal muscleThis paper is one of a selection of papers published in this Special Issue, entitled 14th International Biochemistry of Exercise Conference – Muscles as Molecular and Metabolic Machines, and has under. *Applied Physiology, Nutrition, and Metabolism*, *34*(3), 433–439.

Zorzano, A., Liesa, M., Sebastián, D., Segalés, J., & Palacín, M. (2010). Mitochondrial fusion proteins: Dual regulators of morphology and metabolism. *Seminars in Cell & Developmental Biology*, *21*(6), 566–574.